

Yale University

## EliScholar – A Digital Platform for Scholarly Publishing at Yale

---

Yale Medicine Thesis Digital Library

School of Medicine

---

1979

# A study of maximal renal potassium transport function

Forrester Ashe Lee Jr.

*Yale University*

Follow this and additional works at: <http://elischolar.library.yale.edu/ymtdl>

---

### Recommended Citation

Lee, Forrester Ashe Jr., "A study of maximal renal potassium transport function" (1979). *Yale Medicine Thesis Digital Library*. 2837.  
<http://elischolar.library.yale.edu/ymtdl/2837>

This Open Access Thesis is brought to you for free and open access by the School of Medicine at EliScholar – A Digital Platform for Scholarly Publishing at Yale. It has been accepted for inclusion in Yale Medicine Thesis Digital Library by an authorized administrator of EliScholar – A Digital Platform for Scholarly Publishing at Yale. For more information, please contact [elischolar@yale.edu](mailto:elischolar@yale.edu).





A STUDY OF  
MAXIMAL RENAL POTASSIUM TRANSPORT FUNCTION

---

Forrester Ashe Lee, Jr.

1979

YALE




MEDICAL LIBRARY











Digitized by the Internet Archive  
in 2017 with funding from  
The National Endowment for the Humanities and the Arcadia Fund





Permission for photocopying or microfilming of "

A

Study of Maximal Renal Transport Function "

(TITLE OF THESIS)

for the purpose of individual scholarly consultation or reference is hereby granted by the author. This permission is not to be interpreted as affecting publication of this work or otherwise placing it in the public domain, and the author reserves all rights of ownership guaranteed under common law protection of unpublished manuscripts.

Forrestell Fred

Signature of Author

30 April 1979

Date



A STUDY OF MAXIMAL RENAL POTASSIUM TRANSPORT FUNCTION

- I: MAXIMAL K EXCRETION RATES IN SALINE AND  
K-INFUSED NORMAL AND HIGH-K DIET RATS
- II: MATHEMATICAL MODELS OF FLOW-DEPENDENT  
DISTAL TUBULAR POTASSIUM SECRETION

A Thesis Submitted to the Yale University School of Medicine  
In Partial Fulfillment of the Requirement for the Degree of  
Doctor of Medicine

1979

FORRESTER ASHE LEE, JR.





## ABSTRACT

Clearance measurements were made in saline-loaded rats to determine whether a maximal rate of renal K excretion (K excretory plateau) could be demonstrated during high rates of volume and solute diuresis. Normal and High-K diet rats were studied. Clearance results were analyzed from a control period and 2 hours after K loading (K infusion period) for low, moderate, and high rates of volume expansion (LMH-VE).

During the K infusion period, High-K and normal diet rats exhibited a similar relationship between potassium excretion and urine flow rate or sodium excretion. K excretion rose in parallel with natriuresis and urine flow until an apparent K excretory plateau was attained for urine flow rates greater than  $20 \text{ ul min}^{-1} 100\text{gBW}^{-1}$ . The plateau level of K excretion was not significantly different between the two diet groups and represented approximately 85% of the rate of K infusion. However, the mean plasma K of the High-K diet group was in the normal range while that of the normal diet group was elevated.

A second series of experiments were carried out in the normal diet group in which the K infusion was extended for a total of 6.5 hours. With prolonged K infusion, rats achieved potassium excretion approximately 58% greater than the K excretory plateau present after two hours of K loading in the LMH-VE experiments. This enhancement of renal K excretion during prolonged K infusion appeared to represent a response to the duration of K loading independent of plasma K, Na excretion or urine flow rates.





It is concluded that a K excretory plateau exists during K loading and that it represents a temporally-bound characteristic parameter of renal K excretory function that may change dynamically depending on the degree, efficacy, and duration of the stimulus to K excretion. Correlations with flow-dependent distal tubular K secretion are discussed.

In order to analyze at a theoretical level the basis for flow-dependent distal tubular K transport, mathematical models based on kinetic formulations of distal tubular membrane transport behavior were developed and analyzed. In vivo kinetic data from other studies was used to test and quantify the K secretory kinetics of the models. The results of the analysis suggest that distal tubular flow-dependent K secretion is characteristic of an epithelium that is kinetically defined by its ability to maintain a constant cell K concentration and luminal membrane voltage independent of luminal flow rate or ionic composition and by the presence of a nonsaturable K reabsorptive pump in the luminal membrane. Other models based on alternative postulates of distal tubular membrane transport and cell properties - for example, cell K concentration dependent on transepithelial K transport rates, a luminal membrane voltage determined by a K diffusion potential, a saturable luminal membrane K reabsorptive pump - are examined and contrasted.



"To exist humanly is to name the world, to change it. Once named, the world in its turn reappears to the namers as a problem and requires of them a new naming. Men are not built in silence, but in word, in work, in action-reflection."

Paulo Freire  
Pedagogy of the Oppressed





## PREFACE

The thesis requirement of the Yale School of Medicine poses to the student, already challenged by the enormous task of establishing competency in his or her medical training, a responsibility that is at once an additional, at times unwelcomed, burden and a special opportunity to personalize one's relationship with investigative medical science. That the opportunity for me was indeed especially rewarding reflects on the outstanding qualities of the people with whom I worked.

The excellence of the renal physiology group at Yale was continually inspiring. My thanks are particularly extended to Drs. Josephine Briggs, Emile Boulpaep, Gerhard Giebisch, and Henry Sackin who always found a way to clarify and add new dimensions to the problems I posed. In the laboratory, I was skillfully guided by George Baron and Nicole Fowler. My thanks are especially offered to Tom Duplinsky who worked with exceptional diligence while assisting on the many not so "routine" laboratory determinations. Likewise, Mrs. Donna Belli, who prepared the typed manuscript, was particularly helpful in her expert transcription of the many mathematical expressions with clarity and precision.

My advisor, Dr. Fred S. Wright, stands alone as one committed to personal excellence and integrity while always finding the time and having the patience to share the fruits of these qualities with others. In challenging me to be honest with my ideas and thoughtful with their application, Dr. Wright truly represented a wellspring of enthusiasm, creativity, and support which guided this project to a completion. This thesis is dedicated to Dr. Wright.



Finally, to my family I owe a special debt. Especially to my daughter, N'Tanya, who sought me out late each afternoon in the laboratory to remind me that the scientist, the doctor, and the father are all one person, each committed in their various ways to the same pursuit - to find and share in an enduring, human existence in this world.



TABLE OF CONTENTS

PART I: MAXIMAL K EXCRETION RATES IN SALINE AND  
K-INFUSED NORMAL AND HIGH-K DIET RATS

Introduction . . . . .	2
Methods . . . . .	13
Results . . . . .	18
A. Effects of K infusion in normal diet and High-K diet rats: LMH-VE . . . . .	18
B. Potassium excretion in relation to urine flow rate and Na excretion: LMH-VE . . . . .	22
C. Prolonged K infusion experiments . . . . .	28
D. K excretory plateau . . . . .	37
E. Prolonged K infusion vs. short-term K infusion . . . . .	40
Discussion . . . . .	45

PART II: MATHEMATICAL MODELS OF FLOW-DEPENDENT  
DISTAL TUBULAR POTASSIUM SECRETION

A. Introduction . . . . .	62
B. Principal aspects of K secretory kinetics to be characterized by the model mathematical solutions . . . . .	70
C. Basic parameters . . . . .	74
D. Fundamental equations . . . . .	78
E. Working postulates . . . . .	82
F. Models A and B mathematical solutions with no volume reabsorption . . . . .	87
G. Qualitative examination of the K secretory behavior of Models A and B . . . . .	98





H.	Incorporation of <u>in vivo</u> kinetic data into parameters of Models A and B. . . . .	108
1.	Axial K concentration profile as a function of V and K(0). . . . .	113
2.	K(L) as a function of K(0) and V. . . . .	115
3.	Net K absorption as a function of V and K(0). . . . .	115
4.	Total K axial flux at x = L . . . . .	118
5.	Net K absorption as a function of K(0). . . . .	120
6.	Cell potassium concentration variability in Model B. . . . .	123
I.	Volume reabsorption effects on K secretion. . . . .	127
1.	Approximating flow function . . . . .	130
2.	Net K absorption vs. $\bar{V}$ for DeMello-Aires five experimental groups. . . . .	134
J.	Non-linear luminal reabsorptive pump kinetics . . . . .	139
1.	No luminal K reabsorptive pump model. . . . .	140
2.	Non-linear, saturable K reabsorptive pump model. . . . .	143
K.	Non-constant luminal membrane PD model. . . . .	150
L.	<u>In vivo</u> net K absorption vs. K(0) results compared to model predictions . . . . .	155
	Appendices . . . . .	164
	References . . . . .	169



LIST OF TABLES

PART I

1. Effects of K infusion in normal and High-K diet rats, LMH-VE	19
2. Changes in mean clearance values between control and K infusion period for normal and High-K diet rats, LMH-VE	20
3. Clearance results, prolonged K infusion	30
4. Maximum K excretion rates, normal and High-K, control and K infusion, LMH-VE	39
5. Normal diet: short-term vs. long-term K infusion	41

PART II

1. Model A and B equations	95
2. Comparisons of exponential functions	102
3. Experimental groups of DeMello-Aires	109
4. DeMello-Aires kinetic data	110
5. Adjusted DeMello-Aires kinetics data for use in Models A and B equations; calculated parameter values	112
6. Good and Wright distal tubule microperfusion data	160



LIST OF ILLUSTRATIONS

PART I

1. Late distal K concentration vs. flow rate: results from other studies	7
2. Hypothetical flow-limited and transport-limited secretion models of Giebisch	9
3. NaCl and KCl loading schedules	16
4. $E_{Na}$ vs. $V_u$ , all experimental groups	24
5. $E_K$ vs. $V_u$ and $E_{Na}$ , normal and High-K diet, LMH-VE, control period	25
6. $E_K$ vs. $V_u$ and $E_{Na}$ , normal and High-K diet, LMH-VE, K infusion period	27
7. $E_K$ vs. $V_u$ , prolonged K infusion	31
8. $E_K$ vs. $E_{Na}$ , prolonged K infusion	32
9. $E_K$ vs. $V_u$ , prolonged K infusion, 2 High-K diet rats	34
10. Potassium balance during prolonged K infusion	36
11. $E_K$ vs. $P_K$ , prolonged K infusion and LMH-VE, normal diet	43
12. $E_K$ vs. $V_u$ , control period, normal diet, LMH-VE and results from <u>Khuri et al</u> study	47
13. $V_u$ vs. $V_{LD}$ , results from other studies	51

PART II

1. Late distal tubule cell diagram	63
2. Hypothetical flow-limited and transport-limited K secretion diagrams	66





3. Hypothetical net K absorption vs. $K(0)$ and K secretion vs. flow rate	73
4. Model tubule diagram	75
5. Normalized $K(L)$ and net K secretion vs. flow rate and net K absorption vs. flow rate	100
6. Normalized K secretion vs. flow rate and net K absorption vs. flow rate	103
7. $K(x)$ vs. $x$ , $V$ varied, Models A and B	114
8. $K(x)$ vs. $x$ , $K(0)$ varied, Models A and B	116
9. $K(L)$ vs. $V$ , $K(0)$ varied, Models A and B	117
10. Net K absorption vs. $V$ , $K(0)$ varied, Models A and B	119
11. Potassium flux at $x = L$ and net K secretion vs. $V$ , $K(0)$ varied, Model A	121
12. Net K absorption vs. $K(0)$ , $V$ varied, Models A and B	122
13. Mean Cell K vs. $V$ , $K(0)$ varied, Model B	124
14. $V(0)$ vs. $V(L)$ , $V(x)$ vs. $x$ , approximating flow function	133
15. Net K absorption vs. $V$ , fluid reabsorption model, $K(0)$ varied	135
16. K secretion vs. $V$ , DeMello-Aires 5 experimental groups, Models A and B with fluid reabsorption	137
17. $K(L)$ and K secretion vs. $V$ , Model A and no luminal membrane pump model	142
18. $J_{12}$ vs. $K$ , Model A and non-linear pump model	146
19. $K(L)$ and K secretion vs $V$ , Model A and non-linear pump model	137
20. Net K absorption vs. $K(0)$ , non-linear pump model	148
21. Net K secretion vs. $V$ and $K(0)$ , variable luminal membrane PD model	152
22. Good and Wright microperfusion diagram	156
23. Good and Wright net K absorption vs $K_{ED}$	161



PART I: MAXIMAL K EXCRETION RATES IN SALINE AND  
K-INFUSED NORMAL AND HIGH-K DIET RATS



## INTRODUCTION

The experimental studies and theoretical models set forth in this thesis represent an investigation into observations made principally during the pre-micropuncture era of renal physiology study that under certain diuretic conditions, renal potassium excretion rises in parallel with the rate of natriuresis until, as one report noted, "a K excretory plateau is reached; further increases in Na load then have no effect on K excretion" (Cade and Shalhoub, 15). The present study is designed to re-examine the concept of a "K excretory plateau" in the context of present-day understanding of renal K transport physiology.

The laboratory investigations presented in Part I concern an analysis of renal clearance measurements made during isotonic saline loading of rats in order to ascertain:

- (1) whether a K excretory plateau can be demonstrated, and
- (2) whether the existence or magnitude of such a plateau is affected by:
  - chronically high levels of potassium dietary intake ("K adaptation")
  - the length of time that a rat is subjected to an acute IV potassium load

Presented in Part II is an analysis of mathematical models of distal tubular K secretion. Among the various aspects of K secretory kinetics examined in the models is the relationship between distal tubular luminal fluid flow rate and the rate of potassium secretion, the influence of the K load entering the modeled distal tubular segment on net K secretion, and the importance of various distal tubular membrane transport



properties to maximally attainable K secretion rates. An introduction to this theoretical work is deferred until the beginning of Part II.

In the experimental rat, saline diuresis normally induces augmented rates of K excretion over the non-diuretic state (4,20,24,36,42,44,50). This phenomenon is reliably reproducible in a variety of physiological settings and, with exceptions to be noted, extends to most vertebrate species that have been studied and to most natriuretic stimuli: sodium salt loading (36,42,44); such osmotic agents as urea and mannitol (4,50); and several classes of diuretic drugs, including the clinically popular thiazide and "loop" diuretics (20,24).

In a few studies it has been observed that the kaliuresis induced by natriuretic stimuli has an apparent maximal rate; additional increments in fluid and solute excretion are not accompanied by further increases in the rate of potassium excretion. The data plots from Rapaport and West's experiments in 1950 (49) in which a solute diuresis was induced in dogs by IV sodium salt infusions indicate that although sodium excretion rose in direct proportion to urine flow rate with all infusates, K excretion rates increased at a progressively slower rate and tended to plateau as urine flow increased under the stimulus of NaCl, Na<sub>2</sub>SO<sub>4</sub>, Na<sub>2</sub>S<sub>2</sub>O<sub>3</sub>, and NaHCO<sub>3</sub> loading. Cade and Shalhoub reported in abstract (15) that dogs with intact adrenals or subjected to adrenalectomy plus mineralocorticoid replacement demonstrated augmented rates of K excretion with Na<sub>2</sub>SO<sub>4</sub> loading until a "plateau" level was reached after which further loading induced no additional stimulation of K excretion.





Gonick et al (25) studied the effects of acute K loading on potassium excretion in dogs during a urea promoted osmotic diuresis and concluded that "once distal K secretion was maximally stimulated by K loading... it was not further affected by solute diuresis or augmented Na excretion." Rabinowitz and Gunther (48) observed a similar phenomenon in sheep, herbivores with a high potassium dietary intake. The infusion of saline, hypertonic sodium phosphate or hypertonic sodium sulfate induced a strong Na solute diuresis but no consistent change in K excretion over basal rates. The results were interpreted as indicating "maximally-active" distal nephron K secretory function in the pre-diuretic state.

On the basis of the above reports, it is tempting to speculate, as did Rabinowitz and Gunther, that the demonstration of a K excretory plateau at the urinary level during a solute diuresis might have a correlate with potassium transport in the renal tubule. In view of the well established primacy of the distal tubule as the source of potassium ultimately destined for urinary excretion (7,12,23,42-44,63-65), is it possible that distal tubular K secretion is physiologically limited by a secretion transport maximum? As will be discussed, the limited micropuncture experimental evidence bearing on this question does not directly support the notion of a transport maximum for K secretion in the distal tubule. While it is not the purpose of the clearance experiments described in the present study to evaluate single nephron K transport activity, the work undertaken here is grounded in the view that if a urinary K excretory plateau can be confirmed to exist in the rat, important implications are then posed for mechanisms and determinants of K transport along



the renal tubule. In order to illuminate this point of view, it will be helpful to briefly review some pertinent aspects of renal K handling.

Prior to the full exploitation of the micropuncture technique in the study of renal physiology, the prevailing view of mechanisms of renal K transport was set forth by R. W. Berliner in the Harvey Lectures of 1961 (7). Berliner summarized a body of renal clearance and "stop-flow" experimental studies which pointed convincingly to the probability that urinary potassium was derived largely if not exclusively from secretion of potassium by the distal nephron. He further went on to elaborate the view that in the distal nephron, a sodium-potassium exchange mechanism operated to mediate the magnitude of potassium secreted into the nephron lumen. The delivery of a large sodium load to the postulated mechanism would obligate a high rate of sodium exchange for potassium thus resulting in a high rate of urinary potassium excretion. Conversely, under certain circumstances, it was theorized that the supply of sodium to the distal nephron could become the rate-limiting factor in potassium excretion.

By the late 1960's, it became evident from micropuncture studies that the ratio of exchange of sodium for potassium in the distal tubule was quite variable since differences ranging over an order of magnitude between distal tubular sodium reabsorption and K secretion could be demonstrated under varied physiological conditions (23,43). However, since in all but a few experimental settings, rates of distal tubular K secretion changed in parallel with the rate of Na load delivery to the nephron segment, the view that Na played a primary role in mediating distal tubular K secretion remained unchallenged.



In the early 1970's, the concept of "flow dependency" of K secretion was offered by G. Giebisch (22). Giebisch proposed that tubular fluid flow rate had an important effect on the magnitude of distal tubule K secretion. However, not until recently in the microperfusion experiments of Good and Wright (26,27) was it clearly demonstrated that distal tubular flow rate per se was the important determinant of K secretion independent of delivered sodium load when other physiological determinants of K secretion were controlled.

Shown in Figure I.1 (adapted from Wright 65), are a variety of rat micropuncture experimental results which demonstrate the dependency of K secretion on flow rate. Late distal tubular K concentration is plotted against late distal flow rate. The experimental data from several studies (27,36,39,44,46,51) is superimposed on a series of hyperbolas which represent "constant K secretion isopleths." For tubular K secretion to remain unchanged during variations in luminal flow rate, the functional relationship between K concentration and flow rate would have to follow the profile of one of the isopleths. Connected experimental data points cutting from a lower to a higher constant K secretion isopleth indicate that K concentration is not falling in proportion to luminal flow rate, and therefore that K secretion is being augmented by increments in flow rate.

With the exception of the data from the Khuri et al study (36), the depicted experimental findings indicate that late distal K concentrations tend to fall with higher flow rates, but by a degree that is less than proportional to the rise in luminal flow rate. Therefore, K secretion is enhanced when tubular flow rate is increased. The data





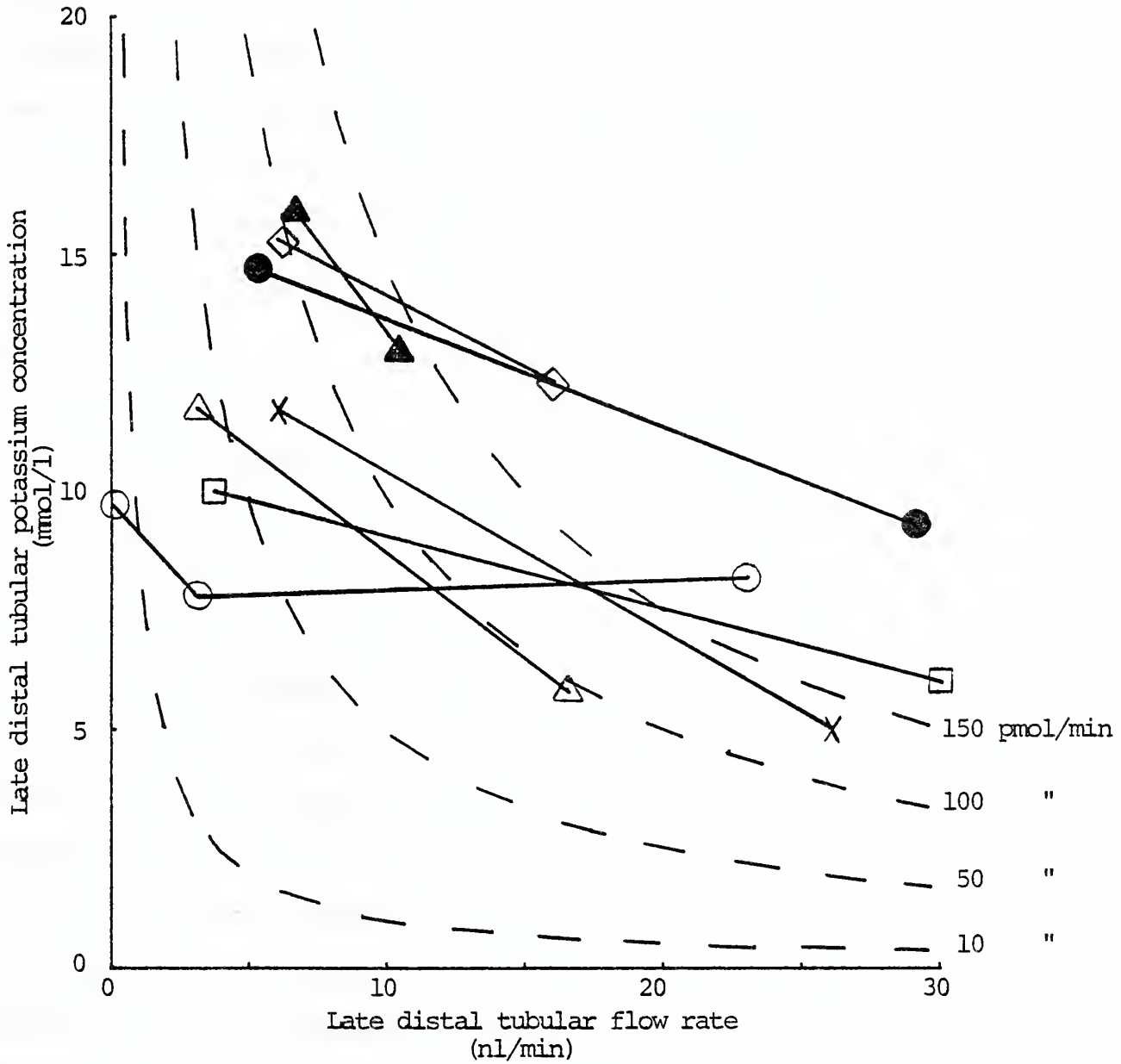


Figure I.1 Late distal K concentration in relation to late distal tubular flow rate. Open symbols indicate rats with normal plasma K; closed symbols, rats with elevated plasma K resulting from K infusion. Circles are from reference 36 and 44, triangles from 51, diamonds from 46, squares from 39, and X's from 27. The hyperbolas represent constant K secretion isopleths (see text).



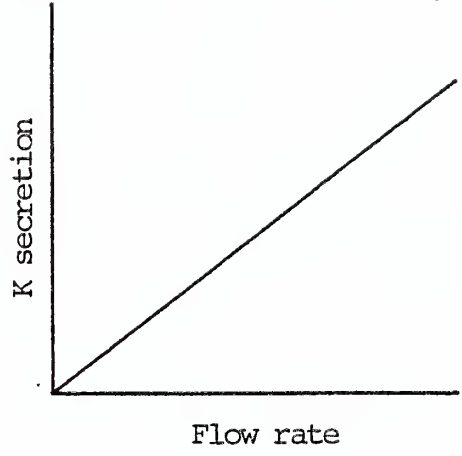
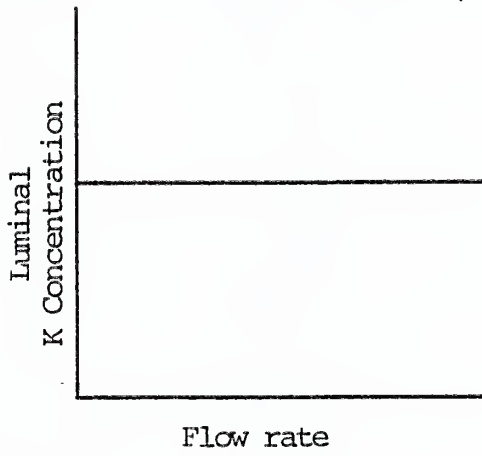
include results from "stationary drop" experiments (44), loop of Henle (46) and direct distal tubule (27) microperfusion experiments in hydro-penic animals, and measurements of free-flow late distal K concentrations and flow rates under hydro-penic and saline loading conditions (36, 39,51). The effect of concurrent KCl loading was also investigated in the Khuri et al (K-adapted rats) and Reineck et al (normal diet rats) studies (36,51).

Based in part on the results of the Khuri et al study, Giebisch proposed that potassium secretion in the rat late distal tubule more closely approximated a hypothetical "flow-limited" secretory model than a "transport-limited" model (22). Shown in Figure I.2 (adapted from Giebisch, 22) are graphical representations of the K secretion vs. flow rate and K concentration vs. flow rate relationships for the flow-limited and transport-limited K secretory models. In the flow-limited case, which Giebisch suggests characterizes distal tubular K secretory behavior, the luminal potassium concentration is maintained at a constant level independent of flow rate variability, with the result that K secretion is directly proportional to flow rate. For the transport-limited model, luminal K concentration falls in proportion to the rise in flow rate, and K secretion therefore remains constant and independent of flow rate.

Most of the experimental results given in Figure I.1 indicate that the late distal tubular K secretory system operates at a position intermediate between a flow-limited and a transport-limited model. Whether a distal tubular K secretory maximum exists which would correlate with a urinary K excretory plateau cannot be ascertained from these investi-



Flow-limited K secretion



Transport-limited K secretion

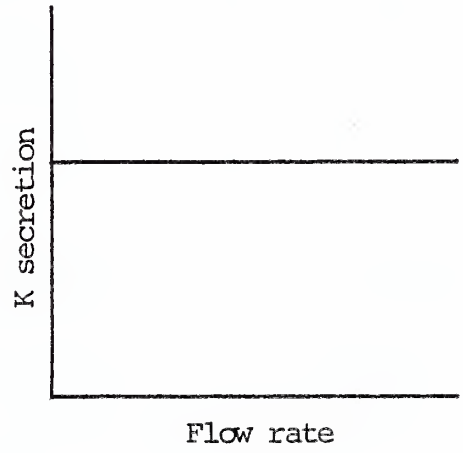
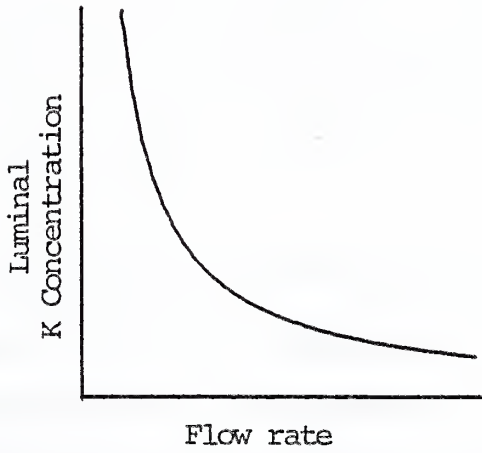


Figure I.2 Contrasting hypothetical models of K transport in relation to luminal fluid flow rate. (Adapted from Giebisch, 22)



gations. The range of flow rates examined is restricted to a few observations in each study.

The rat distal tubule micropuncture studies thus do not provide direct evidence for a distal tubular K secretory maximum within physiological flow rates. Indeed, the proposal advanced by Giebisch that distal tubular K secretion is flow-limited and the results from the Khuri et al study (Figure I.1) imply that any maximal renal K excretory capability measured at the urinary level should reflect a physiological limitation on distal tubular flow rate magnitude, not a maximum K secretory transport capability. However, the concept of a K excretory plateau and its postulated correlation with a distal tubular K transport maximum emerged from the reports noted earlier in which dogs were infused with a K excretion stimulus (for example, KCl and Na<sub>2</sub>SO<sub>4</sub>) and from studies of sheep maintained on their normal high dietary K intake. Whether under similar circumstances of acute or chronic stimulation of renal K excretion, the same phenomenon could be demonstrated in rats is not certain.

The stimulatory effect of acute IV K loading on renal K excretion (5,6,47,54) and the enhancement of the ability of rats fed diets rich in potassium to excrete acute K load challenges more efficiently than normal diet rats, so-called "K-adaptation" or "K tolerance" (1,55,57,62), have been well described. In addition, several reports have shown that during IV K loading, the rate of kaliuresis tends to stabilize after a time in spite of a continually rising plasma K concentration. For instance, Orloff and Davidson (47) found that during perfusion of the portal circulation of the chicken (which directly elevates renal peritubular





K concentration), K excretion leveled off after one hour while plasma K concentration continued to increase. In a recent micropuncture study of the hydropenic rat, Stanton and Giebisch reported in abstract (56) that with acute IV K loading, distal tubular K secretion rates increased over time during a period of relative stability of plasma K concentration. However, similar to the findings reported in the chicken, further K loading raised plasma K concentration but induced no additional increment in distal tubular K secretion. Finally, concerning chronic K loading, Rabinowitz and Gunther observed in a study mentioned earlier (48) that high K diet sheep exhibited rates of K excretion in the hydropenic state that could not be further augmented by sodium salt loading. These reports raise the possibility that a K excretory plateau might be more readily demonstrable during saline volume expansion if the kidney's K excreting capability were concurrently stimulated. Is it possible that in the setting of acute or chronic K loading, progressive saline volume expansion would "unmask" a renal K excretory plateau in the rat?

The foregoing discussion and the questions raised introduce the principal considerations important to the design of the present investigation. The studies in Part I aim to ascertain whether a K excretory plateau exists in the rat during saline volume expansion, and whether its existence or magnitude is conditioned by prior dietary K intake and/or acute IV K loading. The results of these experiments strongly suggest that a renal K excretory plateau can be demonstrated when rats are subjected to acute IV K loading and further indicate that the K excretion rate at which the plateau level is "set" may be dependent on



interrelationships among such variables as plasma K concentration, prior dietary K intake level, and the duration of exposure to an acute IV KCl infusion.

The discussion in Part I centers on an assessment of intra- and extra-renal factors which may be important to setting the magnitude of a K plateau. Implications posed for distal tubular K transport are noted. Part II examines mathematical models of distal tubular potassium transport kinetics as a means of analyzing at a theoretical level a postulated basis for flow-dependent, transport maximum-limited K secretory behavior.



## METHODS

Male Sprague-Dawley rats (Charles River Breeding Lab) weighing from 200 to 325 g were prepared for experimentation on two dietary regimens: (1) a normal diet group was maintained on standard laboratory chow (Purina), Na = 0.10 mmol/g and K = 0.22 mmol/g; and (2) High-K diet rats were fed an enriched potassium diet (General Biochemicals) for 20 to 35 days, Na = 0.18 mmol/g and K = 2.00 mmol/g. Tap water, ad libitum, was provided for both diet groups. Prior to experiments, rats were deprived of food for 15 hours but allowed free access to tap water.

Anaesthesia was induced by intraperitoneal injection of Inactin (Promota, Hamburg) @ 100 mg/kg body weight. Rats were then placed on an experimental apparatus heated to a constant temperature of 37°C throughout the course of the experiment. Rectal temperature was continuously monitored and recorded. Surgical preparation included a tracheostomy, cannulation of the left external jugular vein for IV infusions, and cannulation of the right carotid artery for blood pressure monitoring and blood sampling. The arterial blood pressure was monitored continuously using a strain-gauge transducer (Ailtech) and recorder (Gulston).

The left kidney was exposed through a left flank incision with care taken to avoid manipulation of the adrenal gland as it was dissected away from the perinephric fat. The kidney was immobilized in a plastic lucite cup, bathed in an isotonic saline solution, and draped with a small piece of tissue to limit fluid and heat loss. The temperature of the medium surrounding the kidney was checked periodically and repeatedly found to match



rectal temperature. A polyethylene catheter was inserted into the left ureter and the tip advanced to the uretero-pelvic junction. Urine was collected under oil in pre-weighed tubes. Experiments in which rats maintained a blood pressure greater than 100 mmHg throughout were judged to be successfully completed.

In all experiments, C-14 inulin (New England Nuclear) was added to the saline infusion solution in an amount sufficient to deliver a minimum of 10 uCi/hour/kg body weight. Two methods of saline volume expansion and KCl infusion were employed.

Method I: Low, moderate, and high rate saline volume expansion (LMH-VE)

An isotonic saline solution (0.15M NaCl) was infused for a period of five hours at three rates, 0.3, 1.0, and 3.0 ml/hour/100g BW corresponding to low, moderate, and high rate volume expansion respectively.

A continuous rate adjustable "Precision Metering Pump" (Instrumentation Specialties Co., Model 300) was used. At the end of the first two hours of saline infusion, a one hour clearance period was begun (Control period).

A KCl infusion (1.0M KCl) @ 5.0 umol/min/100g BW was started at the beginning of the third hour and continued for two hours. A separate infusion pump and catheter (Sage, Model 355) was employed. A one hour clearance period (K infusion period) was begun at the start of the second hour of K infusion.

In order to achieve variability in the rate of volume and solute diuresis among the experimental rats, a modified saline loading schedule was employed as part of the Method I protocol. In the first modified method ("1.0/6.0"), the saline was infused at 1.0 ml/hour/100g BW





for the first 3.5 hours and then increased to 6.0 ml/hour/100g BW for the final 1.5 hours. In the second modification ("1.0/0.3"), saline was infused at 1.0 ml/hour/100g BW for three hours and then reduced to 0.3 ml/hour/100g BW for the last two hours. The KCl infusion time and rate and the clearance periods were the same as in the LMH-VE method. For the control period, data from the two modified saline infusion methods were combined with the moderate rate volume expansion group. For the K infusion period, clearance results from the 1.0/6.0 rats were analyzed with the high rate volume expansion group whereas results from the 1.0/0.3 group were combined with the moderate volume expansion group.

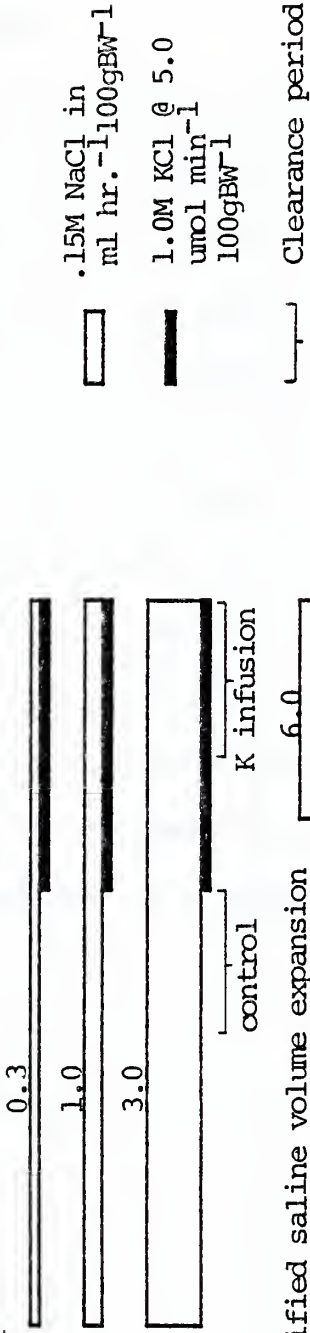
Method II. Prolonged K infusion with graded saline volume expansion

These experiments lasted a total of 8.5 hours. For the first 4.5 hours, isotonic saline was infused at a rate of 0.3 ml/hour/100gBW, advanced to 2.0 for the next two hours, and finally increased to 6.0 for the last two hours. A 1.0M KCl solution infusion @ 5.0  $\mu\text{mol}/\text{min}/100\text{gBW}$  was started at the beginning of the third hour of saline loading and continued for 6.5 hours. Three clearance periods were established: u(1) 2-2.5 hours, u(2) 4-4.5 hours, and u(3) 6-6.5 hours after the start of the K infusion.

The isotonic saline and KCl infusion schedules for Methods I and II are shown in Figure I.3. At the midpoint of each clearance period, blood samples were taken for plasma electrolyte determinations and C-14 inulin radioactive counts.



Method I: Low, moderate, and high rate saline volume expansion with K infusion



Method I: Modified saline volume expansion

Method II: Prolonged K infusion with graded saline volume expansion

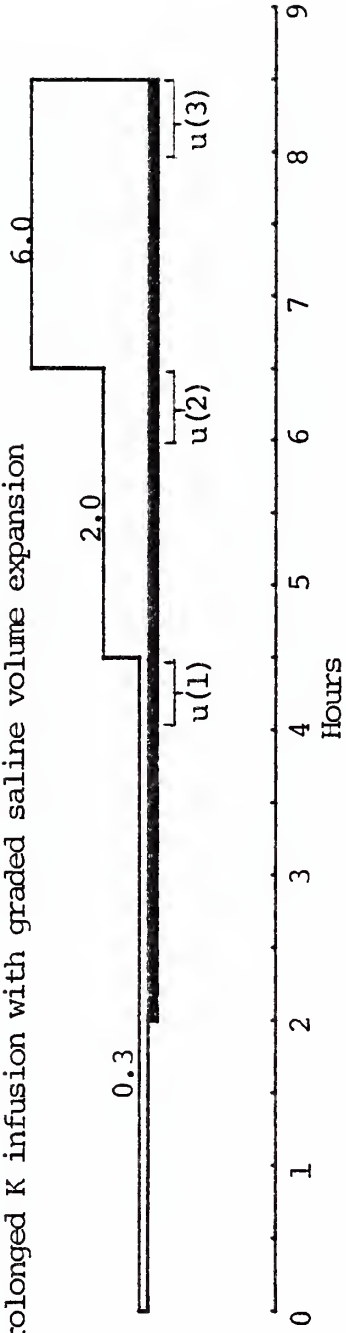


Figure I.3 Saline and potassium loading schedules for Methods I and II.



## Analysis

Sodium and potassium concentrations in urine and plasma were measured by standard laboratory techniques on a flame spectrophotometer (Model 142, Instrumentation Laboratory). For plasma electrolytes, two blood samples were taken at the midpoint of each clearance period and the results averaged. Urine volumes were determined by weighing. For inulin clearance determinations, radioactive counting of C-14 inulin was performed in a liquid scintillation counter (Mark I, Searle) using a gel suspension of sample material mixed with Aquasol (New England Nuclear). Sample counts were at least ten times greater than background counts, and total counts were adequate to establish a minimum 2% accuracy. All urine flow rate, potassium excretion, sodium excretion and GFR results cited in the text represent values normalized to 100g body weight. Statistical analysis of the experimental results utilized Student's t-test.



## RESULTS

### A. Effects of K infusion in normal diet and High-K diet rats: LMH-VE

Clearance data from the low, moderate, and high rate saline volume expansion (LMH-VE) experiments is summarized in Table I.1. Because results for the low and moderate rate volume expansion groups generally were not significantly different, these two groups were combined (LM-VE). Table I.1 is organized in order to facilitate the comparison between the LM-VE and H-VE groups for the control and K infusion periods separately. Presented in Table I.2 are the calculated changes in GFR, plasma K, urine flow, and absolute and fractional excretion rates of Na and K that occurred between the control and K infusion period. The results from experiments in the normal diet group are compared separately from those of the High-K group. Inter-diet group analyses will be deferred until later sections.

#### 1) Normal diet group

The effect of the different saline infusion rates on urine flow and sodium excretion during the control clearance period is substantial, with  $V_u$  averaging only  $1.0 \pm 0.17$  ul/min in the LM-VE group and  $23.24 \pm 5.50$  in the H-VE group. Sodium excretion was elevated by high rate saline volume expansion to a similar degree. Although H-VE produced a brisk saliuresis compared to LM-VE, the GFR was not significantly different.

Plasma K and Na concentrations during the control period did not differ significantly between LM-VE and H-VE animals. However, the





Table I.1 Effects of K infusion in normal and High-K diet rats, LMH-VE

	n =	N O R M A L D I E T				H I G H - K D I E T			
		Control		K infusion		Control		K infusion	
		$\frac{LM-VE}{H-VE}$	$\frac{H-VE}{H-VE}$	$\frac{LM-VE}{H-VE}$	$\frac{H-VE}{H-VE}$	$\frac{LM-VE}{H-VE}$	$\frac{H-VE}{H-VE}$	$\frac{LM-VE}{H-VE}$	$\frac{H-VE}{H-VE}$
$K_p$	9	3.82 ±.18	3.75 ±.12	6.40 ±.27	5.47** ±.06	3.11 ±.19	2.50* ±.12	4.49 ±.20	4.60** ±.15
$Na_p$	6	149.2 ±.7	150.5 ±.7	149.3 ±1.2	150.3 ±.7	151.0 ±.9	149.6 ±.9	151.8 ±1.5	150.1 ±.4
$E_K$	6	0.122 ±.021	0.442*** ±.079	1.719 ±.218	2.185* ±.058	0.432 ±.127	0.892** ±.070	1.177 ±.199	2.003*** ±.060
FEK	8	7.0 ±.9	21.6*** ±2.6	56.6 ±8.2	72.1 ±3.7	34.5 ±8.9	62.6* ±5.6	54.3 ±7.6	84.0** ±4.6
$E_{Na}$	8	0.140 ±.047	3.278*** ±.760	0.642 ±.234	4.533*** ±.535	0.287 ±.100	2.003*** ±.292	0.387 ±.135	3.317*** ±.046
FFeNa	9	0.17 ±.05	3.84*** ±.40	0.89 ±.31	5.36*** ±.53	0.48 ±.17	2.40** ±.39	0.49 ±.15	3.27*** ±.33
GFR	9	0.459 ±.041	0.529 ±.045	0.487 ±.015	0.562* ±.025	0.396 ±.038	0.580*** ±.017	0.476 ±.032	0.674*** ±.011
$V_u$	9	1.00 ±.17	23.24*** ±5.50	7.17 ±.41	27.35*** ±2.37	2.25 ±.79	15.23** ±2.43	3.49 ±.67	22.17*** ±2.87

Differences in mean values between LM-VE and H-VE, when statistically significant, indicated by \*p < .05, \*\*p < .01, \*\*\*p < .001

$K_p$ ,  $Na_p$  mmol/L;  $E_K$ ,  $E_{Na}$   $\mu$ mol  $min^{-1}100gBW^{-1}$ ; FEK, FFeNa %;  $V_u$   $\mu$ l  $min^{-1}100gBW^{-1}$ ; GFR  $ml\ min^{-1}100gBW^{-1}$



Table I.2 Changes in mean clearance values between control and K infusion period for normal and High-K diet rats, LMI-VE

	$\frac{\Delta^K p}{}$	$\frac{\Delta^E k}{}$	$\frac{\Delta^{FEK}}{}$	$\frac{\Delta^E Na}{}$	$\frac{\Delta^{FENa}}{}$	$\frac{\Delta^{GFR}}{}$	$\frac{\Delta^V u}{}$
<u>Normal diet</u>							
IM-VE	+2.58 <sup>***</sup>	+1.597 <sup>***</sup>	+49.6 <sup>***</sup>	+0.502 <sup>*</sup>	+0.72 <sup>*</sup>	+0.028	+6.17 <sup>***</sup>
H-VE	+1.72 <sup>***</sup>	+1.743 <sup>***</sup>	+50.5 <sup>***</sup>	+1.255	+1.52	+0.033	+4.11
<u>High-K diet</u>							
IM-VE	+1.38 <sup>**</sup>	+0.745 <sup>*</sup>	+19.8	+0.100	+0.01	+0.080	+1.24
H-VE	+1.10 <sup>***</sup>	+1.111 <sup>***</sup>	+21.4 <sup>**</sup>	+1.314 <sup>*</sup>	+0.87	+0.094 <sup>***</sup>	+6.94

Changes which were statistically significant are indicated by: \*p < .05, \*\*p < .01, \*\*\*p < .001. Units for variables are given in Table I.1.



high rate of saline loading resulted in a nearly four-fold difference in K excretion:  $0.122 \pm 0.021$  vs.  $0.442 \pm 0.079$   $\mu\text{mol}/\text{min}$  for LM-VE and H-VE rats respectively ( $p < .001$ ). Fractional K excretion rates also differed significantly ( $p < .001$ ),  $7.0\% \pm 0.9$  vs.  $21.6\% \pm 2.6$ .

After the infusion of KCl at  $5.0 \mu\text{mol}/\text{min}/100\text{gBW}$ , mean plasma K concentration rose in the LM-VE group to  $6.40 \text{ mmol}/\text{l}$  ( $\Delta K_p = +2.58$ ) and to  $5.47 \text{ mmol}/\text{l}$  in the H-VE rats ( $\Delta K_p = +1.72 \text{ mmol}/\text{l}$ ). The  $\Delta K_p$ 's were significant ( $p < .001$ ). K excretion was augmented dramatically in both groups, though proportionally more so among LM-VE rats. The H-VE rats continued to demonstrate significantly higher rates of K excretion than LM-VE rats,  $2.184 \pm 0.058$  vs.  $1.719 \pm 0.218$   $\mu\text{mol}/\text{min}$  ( $p < .05$ ). The H-VE group attained this higher rate of kaliuresis in spite of a significantly lower plasma K ( $p < .01$ ). Assuming that K excretion per kidney would have to equal approximately  $2.5 \mu\text{mol}/\text{min}$  to offset the K infusion rate of  $5.0 \mu\text{mol}/\text{min}$ , neither group achieved this level of K excretion proficiency. However, all rats survived the K infusion.

Plasma Na concentrations were not changed significantly in either group following K infusion, but Na excretion rose significantly ( $p < .05$ ) in the LM-VE group as did urinary flow rate ( $p < .001$ ). A tendency towards a higher rate of saliuresis with K infusion was also noted in the H-VE group, though statistical significance was not achieved. Clearly for this group, saline loading and not KCl infusion was the predominant saliuretic stimulus. GFR showed a slight tendency to increase with K infusion in both groups, but this change was not significant.



2) High-K diet group

In most respects, the clearance data from the High-K diet rats paralleled the results from the normal diet group. Of particular note, however, is that the plasma K concentration during the control period was somewhat low in the LM-VE group,  $3.11 \pm 0.19$  mmol/l and decidedly low in the H-VE group,  $2.50 \pm 0.12$  mmol/l. With K infusion, mean plasma K rose to 4.49 mmol/l in the LM-VE rats ( $\Delta K_p = +1.48$ ) and to 3.60 mmol/l in the H-VE group ( $\Delta K_p = +1.10$ ). The  $\Delta K_p$  was significant in both instances. Absolute and fractional K excretion rates were significantly higher among H-VE animals compared to the LM-VE group, both before and during K infusion. The balance of the clearance data reveals responses to the various experimental interventions qualitatively similar to those found in the normal diet group.

B. Potassium excretion in relation to urine flow rate and Na excretion:  
LMH-VE

Early in the course of the experiments, it became clear that for a given rate of volume expansion, rats would manifest considerable variability in rates of diuresis and K excretion. However, such data when plotted as  $E_K$  vs.  $E_{Na}$  or  $E_K$  vs.  $V_u$  revealed a fairly predictable, characteristic relationship among the variables. Accordingly, the experimental results for individual rats have been organized and graphed in this manner. Since it is not the purpose of this study to define separately the effect on K excretion of an induced sodium or volume diuresis, the results are presented utilizing both parameters as independent variables. It should be noted, however, that  $E_{Na}$  and  $V_u$  varied together





in a predictable fashion irrespective of the experimental intervention. This finding is demonstrated in Figure I.4.

In the plot of  $E_{Na}$  vs.  $V_u$  shown in Figure I.4, the X and Y axes have been assigned arbitrarily to  $V_u$  and  $E_{Na}$  respectively. Data is taken from normal and High-K diet rats for both control and K infusion periods and for all rates of volume expansion. The results from the prolonged K infusion experiments to be discussed later are also plotted. The data points appear to approximate a linear relationship between Na excretion and urine flow rate. There is no obvious distribution of data points that suggests a different  $E_{Na}$  vs.  $V_u$  correlation among the different diet groups or between control and K-infused rats. While a linear regression line might conveniently be fitted to the data, this would impart more significance to the results than intended. It is sufficient to note by inspection that  $E_{Na}$  and  $V_u$  are co-variables that change together in a fairly predictable way. Therefore, K excretion data, when plotted against one or the other variable, is not likely to yield significantly different plots.

1) Control period

Shown in Figure I.5a is a plot of K excretion vs. urine flow rate for normal and High-K diet rats during the control period, with data drawn from all three volume expansion rates. A curve representing an "eyeball" estimate of a "best fit" line has been drawn through the data points for each diet group. This curve fitting method was also employed on all  $E_K$  vs.  $V_u$  and  $E_K$  vs.  $E_{Na}$  data plots in later sections.



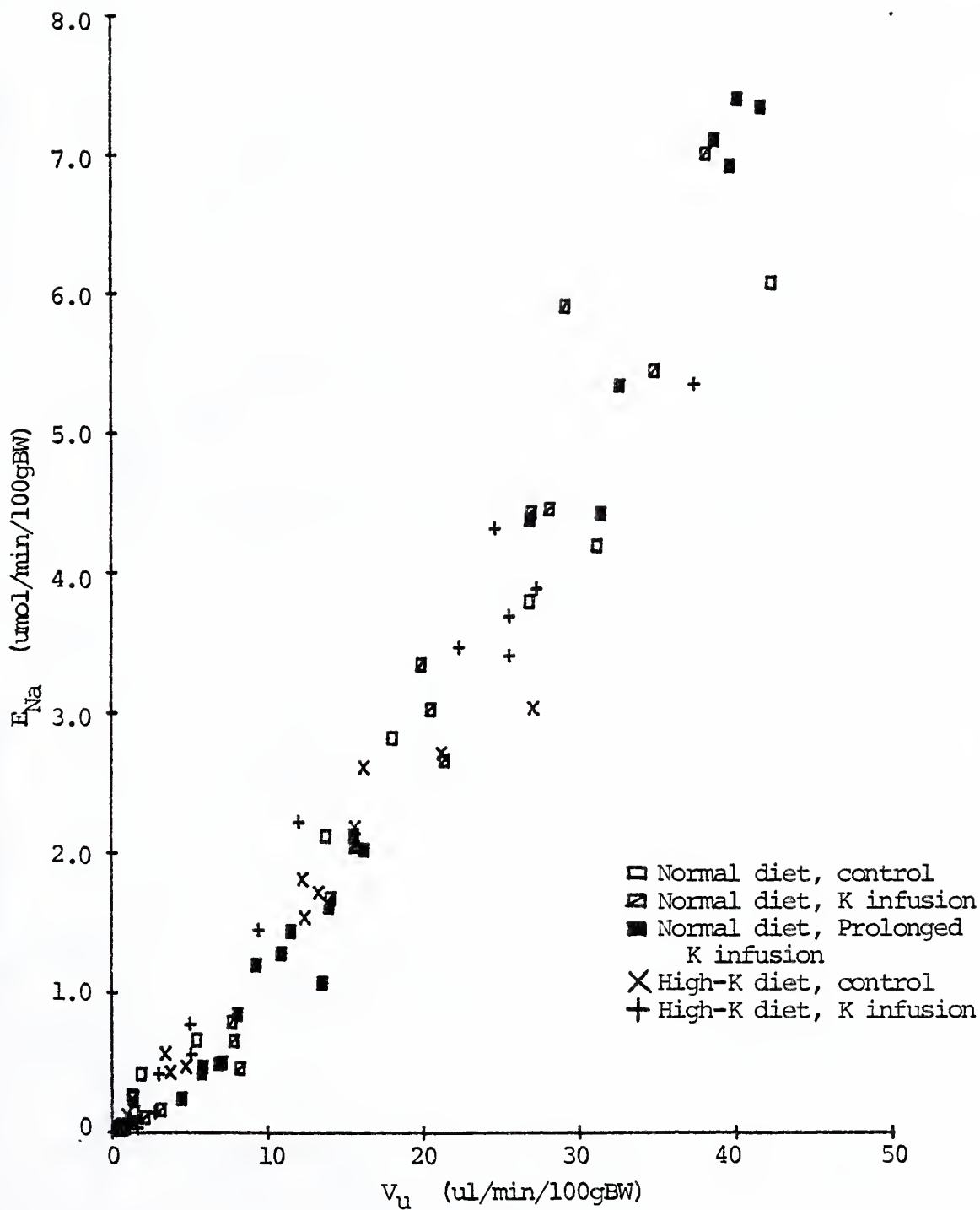


Figure I.4 Sodium excretion plotted as a function of urine flow rate. Data include all rats in LMH-VE and prolonged K infusion experiments.



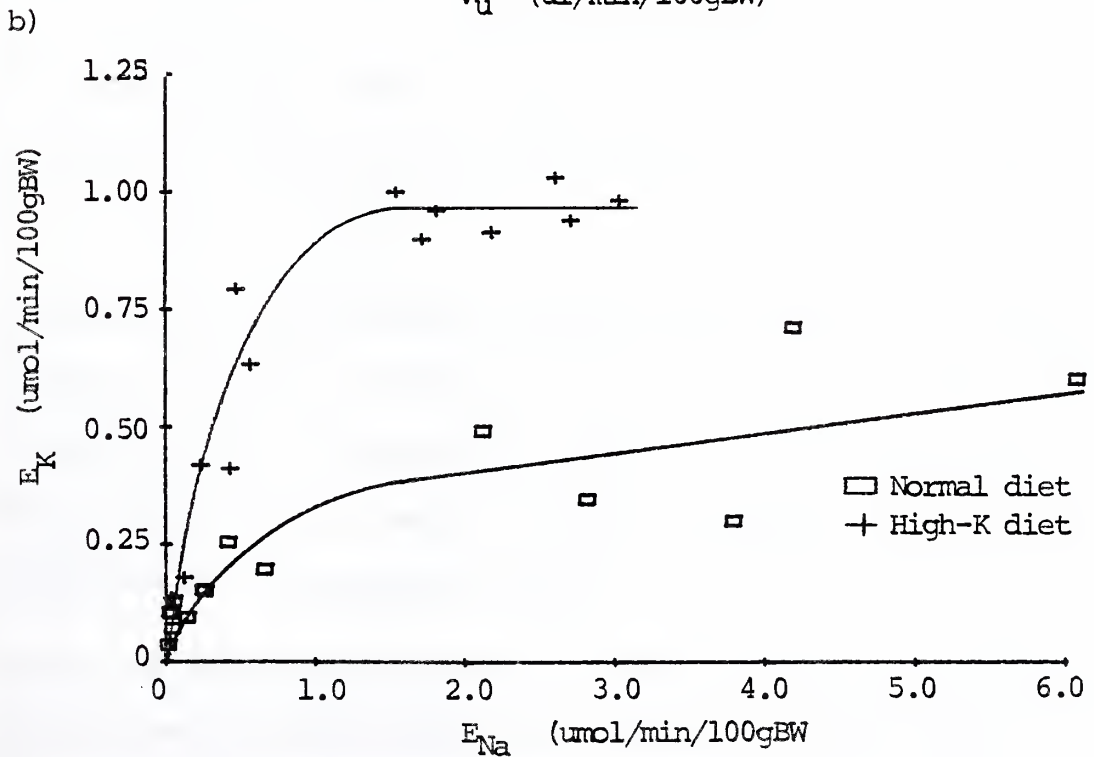
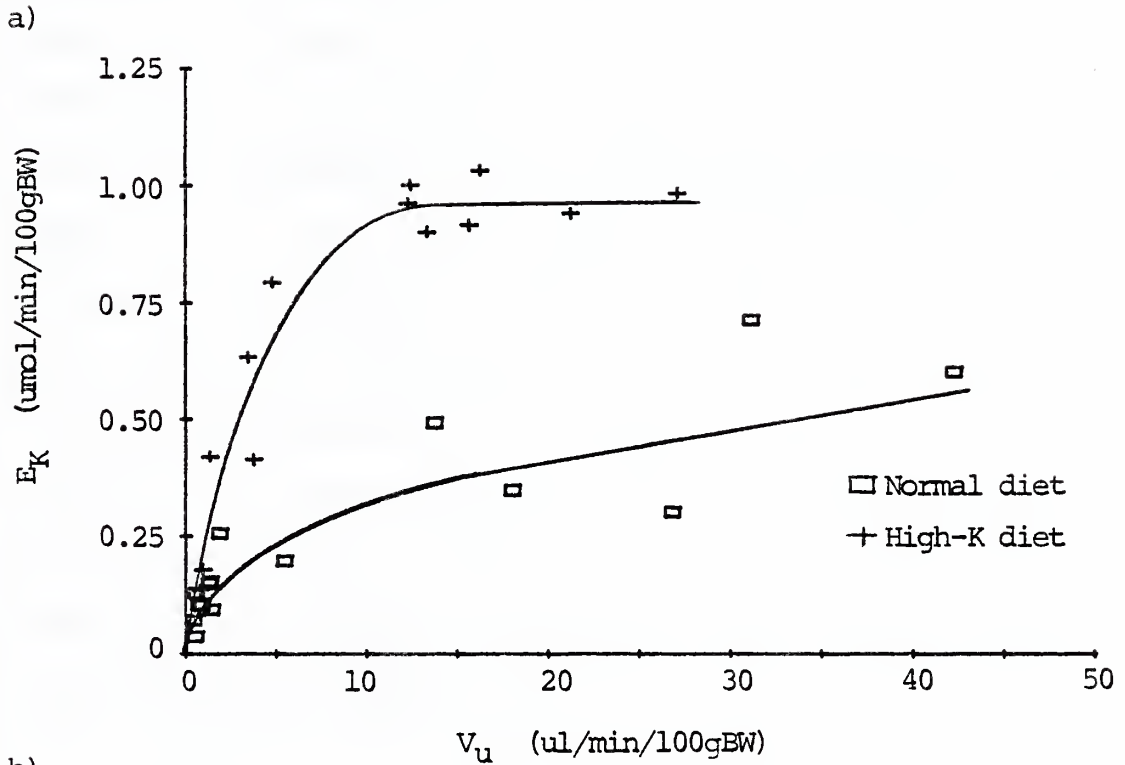


Figure I.5 Potassium excretion plotted as a function of flow rate (a) and sodium excretion (b) for normal and High-K diet rats during control period of LMH-VE.



The trend for K excretion to increase with flow rate is apparent in Figure I.5a, although the normal diet rats showed considerably less predictability in the relationship between  $E_K$  and  $V_u$  at higher urine flow rates. Nonetheless, it can be appreciated that High-K animals excreted K at a rate exceeding that of normal diet rats for all but the lowest urine flow rates. Furthermore, among the High-K rats, animals excreting K in the range of 0.8 to 1.0  $\mu\text{mol}/\text{min}$  had urine flow rates ranging from 12 to 28  $\mu\text{l}/\text{min}$ . Thus a more than two-fold increase in urine flow rate did not significantly alter K excretion. Among normal diet rats, the data in the higher urine flow rate range is quite variable, although the trend appears to be towards a modest elevation of potassium excretion with  $V_u$ .

The K excretion vs. Na excretion plot shown in Figure I.5b is similar in all respects. For the High-K rats, K excretion relatively stabilized for sodium excretion rates greater than 1.5  $\mu\text{mol}/\text{min}$ .

## 2) K infusion period

Data from the clearance period between one and two hours following K infusion is plotted in Figures I.6a and I.6b. A rising rate of kaliuresis with urine flow and sodium excretion is now clearly evident over the low urine flow and sodium excretion rate ranges. Additionally, the graph reveals two important findings.

First, the data from the normal and High-K animals plot in similar manner, and the two diet groups cannot be clearly differentiated based on their K excretion, Na excretion, and flow rate results. Secondly,  $E_K$  appears to rise to a maximum rate which is encountered at moderately high





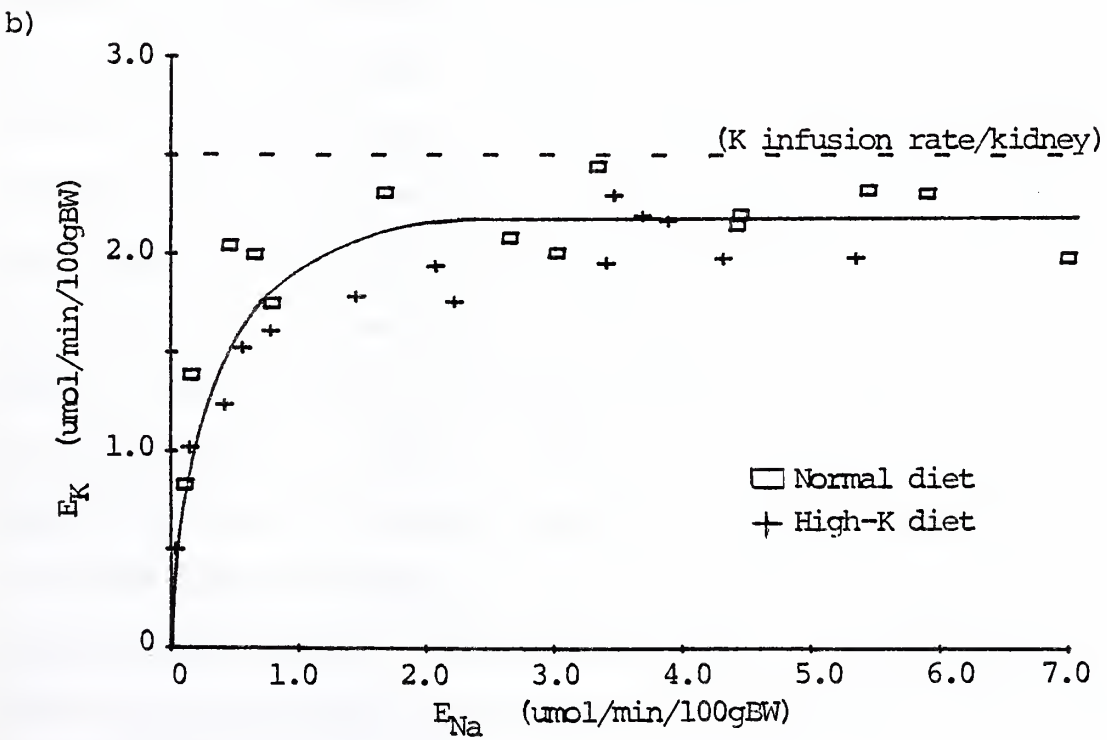
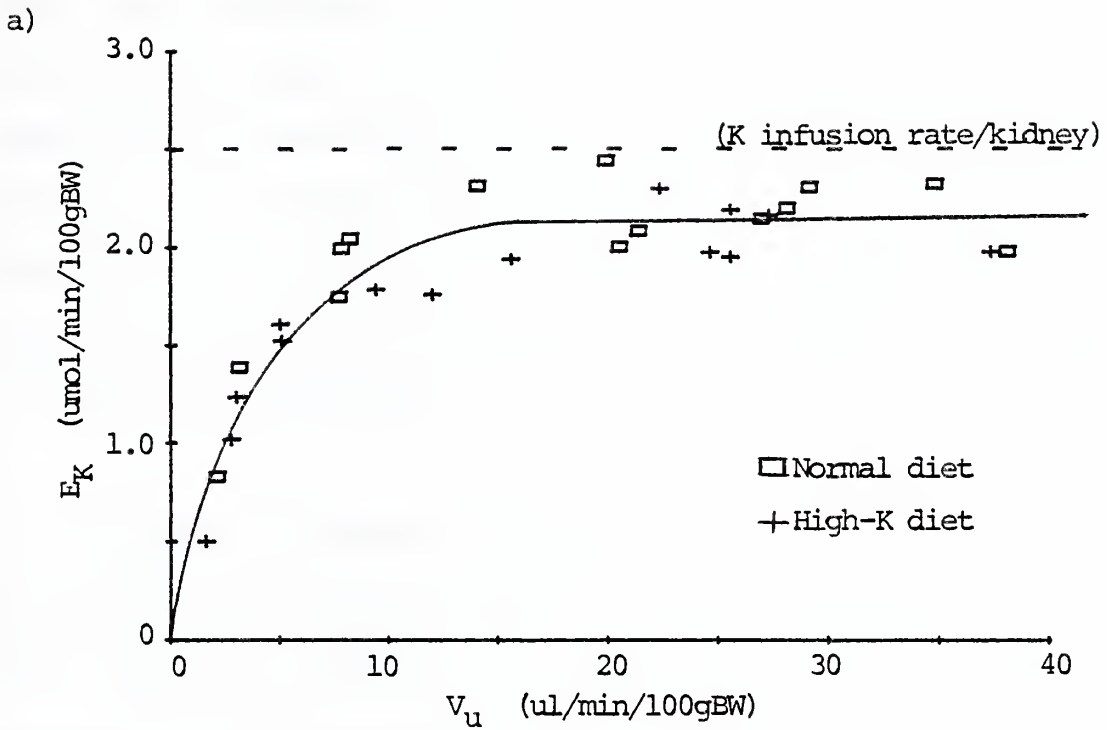


Figure I.6 Potassium excretion plotted as a function of urine flow rate (a) and sodium excretion (b) for normal and High-K diet rats following K infusion during LMH-VE.



rates of  $V_u$  and  $E_{Na}$ . This apparent K excretory plateau lies between 2.0 and 2.5  $\mu\text{mol}/\text{min}$ , somewhat less than the K infusion rate of 2.5  $\mu\text{mol}/\text{min}/\text{kidney}$ . Potassium excretion for normal and High-K diet rats was fixed within this range for urine flow rates exceeding 20  $\mu\text{l}/\text{min}$  and for sodium excretion rates greater than 2.5  $\mu\text{mol}/\text{min}$ . This relatively constant rate of K excretion was maintained up to the highest rates of urine flow and sodium excretion recorded, 38.1  $\mu\text{l}/\text{min}$  and 7.0  $\mu\text{mol}/\text{min}$  respectively.

### C. Prolonged K infusion experiments

In order to study the effect that prolonging the duration of K infusion would have on the rate of K excretion in a manner that would yield results that could be compared with the finding of an apparent K excretory plateau in the LMH-VE expansion experiments, it was necessary to devise an appropriate saline loading schedule. If a low rate saline infusion were given throughout, K excretion would not be augmented sufficiently to preclude a toxic plasma K concentration rise. On the other hand, a continuous high rate of saline loading would be anticipated to induce a rate of kaliuresis sufficiently great that by the end of the prolonged K infusion, plasma K concentrations conceivably would be returned well towards normal. Accordingly, a graded schedule of saline loading was employed with the objective of achieving an approximately stable plasma K concentration from the first through the third urine collection periods. After some trial experiments, the following protocol, briefly summarized from the Methods section, was used.



An isotonic saline infusion was progressively advanced from 0.3 to 1.0 to 6.0 ml/hr/100gBW over an 8.5 hour period. K infusion at the same rate as in the LMH-VE groups (5.0  $\mu\text{mol}/\text{min}/100\text{gBW}$ ) was initiated at the end of the second hour and continued for 6.5 hours. Clearance measurements during K infusion were made for each saline loading rate. Thus each rat experiment yielded three data points on an  $E_K$  vs.  $V_u$  or  $E_K$  vs.  $E_{Na}$  graph. Figure I.3 summarizes the saline and K infusion methods.

1) Normal diet rats

The results from the three clearance periods, u(1), u(2), and u(3) are summarized in Table I.3, and the  $E_K$  vs.  $V_u$  and  $E_K$  vs.  $E_{Na}$  plots are presented in Figures I.7 and I.8. For comparison purposes, the results from the K infusion period (1-2 hours after K infusion) of the LMH-VE experiments are also plotted.

Looking first at the plots,  $E_K$  again rose with  $V_u$  and  $E_{Na}$  and by u(2) the K excretion rate for most rats exceeded the highest rates found among normal and High-K diet animals in the LMH-VE groups. Moreover, by u(2), most rats excreted K at a rate faster than the K infusion rate per kidney.

Examining the data from Table I.3, several points are noteworthy among the otherwise predictable changes that occurred from the first to the third clearance period. Plasma K concentration peaked during u(2) at  $6.84 \pm 0.14$  mmol/l and declined in u(3) to the same mean plasma concentration recorded during u(1), 6.35 mmol/l. The mean K excretion rate rose from 1.781 to 2.833 to 3.393  $\mu\text{mol}/\text{min}$  from u(1)



Table I.3 Clearance results from prolonged K infusion with graded saline volume expansion

	$K_p$	$Na_p$	$E_K$	FEK	$E_{Na}$	FENa	GFR	$V_u$
u(1) n=7	6.35 ±.13	151.9 ±.5	1.781 ±.213	52.2 ±5.9	0.436 ±.091	0.53 ±.10	0.535 ±.021	5.63 ±.82
u(2) n=8	6.84* ±.14	154.7*** ±.8	2.833*** ±.113	77.8** ±3.5	1.599*** ±.148	1.97*** ±.19	0.532 ±.023	13.30*** ±.90
u(3) n=7	6.35* ±.10	154.7 ±.10	3.393** ±.090	94.3* ±5.3	6.128*** ±5.18	6.87*** ±.46	0.576 ±.028	35.85*** ±2.10

Statistical significance indicated for differences in mean values between u(1) and u(2) and between u(2) and u(3): \*p < .05, \*\*p < .01, \*\*\*p < .001. Units for variables are given in Table I.1.





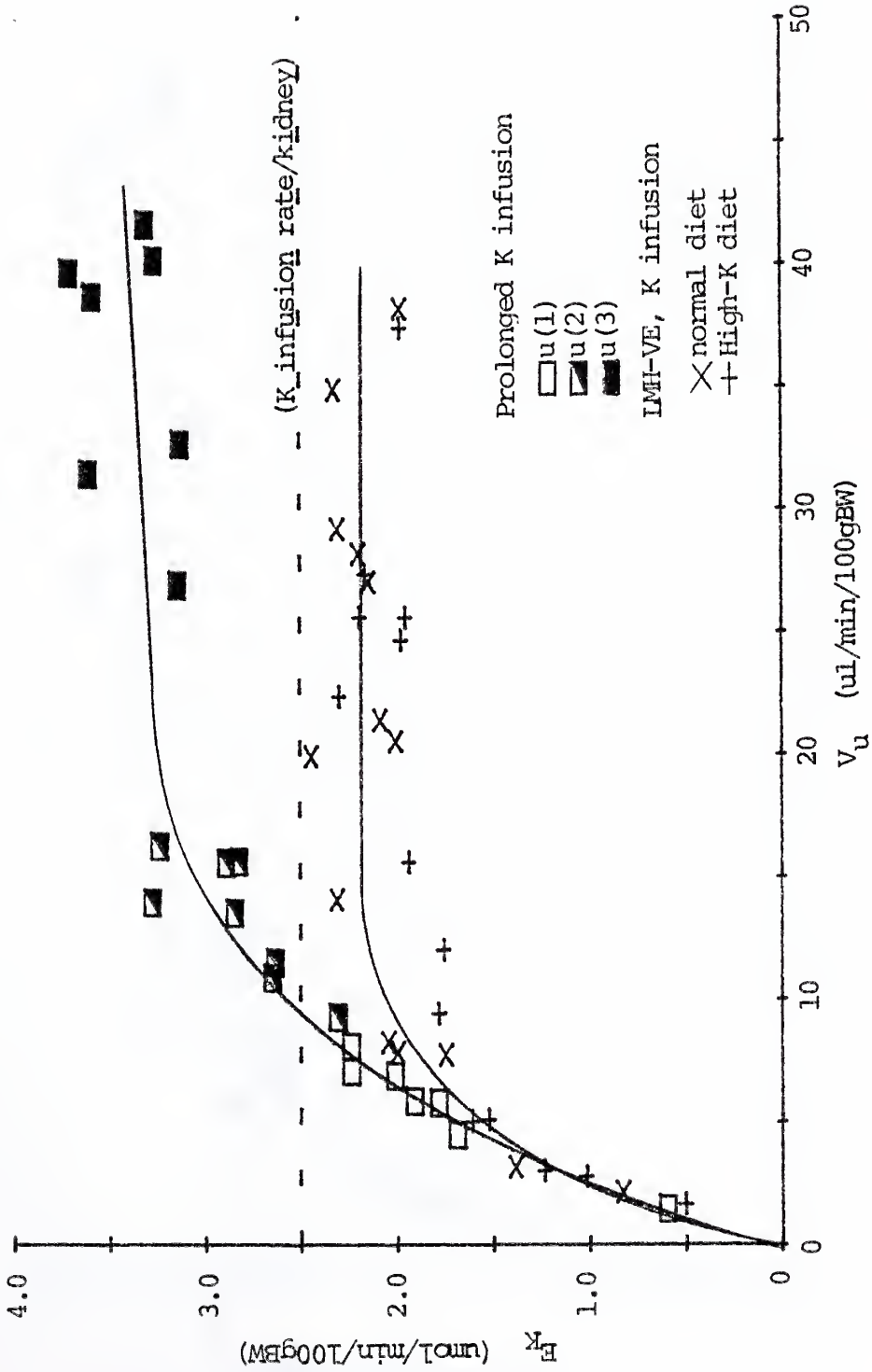


Figure I.7 Potassium excretion plotted as a function of urine flow rate during prolonged K infusion, u(1), u(2), and u(3), and during K infusion period of IMH-VE for normal and High-K diet rats.



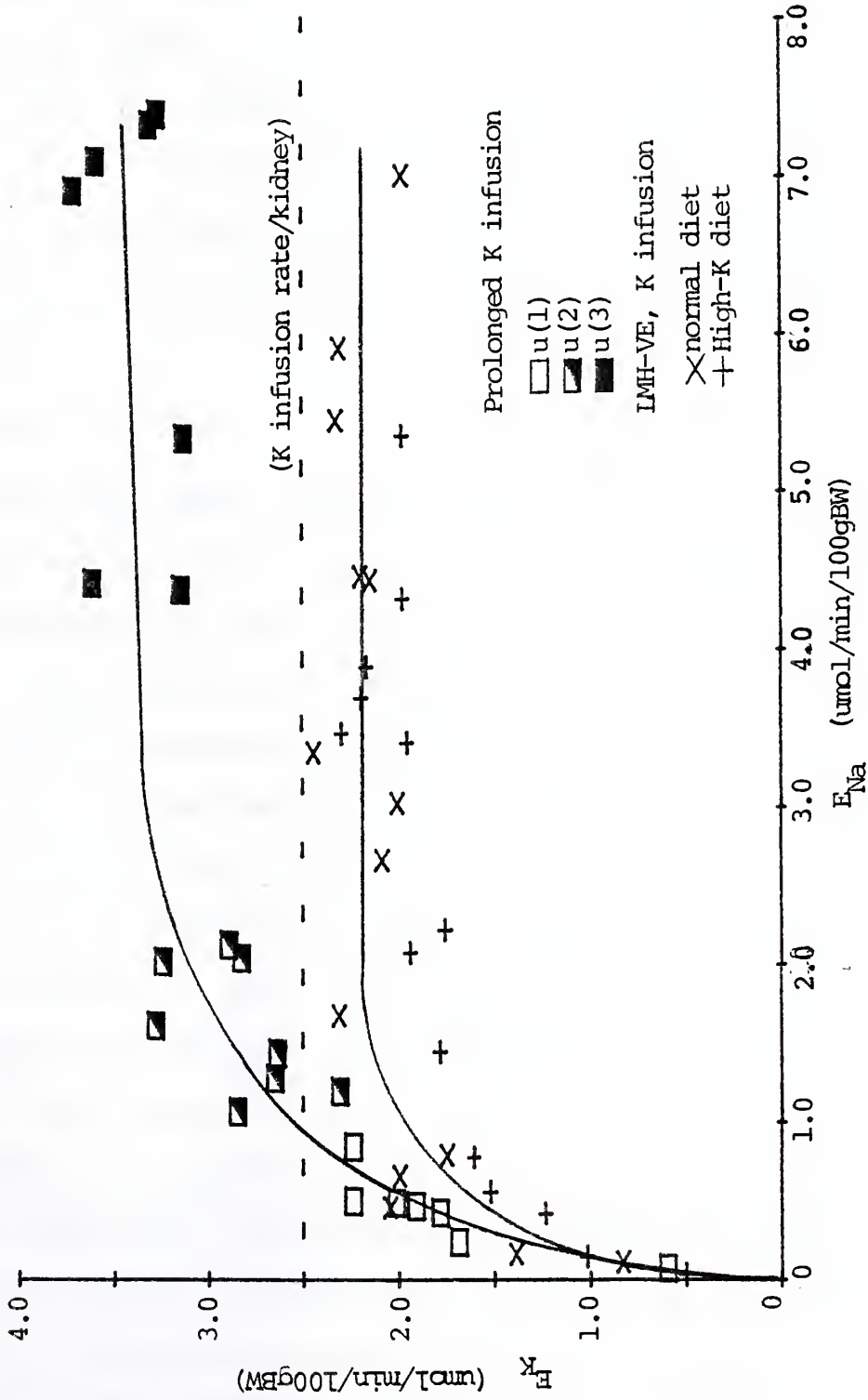


Figure I.8 Potassium excretion plotted as a function of sodium excretion during prolonged K infusion, u(1), u(2), and u(3), and during K infusion period of LMH-VE for normal and High-K diet rats.

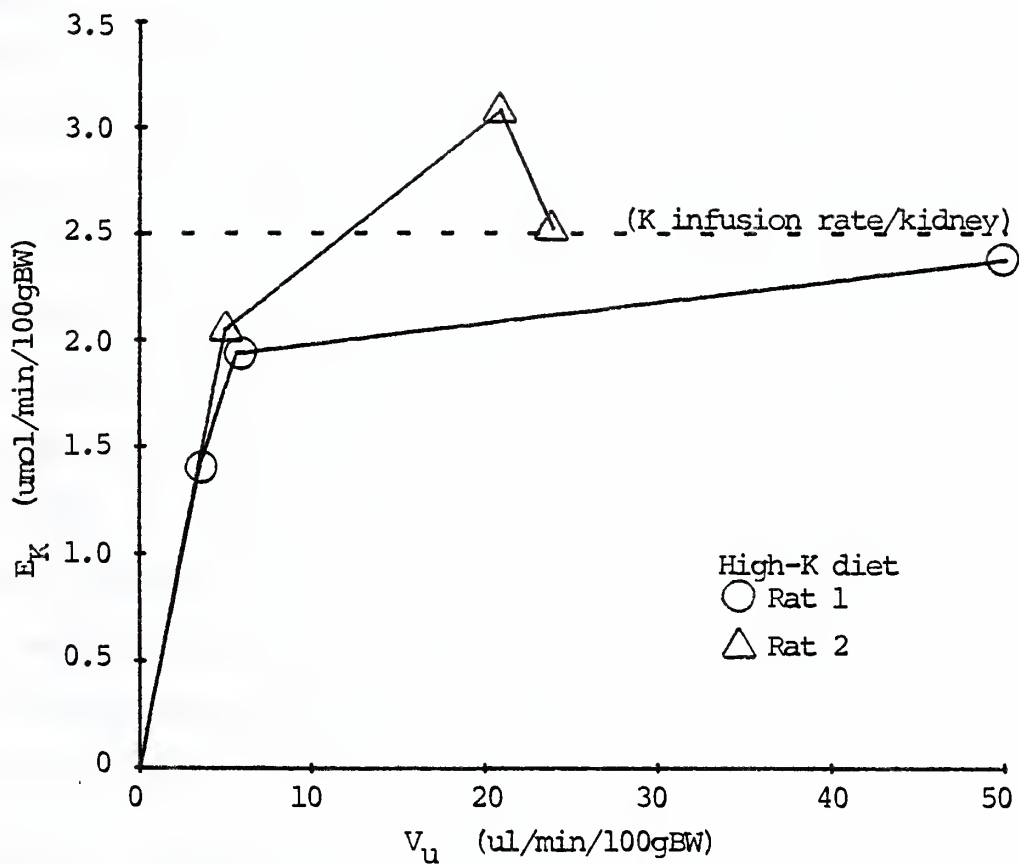


to u(3) and mean fractional K excretion rates similarly progressed from 52.2% to 77.8% to 94.3% by u(3). The changes in the K clearance parameters were all significant. Na excretion rose predictably as the saline loading was progressively augmented, reaching a mean of  $6.158 \pm 0.518$   $\mu\text{mol}/\text{min}$  by the third collection period. In spite of the long period of volume expansion, GFR was stable between u(1) and u(2) and rose modestly but not significantly between u(2) and u(3).

## 2) High-K diet rats

For reasons which remain unexplained, High-K rats had a very varied diuretic response to the prolonged saline and K loading, some animals exhibiting relatively low rates of urine flow and sodium excretion in spite of high rates of volume expansion. Among five High-K animals, three failed to develop urine flow rates greater than 12  $\mu\text{l}/\text{min}$  by u(3), which contrasts markedly with the normal diet group in which urine flow rate averaged 35.85  $\mu\text{l}/\text{min}$  during u(3). The High-K animals were noticeably water logged. No apparent problems were noted in blood pressure or GFR. Since it was not possible to reliably generate high urine flow rates, these experiments were abandoned. Data results from the two High-K diet rats whose urine flow rates did progress more or less appropriately with the graded volume expansion are shown in Figure I.9. Also indicated on the graphs are plasma K concentrations for each clearance period. During u(3), both High-K rats had K excretion rates less than that for any normal diet rat. However, by u(3), plasma K concentration was virtually normal for each High-K rat, and K excretion approximately matched the K infusion rate.





	<u>Plasma K (mmol/l)</u>		
	u(1)	u(2)	u(3)
Rat 1	5.18	5.08	4.14
Rat 2	3.45	3.59	4.57

Figure I.9 Potassium excretion as a function of urine flow rate for two High-K diet rats during prolonged K infusion. For each rat data points are plotted successively for u(1), u(2), and u(3).





3) Estimated potassium balance during the prolonged K infusion:  
normal diet group

Since the K load infused over the 6.5 hour represents an amount approximately equivalent to 50% of total body K content (assuming K body stores equal to 40 mmol/kgBW), it will be useful to assess K balance over this period of time. Shown in Figure I.10a is a plot of K excretion vs. time for the normal diet group. The midpoint of each clearance period, 2.25, 4.25, and 6.25 hours for  $u(1)$ ,  $u(2)$ , and  $u(3)$  respectively is assigned to the time axis. The mean K excretion rate for each clearance period  $\pm$  SEM is plotted against the Y axis. The K excretion rate shown at zero hour, the start of K infusion, represents the value measured for K excretion during the control period of the low rate volume expansion experiments discussed in the previous sections in which the saline infusion rate was also 0.3 ml/hr/100gBW.

In order to roughly calculate cumulative K excretion over the 6.5 hours, the four data points have been connected. The area under the line from zero to any future time following K infusion provides an estimate of cumulative K excretion,  $E_K^C$ , up to that point. The results of this integration, manually performed, are shown in Figure I.10b. On the same graph, a rising straight line is drawn indicating the cumulative amount of infused K "per kidney" ( $K_{in}^C$ ) as a function of time, on the assumption that each kidney excretes one-half of the infused K load. Finally, the cumulative net K balance ( $K_{in}^C - E_K^C$ ) over time is shown by the dashed line.



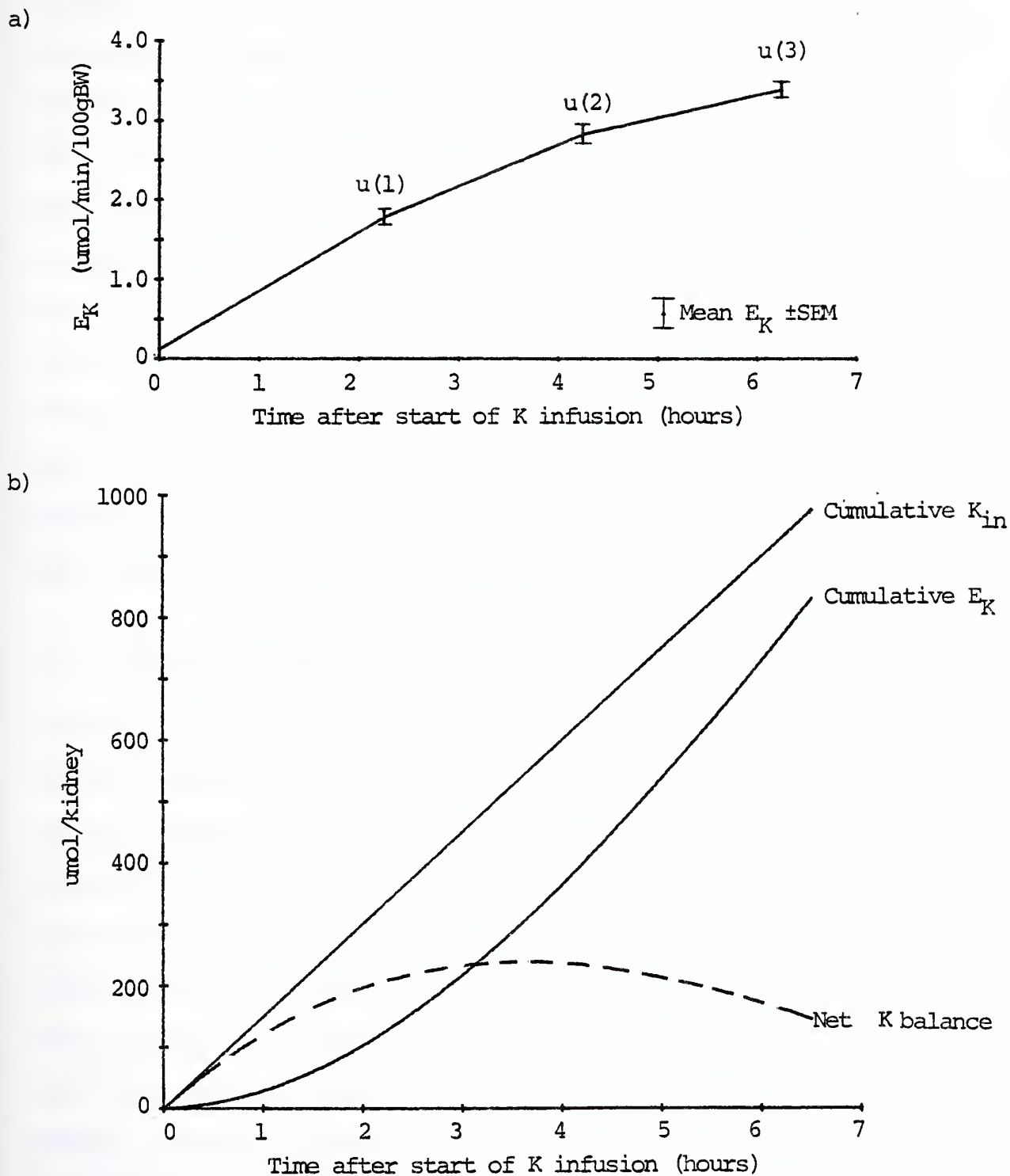


Figure I.10 a)  $E_K$  as a function of time for prolonged K infusion.  
b) Potassium balance over time in prolonged K infusion experiments. See text for explanation of plots.



After 6.5 hours of K infusion, it is clear that the rats were well on their way towards eliminating the positive K balance accumulated earlier. Net positive K balance peaked in the neighborhood of the u(2) clearance period (approximately +225  $\mu\text{mol}/\text{kidney}$ ) at a time when the mean plasma K concentration was also highest among the three clearance periods. By the end of u(3), the positive K balance had been reduced to an estimated +140  $\mu\text{mol}/\text{kidney}$ . To linearly extrapolate the line beyond 6.5 hours would be unwarranted since the falling plasma K concentration would probably have a moderating influence on the rate of potassium excretion. Thus the prolonged K infusion challenge appears to have been effectively met by normal diet rats. No rats died during the course of the experiments.

#### D. K excretory plateau

The results from the K infusion period in the LMH-VE experiments not only demonstrate the apparent existence of a K excretory plateau but also suggest that the magnitude of the plateau may not differ between normal and High-K diet rats. In order to analyze this possibility more rigorously, it will be useful to compare clearance data from the two diet groups for rats which excreted K at the plateau level. An inspection of Figure I.6a indicates that potassium excretion relatively stabilized when urine flow rate exceeded 20  $\mu\text{l}/\text{min}$  for rats in both diet groups. A comparison between the two diet groups will therefore rely on data collected from these rats.

The clearance results for the seven normal diet and six High-K diet rats which excreted K at the plateau level during K infusion is summarized



in Table I.4. The outstanding point differentiating the two groups is the plasma K concentration which was  $3.50 \pm 0.09$  and  $5.47 \pm 0.07$  mmol/l for the High-K and normal diet rats respectively, a difference that is statistically significant ( $p < .001$ ). The mean K excretion rate was virtually the same for both groups: High-K,  $2.092 \pm 0.058$  umol/min and normal diet,  $2.148 \pm 0.052$  umol/min, a difference that is not statistically significant ( $p > .4$ ). The mean fractional K excretion rate for the High-K group was significantly higher ( $p < .01$ ) than the normal diet group, 88.5% vs. 69.3%, reflecting the lower plasma K concentration among the High-K rats. Renal sodium handling was similar for the two groups as was urine flow rate.

These findings for the K infusion period contrast with the results from the control period. Since a K excretory plateau was not definitely demonstrated among the normal diet rats, it is perhaps most useful to compare the results for the two diet groups in the high rate volume expansion experiment. The comparative data is shown in Table I.4. The High-K rats clearly distinguished themselves from the normal diet group by excreting K at a rate nearly twice as great,  $0.892 \pm .079$  vs.  $0.442 \pm .070$  umol/min, in spite of a significantly lower ( $p < .001$ ) plasma K concentration. Accordingly, the fractional K excretion rate for the High-K group was nearly three times greater than normal diet rats. All differences in potassium clearance values were statistically significant. Mean urine flow and sodium excretion rate were lower for the High-K group so these factors would not account for the higher rate of kaliuresis demonstrated by High-K rats.





Table I.4 Maximum K excretion rates for normal and High-K diet rats during control and K infusion periods of LMH-VE

	$\frac{K_p}{p}$	$\frac{Na_p}{p}$	$\frac{E_K}{K}$	$\frac{FEK}{K}$	$\frac{F_{Na}}{Na}$	$\frac{FENa}{Na}$	$\frac{GFR}{ml}$	$\frac{V_u}{ml}$
Control, H-VE normal diet (n=6)	3.75 ±.12	150.5 ±.7	0.442 ±.079	21.6 ±2.6	3.278 ±.760	3.84 ±.40	0.529 ±.045	23.24 ±5.50
High-K diet (n=8)	2.50*** ±.12	149.6 ±.9	0.892** ±.070	62.6*** ±5.6	2.003 ±.292	2.41 ±.39	0.580 ±.017	15.18 ±2.46
K infusion, H-VE normal diet (n=7)	5.47 ±.07	150.7 ±.7	2.148 ±.052	69.3 ±2.8	4.702 ±.586	5.46 ±.60	0.572 ±.027	28.41 ±2.44
High-K diet (n=6)	3.50*** ±.09	150.5 ±.3	2.092 ±.058	88.5** ±4.5	4.018 ±.298	3.93* ±.25	0.681** ±.016	27.09 ±2.15

Data for control period includes all rats given high rate saline volume expansion (H-VE). K infusion data is for all rats achieving urine flow rates greater than 20  $ul \cdot min^{-1} \cdot 100gBW^{-1}$  during H-VE. Differences in mean values between diet groups, when statistically significant, indicated by \* $p < .05$ , \*\* $p < .01$ , \*\*\* $p < .001$ . Units for variables are given in Table I.1.



Thus it appears that the High-K rats, which prior to K infusion clearly outdistanced normal diet animals in K excreting capability, were remarkably similar to normal diet animals in their renal K excretion response to K infusion. However, with the K infusion, High-K rats showed the remarkable ability to excrete potassium at a rate comparable to normal diet animals in spite of a plasma K concentration that was in the low normal range.

#### E. Prolonged K infusion vs. short-term K infusion

Since the mean K excretion rate during u(3) of the prolonged K infusion experiment substantially exceeded the K excretory plateau demonstrated during the LMH-VE experiments, it is appropriate to consider the question of whether the time of exposure to K loading was an important determinant of renal K excreting capability. Complicating such an appraisal is the fact that the plasma K concentrations during u(3) of the prolonged K infusion experiment averaged 6.35 mmol/l, a value significantly higher ( $p < .001$ ) than the 5.47 mmol/l mean plasma K among normal diet rats excreting potassium at the K excretory plateau level after two hours of K infusion. Also to be considered are whether other parameters of renal function differed. To explore these questions, the data from u(3) of the prolonged K infusion experiment will be compared with the results of those normal diet animals excreting K at the plateau level in the LMH-VE experiment ("short-term K infusion"). The comparison is presented in Table I.5. The mean GFR was nearly identical for the two groups. The prolonged K-infused rats demonstrated a mean K excretion rate approximately 58%



Table I.5 Normal diet group: short-term vs. prolonged K infusion

	$\frac{K_p}{}$	$\frac{Na_p}{}$	$\frac{E_K}{}$	$\frac{FEK}{}$	$\frac{E_{Na}}{}$	$\frac{FENa}{}$	$\frac{GFR}{}$	$\frac{V_u}{}$
Short-term K infusion (n=7)	5.47 ±.07	150.7 ±.7	2.148 ±.052	69.3 ±2.8	4.702 ±.586	5.46 ±.60	0.572 ±.027	28.41 ±2.44
u(3), prolonged K infusion (n=7)	6.35*** ±.10	154.7** ±.10	3.393*** ±.090	94.3** ±5.3	6.128 ±.518	6.87 ±.46	0.576 ±.028	35.85* ±2.10

Short-term K infusion includes normal diet rats with urine flow rates greater than  $20 \text{ ul min}^{-1} 100\text{gBW}^{-1}$  during K infusion period of H-VE. Prolonged K infusion results are for u(3). Differences in mean values between groups, when significant, are indicated by \* $p < .05$ , \*\* $p < .01$ , \*\*\* $p < .001$ . Units for variables are given in Table I.1.



higher than the short-term K infusion group and 36% greater than the K infusion rate of 2.5  $\mu\text{mol}/\text{min}/\text{kidney}$ . The difference in the K excretion rate between short-term and prolonged K-infused rats was significant ( $p < .001$ ). The mean fractional K excretion rate was also significantly greater ( $p < .01$ ) among prolonged K-infused rats, 94.3% vs. 69.3%, notwithstanding the higher plasma K concentration among the prolonged K-infused rats. Mean Na excretion and urine flow rates were also somewhat higher in the prolonged K-infused group compared to the short-term K-infused rats, although only the difference in urine flow rate was statistically significant. However, it seems improbable that these factors accounted for the difference in K excretion between the two groups since an inspection of Figures I.7 and I.8 clearly indicates that the prolonged K-infused rats with the lowest urine flow and Na excretion rates during u(3) had K excretion rates substantially greater than the highest K excretion rate for any rat in the short-term K-infused group.

In order to assess whether the difference in mean plasma K concentration between the short-term K-infused rats (5.47  $\text{mmol}/\text{l}$ ) and the prolonged K-infused group (6.35  $\text{mmol}/\text{l}$ ) was a significant factor in causing the different K excretion rates, plasma K concentration in relation to K excretion rate was examined. Figure I.11 shows a plot of potassium excretion vs. plasma K for all rats in the two groups. In both groups a degree of correlation between plasma K concentration and K excretion is evident, with kaliuresis tending to be greatest among rats with the higher plasma K concentrations.





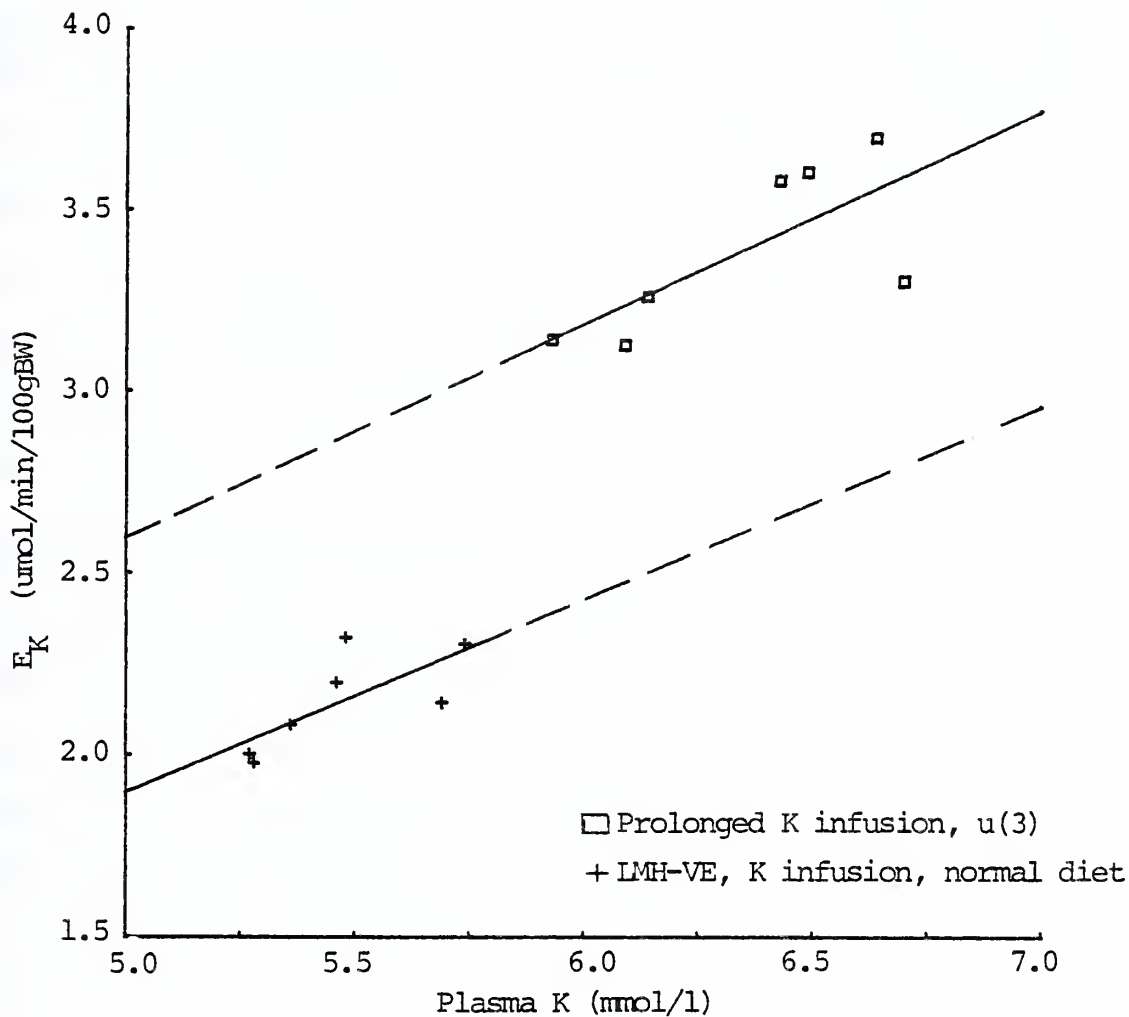


Figure I.11 Potassium excretion in relation to plasma K concentration during u(3) of prolonged K infusion experiments and during K infusion period of LMH-VE for normal diet rats. Regression equations for plotted lines are:

LMH-VE  $y = 0.532x - 0.760$  ( $r=.73$ )

Prolonged K infusion  $y = 0.592x - 0.363$  ( $r=.73$ )



Visual inspection of the plots suggests that the two groups appear to define different  $E_K$  vs.  $K_p$  relationships which if extrapolated would not overlap. Indeed, a statistical analysis of the data indicates that the linear regression equations fitted to the data for each group have slopes which are not significantly different ( $p > .5$ ). The two regression equations may therefore be judged statistically to represent parallel lines separated by a difference in  $K$  excretion of  $0.74 \pm .7$   $\mu\text{mol}/\text{min}$  ( $p < .001$ ). However, the size of the data sample is quite small and the validity of extrapolating the regression lines beyond the limits of the respective data values for each group uncertain. Accordingly, it would be unreasonable to place great reliance on the statistical inferences.

Taking all the factors discussed in this section into account, it seems fair to conclude that the prolonged  $K$ -infused rats manifested a higher renal  $K$  excretion capability than short-term  $K$ -infused rats. This renal response appears to be conditioned more by the difference in the duration of  $K$  loading than by differences between the two groups in plasma  $K$ , sodium excretion, or urine flow rate.



## DISCUSSION

The principal findings of this investigation can be summarized as follows:

During the control period of LMH-VE, at moderate to high rates of Na excretion and urine flow, High-K diet rats excreted potassium at a rate two to three times greater than normal diet rats. While undergoing high rate saline volume expansion, the High-K group demonstrated a relatively stable rate of K excretion independent of the rate of solute or volume diuresis, whereas normal diet rats showed a tendency towards a modest stimulation of K excretion with higher urine flow and sodium excretion rates.

During the K infusion period of LMH-VE (1-2 hours after initiating K loading), High-K and normal diet rats exhibited a similar relationship between potassium excretion and urine flow rate or sodium excretion. K excretion rose in parallel with natriuresis and urine flow until an apparent maximal rate of K excretion was established for urine flow rates greater than 20 ul/min and for sodium excretion greater than 2.5 umol/min. The plateau level of K excretion was not significantly different between the two diet groups and represented approximately 85% of the rate of K infusion. Among rats excreting at the plateau level, the High-K diet group had plasma K concentrations in the normal range whereas the plasma K of normal diet rats was significantly elevated.

During prolonged K infusion with concurrent graded saline volume expansion, normal diet rats achieved rates of potassium excretion between 6.0



and 6.5 hours of K loading approximately 58% greater than the K excretory plateau present after two hours of K loading in the LMH-VE experiments. The rate of K excretion was 35% higher than the rate of K infusion. This enhancement of renal K excretion during prolonged K-infusion appeared to represent a response to the duration of K loading, independent of plasma K concentration, sodium excretion or urine flow rates.

### 1. Renal K excretory plateau

Prior to K infusion in the LMH-VE experiments, K excretion in the normal diet group tended to increase with sodium excretion and urinary flow rate for all levels of saline volume expansion. The presence of a K excretory plateau was not demonstrated. However, K excretion rates were quite scattered in the high flow rate range, and therefore a firm conclusion regarding a renal K excretory plateau cannot be reasonably drawn.

The urinary K excretion data from the experiments of Khuri et al (36) in which rats were also subjected to three different rates of saline volume expansion reveal findings similar to those in the present experiments. Shown in Figure I.12 is a comparison of the Khuri et al results with those from the present study. The potassium excretion and urine flow rate data for normal diet rats in the LMH-VE experiments have been grouped into four flow rate ranges: 0-1, 1-5, 5-20, and > 20 ul/min with the mean  $E_K$  and  $V_u \pm SEM$  shown for each group. In comparing the plots from the two studies, it appears that saline loaded rats have the capacity to augment K excretion as the rate of diuresis increases, but





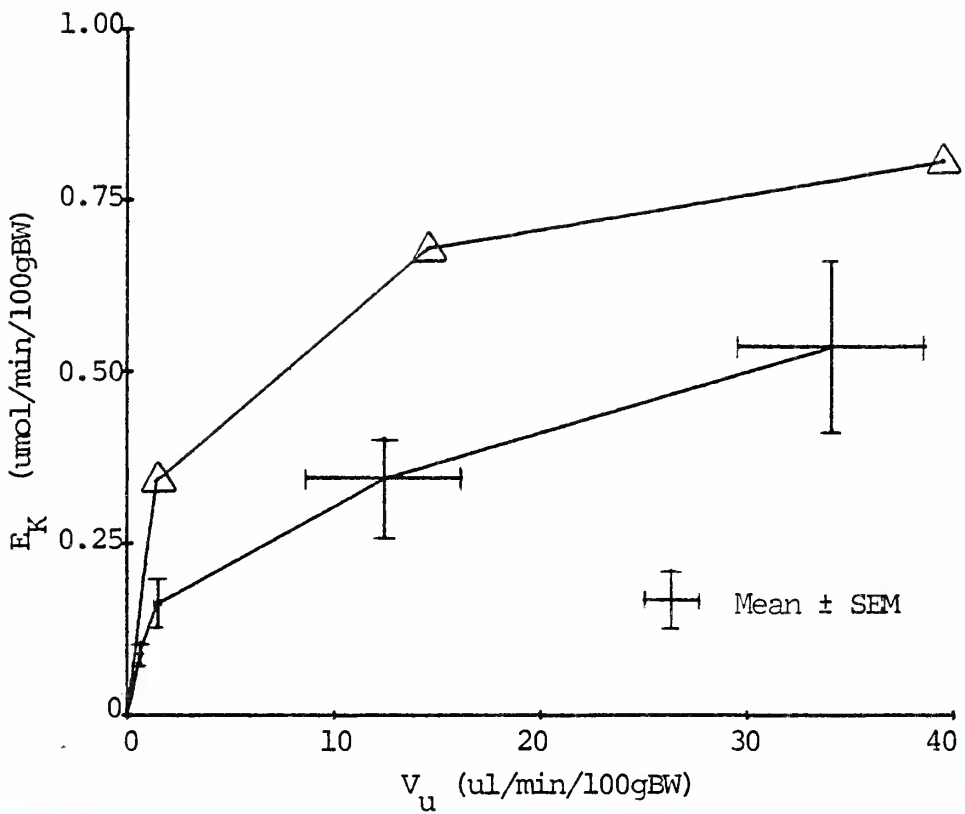


Figure I.12 Potassium excretion in relation to urine flow rate. The line connecting the triangles represents data from Khuri et al (36). The results from control period of the LMH-VE experiments in normal diet rats are plotted in the lower line. Mean  $E_K$  and  $V_u \pm$  SEM are shown for the data which has been grouped into four flow rate ranges: 0-1, 1-5, 5-20, and greater than 20  $\text{ul}/\text{min}/100\text{gBW}$ .



that the enhancement of K excretion with increased urine flow rate progressively diminishes.

The High-K diet rats during the control period maintained a relatively constant potassium excretion rate, approximately two to three times that of normal diet rats, when urine flow ranged from 12 to 28 ul/min. A K excretory plateau appears to be present for High-K diet rats over this flow rate range. Whether higher rates of solute and volume diuresis (as seen subsequently during the K infusion period) would have further enhanced K excretion is not known.

A higher pre-K loading K excretion rate among K-adapted rats as compared to normal diet rats was also observed by Adam and Dawborn (1).

"Basal" K excretion rates in unanaesthetized, fasted rats following a 4 ml intra-gastric water load were nearly five times greater for K-adapted animals as compared to normal diet rats. Wright et al (62), on the other hand, found rates of kaliuresis in fasted, K-adapted rats prior to K loading to be approximately one-half that of normal diet rats. Mannitol was added to the saline infusion in the Wright et al experiments, and mean urinary flow rate for both normal and High-K diet rats was approximately 9 ul/min/100gBW, somewhat below the urine flow rate at which differences in K excretion rates between normal and High-K rats became most obvious in the present study. However, these considerations would not appear to explain the discrepant results. The reason for the different findings is not apparent.

Once K excretion is stimulated by IV K loading, an apparent maximal renal K excretion capability in response to saline loading is demonstrated in both diet groups. This finding is in accord with the results



of Rapaport and West (49), Cade and Shalhoub (15) and Gonick et al (25) discussed in the Introduction. In these studies on dogs, a K excretory plateau was demonstrated similarly in the setting of an acute IV loading stimulus to K excretion:  $\text{Na}_2\text{SO}_4$  (15,49) or KCl (25). The K excretory plateau observed by these investigators and in the present experiments may have resulted from a number of renal and/or extra-renal factors which are known to influence K excretion. Discussed below are a number of these considerations.

a) Distal tubular flow rate

As discussed in the Introduction, luminal fluid flow rate is a primary determinant of the magnitude of K secretion in the late distal tubule (26,27). If it is assumed that urinary K excreted during high urine flow rates induced by saline loading originates largely from distal tubular K secretion, it can be argued that the excretory plateau arises as a consequence of a constant, perhaps maximal rate of distal tubular flow rate. That is, the range of urine flow rates over which K excretion stabilized may reflect a variable rate of collecting duct fluid transport and not variability in distal tubular flow rate.

Distal tubular flow rates were not measured during the course of this study so the validity of this argument has not been established. However, it is well established that greater volume and solute loads are delivered to the distal tubule during Na and/or K loading (11,16,36, 37,40,43,62). Since both the late distal tubule and the collecting duct are target sites for the action of ADH (28,30,45,61,65), it would be anticipated that late distal tubular flow rates would correlate to some



extent with urinary flow rate. The data presented in Figure I.13 offers some substantiation of this possibility. Shown are the results from three experiments during which distal tubule and urine flow rate were measured during the course of saline volume expansion (36,39,51). Apparent from the figure is that increases in late distal flow rates correspond to proportionate elevations of urine flow rates. The range of urine flow rate recorded among these studies is comparable to that observed in the present investigation. However, since only a limited number of late distal tubule and urine flow rate measurements were documented in each study, the exact nature of the late distal tubule-urine flow rate correlation is uncertain.

b) Suppression of aldosterone secretion by volume expansion

Because of the wide variation in measured urine and Na excretion rates among the H-VE rats during the K infusion period, it is possible that some rats retained relatively more of the isotonic solution infused prior to this time (four hours) and thus were more severely volume expanded than others. By this reasoning, the rats demonstrating the highest rates of diuresis during the K infusion period may have sustained a higher degree of ECF volume expansion earlier than rats with lesser urine flow rates. Since aldosterone secretion, an important stimulus to K excretion (18,21,31,59,60), is suppressed by volume expansion (52), it may therefore be argued that circulating aldosterone levels in the H-VE rats with the highest urinary flow rates were less than those H-VE rats with lower urine flow rates. This then would tend to suppress any tendency towards higher rates of K excretion among rats having the highest rates of diuresis.





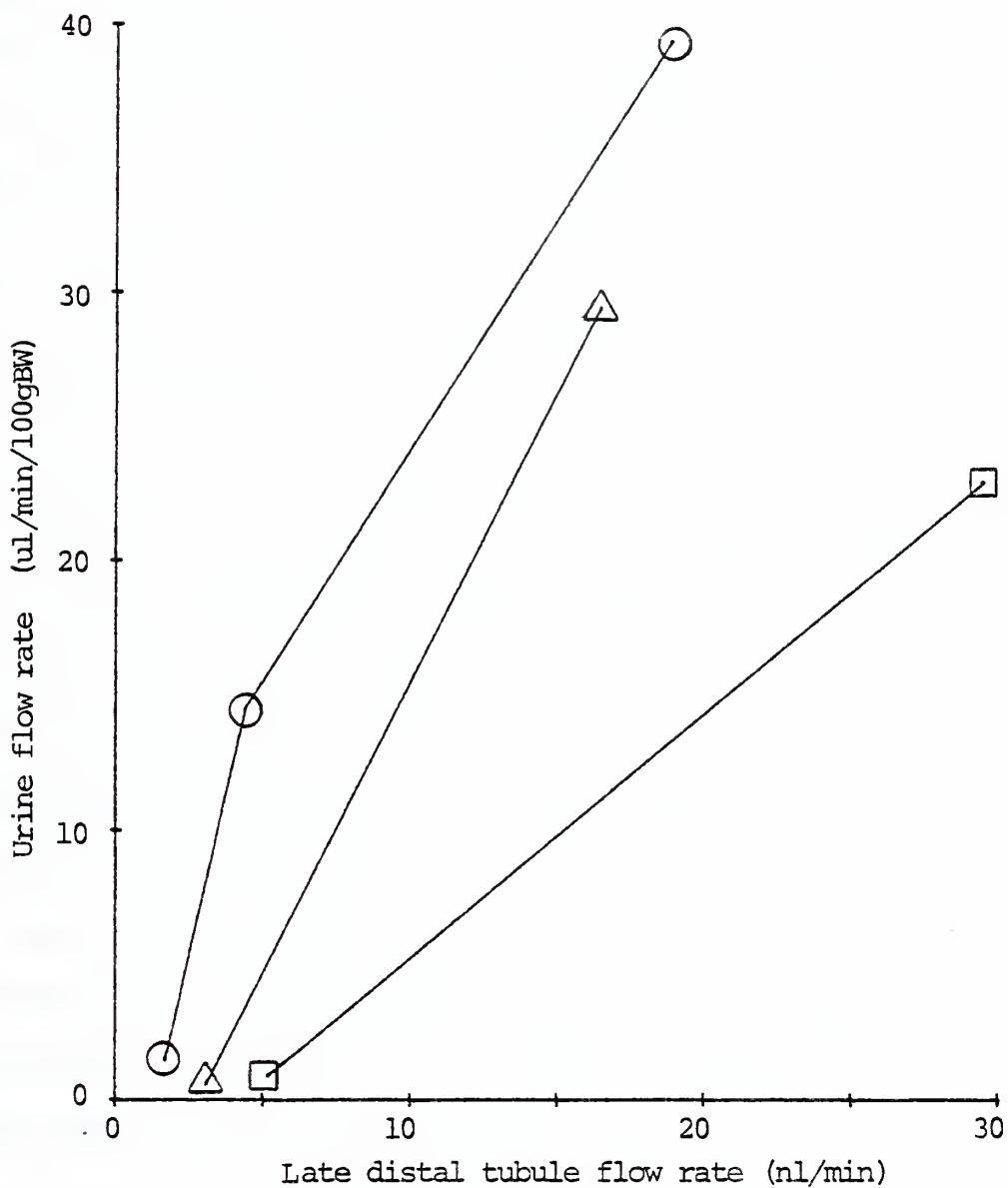


Figure I.13 The relationship between late distal tubular flow rate and urine flow rate. Data is taken from reference 36 (circles), 51 (triangles), and 39 (squares). Urine flow rate data normalized to 100gBW per kidney as appropriate.



It is well documented that adrenal aldosterone secretion is enhanced directly by elevated plasma K concentrations, an effect that has been shown to be independent of volume status or sodium balance (9,10,17). Even so, it is not known whether the direct stimulatory effect of elevated plasma K concentration on aldosterone secretion can be significantly blunted by the high rates of volume expansion employed in this study. This has not been specifically investigated in the rat.

c) Collecting duct reabsorption

The possibility that the collecting duct reabsorbs a greater proportion of K secreted by the distal tubule with increased collecting duct flow rates, thereby offsetting any tendency towards increased K excretion, seems quite remote. K transport activity in the rat collecting duct is generally believed to be dependent on the "contact time" of the luminal fluid passing the collecting duct epithelial cells (23,51,65). Higher flow rates reduce contact time and as a consequence net K transport rates. The results from several studies point to the fact that during high rates of saline induced diuresis with concurrent K infusion, the fractional excretion of K is virtually unchanged from the end of the late distal tubule to the collecting duct (36,43,51).

d) Distal tubule K secretion transport maximum

The urinary potassium measured in these experiments arose potentially from several sources which correlate with presently known segmental nephron handling of potassium: K filtered at the glomerulus which escapes reabsorption by the proximal tubule and loop of Henle, net secretion of potassium by the distal convoluted tubule, and net secretion by the various



anatomical segments of the collecting duct (66). There is no experimental evidence to suggest that the collecting duct makes a substantial contribution to urinary potassium during high rates of saline volume expansion. As already noted, fractional excretion of potassium as measured at the end of the late distal tubule has been found to approximate that measured in the urine.

Unreabsorbed filtered potassium, however, may have been a significant factor in these experiments. As pointed out by Giebisch, the increased K load delivered to the distal tubule with high rates of volume expansion may contribute significantly to urinary K (23). Since early distal K concentrations during volume expansion tend to remain unchanged or perhaps slightly increased relative to hydropenic conditions (36,39,51), the unreabsorbed proximal K delivered ultimately to the urine would, if anything, tend to rise with increased rates of volume expansion. Accordingly, a proximal nephron role in limiting K excretion capability seems unlikely, unless the increased proximally delivered K loads to the distal nephron actually serve to depress distal tubular secretion.

There remains, then, the possibility that the distal tubule's K secreting capability was maximized during the saline loading. Prior to K infusion, it seems probable that even with high rates of saline volume expansion, K secretion in the distal tubule was not maximal in normal diet rats since urinary K excretion showed a tendency to rise over the entire range of observed urine flow and Na excretion. However, with K loading, although the distal tubule's K secreting capability was undoubtedly enhanced, a maximal rate of secretory transport may have



become manifest within the range of distal tubular flow rates induced by the volume expansion.

The micropuncture experiments relevant to this question (summarized in the Introduction) were primarily designed to characterize flow-dependent K secretion in the distal tubule; the existence of a K transport maximum was not specifically examined. As noted earlier, the findings of these studies cannot be reasonably interpreted in a manner germane to the question of a K secretion transport maximum.

In the context of the present study, among the known mediators of distal tubular K secretion, two can quite reasonably be implicated as determinants of the magnitude of a presumed maximal distal tubular K transport capacity: plasma K concentration and circulating aldosterone levels. As K loading raises plasma K, two effects of consequence to the distal tubule would follow: (1) a direct stimulation of the adrenal gland's aldosterone output (9,10), and (2) enhanced rates of peritubular K uptake by the distal tubule cells leading to an increased cellular K content and an augmented secretory capability (19,23). The degree of stimulation afforded by these linked mechanisms would determine the magnitude of distal tubular response to K loading.

## 2. High-K vs. Normal diet rats

An important question arising from the experiments is why the K secretory behavior of High-K diet rats was so remarkably similar to normal diet rats during K loading, with the important distinction, of course, that High-K animals manifested K secretion rates comparable to normal diet animals in spite of a significantly lower plasma K concentration.





First, it should be noted that since the purpose of the study was not to investigate K adaptation per se, a moderate rate of K infusion was chosen so that the lethal effects of an acute K challenge would not be encountered. Indeed, none of the experimental animals died. It seems certain that the High-K diet rats were not significantly stressed by the IV K load since plasma K's in this group did not exceed the normal range. This undoubtedly accounts for, in part, the "failure" to document an enhanced rate of K excretion by K-adapted compared to normal diet rats during an acute K challenge. Studies describing this phenomenon employed K loads that resulted in significant lethality to normal diet animals (1,47,62).

Also of importance in judging the results of normal and High-K rats is that the latter group, when subjected to H-VE, had plasma K concentrations averaging only 2.50 mmol/l during the control period. This suggests that total body potassium stores may have been somewhat depleted. High-K rats might have had inappropriately high rates of K excretion during the pre-experimental fasting period, a possibility that is emphasized by the significantly higher rates of K excretion exhibited by the High-K group compared to normal diet rats during the experimental control period. It appears that High-K rats may be quite sensitive to an acute withdrawal from dietary K intake, perhaps reflecting an inability to readjust homeostatic mechanisms tuned to a high daily rate of K excretion. After 15 hours of fasting (during which access to tap water was permitted), it seems probable that K-adapted but relatively K-depleted rats were brought to the experimental table.



If it is assumed that the High-K animals had developed pre-experimentally a degree of K depletion, then the K infusion served in part to replete body K stores. Hence the excretory plateau observed for the High-K rats approximated 85% of the K infusion rate (as it was for the normal diet group). It is noteworthy that at the end of the two hour K infusion period, plasma K concentrations among the High-K rats were within the normal range irrespective of the rate of saline loading. This observation further emphasizes the remarkability of the High-K rats' homeostatic adaptation to the enriched potassium diet, for they are able to excrete K at a relatively high rate even at normal plasma K concentrations.

As pointed out by Silva et al (56), some of the controversy in the literature regarding the role of renal and non-renal factors in K adaptation (see for example references 1-3) may arise from different states of K balance among K-adapted rats in the various experimental studies, some of which included pre-experimental fasting while others did not. Silva et al theorized that extra-renal K adaptation, that is, the buffering of plasma K concentration by body tissues during an acute K load challenge, may be accounted for in part by unrecognized relative total body K depletion among K-adapted animals in some studies.

Finally, it should be noted that although K loading induced a similar renal K excretory response among High-K and normal diet rats, the difference in systemic consequences was particularly underscored when the duration of the K infusion was extended. Normal diet rats augmented their rate of kaliuresis substantially during prolonged K infusion thus avoiding a toxic accumulation of body potassium. High-K rats on the other hand responded to the short- and long-term K loading with a K excre-



tion rate which, though equal to or less than the normal diet group, easily afforded protection from systemic K toxicity while simultaneously repleting apparently low potassium body stores. K excretion rates for the High-K group appeared to be entirely appropriate to the level of the K load challenge.

### 3. Prolonged acute K infusion

That prolongation of acute IV K loading beyond two hours most likely resulted in an augmented renal K excretory capability is an important conclusion of this study. Normal diet animals that were K infused for 6.5 hours demonstrated K excretion rates averaging 136% of the rate of K infusion compared to 86% for rats K infused for a period of 2 hours. K excretion for the latter group was found to be the highest rate inducible by high rate saline loading. This enhancement of renal K excretion response to K loading over time might be characterized as "acute K adaptation" in contrast to the well documented phenomenon of K adaptation associated with chronic high potassium dietary intake (1,3,57,62).

Other studies in rats have reported an induction of the K-adapted physiological state after a relatively short period of dietary K supplementation. Adam and Dawborn (1) found that adaptation could be demonstrated after 24 hours of high dietary K intake. Hohenneger (34) observed that 48 hours following K dietary supplementation, rats could "escape" an amiloride induced depression of K excretion. Recently, Stanton and Giebisch reported in abstract (57) that distal tubular K secretion in hydropenic rats was significantly increased over time during acute KCl loading.



Since in the present experiments, the enhanced rate of K excretion during prolonged K infusion was associated with higher plasma K levels when compared to rats subjected to short-term K loading, the stimulatory effect of the more elevated plasma K may have contributed at least in part to the observed difference in K excretion. However, for several reasons, the duration of K loading most likely had an effect independent of plasma K concentration. First, after 4.5 hours of K loading (u(2)), the mean plasma K concentration was actually higher than after 6.5 hours (u(3)). In spite of the falling plasma K between the second and third clearance periods, the absolute and fractional K excretion rates rose significantly. Secondly, the comparison of the plasma K and K excretion data for individual rats shown in Figure I.11 demonstrates that among the short-term K-loaded rats, those with the highest plasma K values still had K excretion rates substantially below those of rats in the prolonged K infusion experiments.

The presumed enhanced K excretory capability of the kidney after prolonged K loading may have resulted from a number of factors. First, it seems probable that aldosterone plasma levels may have been progressively augmented by the prolonged K infusion. Also, it is relevant to point out that the time course of the renal response to aldosterone stimulation, which involves RNA and protein synthesis, evolves over time. Fignognari et al found that after a single subcutaneous injection of aldosterone into rats, plasma aldosterone concentrations peaked after one-half hour but the maximum rate of kaliuresis did not occur until after 3 hours (21). Thus the level of the endogenous aldosterone "dose" as well as the time course of the renal response to its effect may have been





significant factors in the enhancement of K excretion rates after 6.5 hours of K loading. Finally, it is conceivable that the prolonged period of volume expansion and/or K loading may have progressively inhibited proximal tubule and loop of Henle K reabsorption resulting in the delivery of a greater proportion of filtered K to the urine.

Irrespective of the mechanisms involved, the response of normal diet rats to prolonged acute IV K infusion is clearly adaptive. As demonstrated in the analysis of estimated K balance during the 6.5 hour K infusion period, by the end of the experiment, the rats have clearly augmented K excretion sufficiently to begin lowering the elevated plasma K as well as eliminating an accumulated body K surplus.

Whether such an adaptive response would have been demonstrated in the absence of the very high rates of saline volume expansion employed in this experiment is not known. However, it is significant that after 4.5 hours of K infusion, up to which point saline had been infused at a relatively modest rate, all but one of the seven rats were already excreting K more rapidly than the K infusion rate.

In summary, the results of this investigation suggest that saline loading with concurrent IV K loading in the rat induces a parallel rise of kaliuresis with urine flow and Na excretion until a plateau level of K excretion is reached after which further progression in the diuresis produces no additional increase in K excretion. A K excretory plateau is demonstrated both for normal and High-K diet rats. However, High-K rats exhibit a plateau K excretion rate comparable to normal diet animals but at a significantly lower plasma K concentration. The maximum K



excretion rate in response to K loading appears to depend on the length of time that the rat is exposed to acute IV K loading; over time, the renal K excretory capability is progressively enhanced. It seems probable that the renal K excretory plateau represents a temporally-bound, characteristic parameter of renal K excretory function which may change dynamically depending on the degree, efficacy, and duration of the stimulus to K excretion.



PART II: MATHEMATICAL MODELS OF FLOW-DEPENDENT  
DISTAL TUBULAR POTASSIUM SECRETION



## A. INTRODUCTION

The rate of tubular fluid flow has been shown to be an important determinant of the magnitude of potassium secretion in the rat distal convoluted tubule (27,36,39,51). The presentation here in Part II explores at a theoretical level, a number of known and postulated aspects of distal tubular membrane transport behavior which may account for this flow-dependent K secretory phenomenon. Several models of distal tubule K secretion based on mathematical formulations of membrane transport kinetics will be developed and analyzed. The modeling approach will also permit a theoretical assessment of the suggestion raised in Part I that distal tubular K secretory capacity may be bounded by a transport maximum. Experimentally derived in vivo kinetic data will be utilized to provide meaningful quantification of the K secretory behavior of the mathematical models.

Preliminarily, it will be useful to consider the cellular model of distal tubular K transport proposed by Giebisch (22), which conveniently identifies and characterizes the generally agreed upon key features of membrane transport in a "typical" distal tubular K secretory cell (Figure II.1). The transepithelial electrical gradient (-20 to -40 mv, lumen negative) is favorably poised to promote secretion of the potassium cation. The potential gradient arises in part from the indicated differences in ion permselectivity of the basolateral and luminal membranes, the latter being relatively more permeable to sodium and as a consequence, depolarized in relation to the basolateral membrane. An active "reabsorptive potassium pump" transporting K from the lumen to the cell is postulated





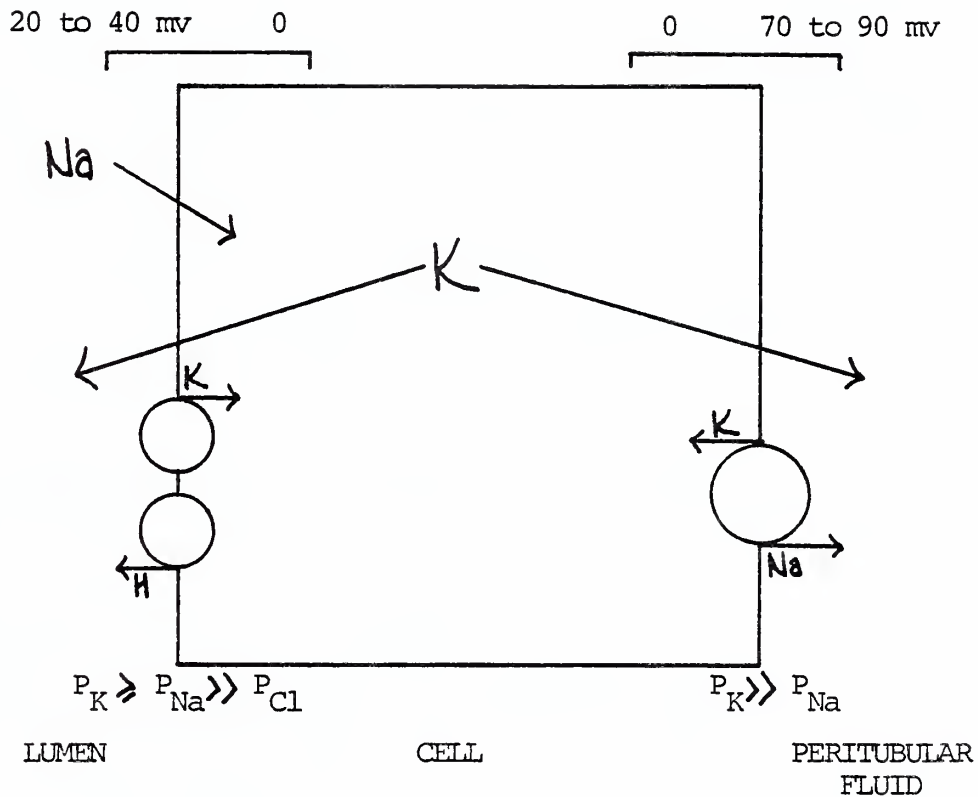


Figure II.1 Schematic diagram of late distal tubule potassium secretory cell (adapted from Giebisch, 22). See text for description.



to lie within the luminal membrane. On the blood side, K is accumulated and Na extruded from the cell by the familiar Na-K-ATPase dependent membrane transport system. Rheogenic ion pumping by any of the carrier-mediated transport mechanisms depicted would contribute to the electrical polarization of the respective membranes. Cellular potassium is concentrated relative to the blood and luminal fluid, though estimates of its chemical activity vary considerably - from 45 to 150 mmol/l (13, 14,35,60,65). The cellular units of the distal tubule are generally considered to be tightly linked at their apical borders by "tight junctions." The distal tubule is thus categorized among the so-called "tight epithelia" in which the predominant mode of transepithelial ion and fluid transport is transcellular rather than paracellular (8).

In order to appreciate the kinetic basis for and mechanisms of flow-dependent K secretion in light of this briefly described cellular model, consideration must be given to the manner in which the ion fluxes across each membrane, both passive and carrier-mediated components, are modified by changes in the rate and composition of fluid flowing past the luminal membrane. It might be said that we need to characterize the dynamic behavior of such a cell and its response to imposed luminal changes. For instance, presume for the moment that the cell as depicted is in a steady state wherein, among other kinetic events, a net secretory flux of K is being transported from blood to lumen. The concentrations of K in the cell and in the fluid flowing past the luminal membrane would be constant in this steady state. If then, tubular fluid with a higher rate of flow is abruptly directed past the luminal membrane (which for the purposes here will be assumed to result initially in a lowering of the luminal K



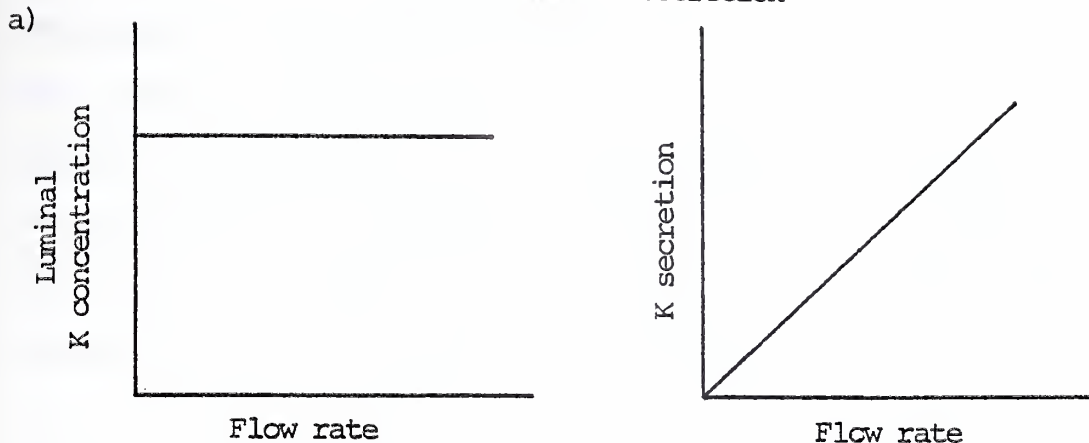
concentration), the steady state will be transiently perturbed, thus initiating potentially, though not necessarily, a number of alterations in the transmembrane ion fluxes and possibly a set of responses by the various membrane transport mechanisms.

If the sum effect of this cellular response results in a fall in the luminal K concentration directly proportionate to the rise in the luminal flow rate, then such a cell would be characteristic of a cell in the Giebisch "transport-limited" secretion model. K secretion would be constant and independent of flow rate. If, on the other hand, appropriate adjustments in transmembrane ion fluxes occur which permit the restoration of the luminal K concentration to that which was present at the lower flow rate, a "flow-limited" secretory behavior would result - the rate of K secretion would be linearly proportional to the rate of tubular flow. These two Giebisch paradigms of secretory epithelial transport behavior (22) have been discussed earlier, and the graphical schematization of each model is again depicted in Figure II.2a.

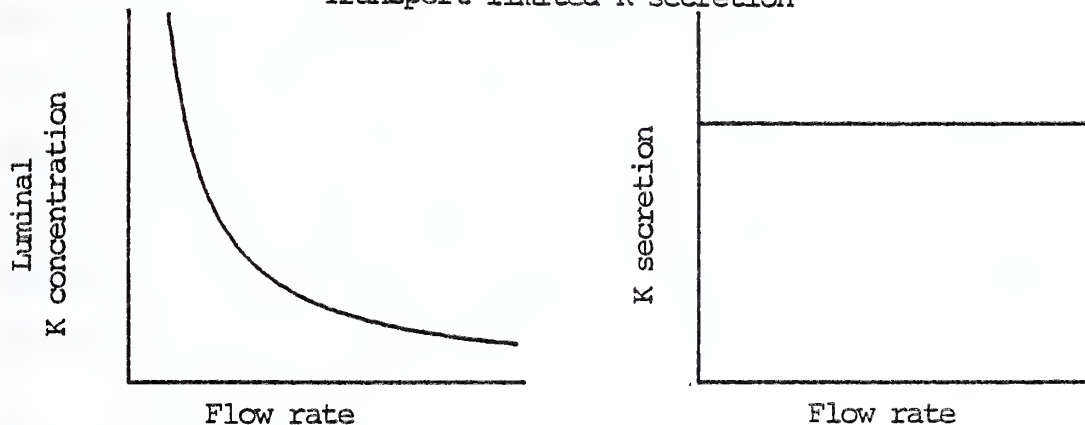
The Giebisch cellular model, together with the two described secretory paradigms, are particularly helpful here, for they direct our attention very specifically to questions that if answerable, would offer considerable insight into the basis of flow-dependent K secretion. For instance, what effects do changes in luminal flow rate and ionic composition have on membrane electrical potentials, the activity and rheogenicity of the carrier-mediated transport mechanisms, cellular K concentration, and membrane ion permeability characteristics? By and large, data regarding such dynamic aspects of the distal tubular epithelium is limited to a



Flow-limited K secretion



Transport-limited K secretion



b) Flow-limited/Transport-limited K secretion with a secretion maximum

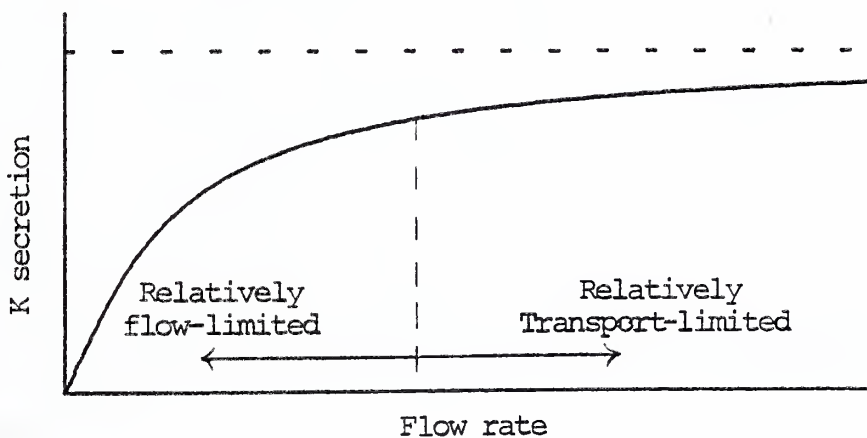


Figure II.2 Hypothetical relationship of luminal flow rate to luminal K concentration and K secretion. a) is adapted from Giebisch (22).





small number of experimental observations. Thus the Giebisch models, while helpful in defining some of the questions to be explored, in the absence of further data, do not a priori define the mechanism or basis of flow-dependent K secretory transport. Indeed, it should be evident that the cellular model, as characterized, would be consistent with flow-limited or transport-limited K secretory behavior.

Additionally, it should be recognized that an inherent limitation of a single cell, static model of K transport is that it may obscure or inadequately prepare one to anticipate the aggregate operation of such single cell units disposed along a tubular epithelium, the axial dimension of which is two orders of magnitude greater than the transepithelial dimension. For this reason, compartment kinetics and the mathematical approaches applied to such systems are inappropriate here.

What then are the dynamic properties of K transport in the distal convoluted tubule which mediate the flow-dependent K secretory phenomenon? While a full answer to this question necessarily awaits further experimental data and observation regarding distal tubule membrane transport processes, it is the purpose of this presentation to propose, at a theoretical level, a more dynamic description of the distal tubule which builds on the precepts of the Giebisch cellular model. The objective is to provide a theoretical basis for conceptualizing flow-dependent K secretory kinetics.

The theoretical analysis will focus chiefly on a detailed examination of one model of K secretion which incorporates a number of physiologically



plausible membrane and cellular properties which are postulated to optimize the potential for flow-limited secretory behavior. Briefly stated, the "optimized model" develops from the following considerations. If we presume that increases in luminal flow rate have a tendency to lower luminal K concentration, two direct consequences can be predicted to result that would tend to limit the epithelium's capability to augment K secretion with increased flow rate. First, the reduced luminal K concentration would establish a chemical gradient favorable at least transiently to a net efflux of K from the cell to lumen. If the net influx of K across the basolateral membrane were not increased to compensate, the consequence would be a tendency towards a lower steady state cell K concentration, and all other things being equal, a reduced net secretory flux of K from cell to lumen. Secondly, the lowered luminal K concentration would tend to increase the polarization of the luminal membrane (which in part arises from a K diffusion potential) thus favoring a reduced net K secretory flux across the luminal membrane. In sum, the net result would be a reduction of the electrochemical potential for K secretory transport.

An optimal K secretory cell is therefore viewed as one which would resist these two changes: it would maintain a constant cell K concentration and luminal membrane PD independent of luminal conditions. To complete the description of such a cell in a manner amenable to mathematical modeling, it remains to define the kinetics of the luminal membrane reabsorptive pump, a discussion which, for the present, will be deferred. Beginning with a model incorporating these principles, the analysis proceeds to consider alternative postulates regarding the luminal membrane



PD, cell K variability, and the kinetics of the luminal membrane reabsorptive pump.

The purpose of the mathematical modeling is not to argue strongly in favor of a particular view of distal tubule mechanisms and epithelial properties important to K secretory kinetics. Rather, the aim is to define a plausible set of alternative postulates regarding distal tubular membrane and cell properties, to examine the K secretory behavior of a tubular epithelium modeled on the basis of such properties, and to identify the distinctive kinetics of each model in a manner that permits the correlation of in vivo experimental data regarding flow-dependent K secretion with theoretical considerations of K transport processes in the distal tubule.



B. PRINCIPAL ASPECTS OF K SECRETORY KINETICS TO BE CHARACTERIZED BY THE MODEL MATHEMATICAL SOLUTIONS

In order to conceptually facilitate the comparison and analysis among the various secretory models, attention will be focused on three particular areas of K secretory behavior: (1) the dependency of K secretion on luminal-flow rate - "Flow Dependency", (2) the effect that the initial concentration of K entering the secretory tubule,  $K(0)$ , has on the magnitude of net K transport - " $K(0)$  Sensitivity", and (3) the range of K secretion rates attainable by a given model - "Secretory Potency." Before proceeding with the mathematical formulation of the models, it will be useful to describe briefly the types of behavior which will be exhibited among the models in these three areas.

1. Flow dependency

The terminology employed by Giebisch in characterizing the relationship of secretion to flow rate will be used here (23):

Transport-limited: K is secreted at a constant rate, independent of luminal flow rate

Flow-limited: K secretion is directly proportional to the luminal flow rate

Since none of the models will conform strictly to the secretory behavior characterized by the Giebisch paradigms, flow dependency will be described as more closely approximating either flow-limited or transport-limited behavior. Also, it will be seen that for most of the models, the nature of flow dependency will vary over different flow rate ranges. For instance, Figure II.2b depicts the K secretion vs. flow rate profile





of a hypothetical epithelium in which K secretion plateaus at higher flow rates. K secretion flow dependency would be characterized as relatively flow-limited at low flow rates and relatively transport-limited at higher flow rates.

In passing, it should be noted that some difficulty arises in the concept of flow dependency when volume reabsorption is taken into account. What luminal flow rate in a tubular segment, the initial, the final, or the mean should be used as the appropriate value for the flow variable?

Since most of the discussion of the models will center on the special case of zero volume reabsorption along the tubule, this problem is generally obviated. The effects of volume reabsorption on K secretion will be considered specifically in one section of Part II.

## 2. K(0) sensitivity

An interesting and valuable result of the model mathematical solutions is that net K secretion is influenced by the initial K concentration entering the secreting segment,  $K(0)$ , in a characteristic way. In general, it will be seen that as  $K(0)$  rises, net K secretion falls, and in most cases converts to net K reabsorption if the initial K concentration is sufficiently high. In a sense, then, it might be said that the potassium load entering the segment can exert an "inhibitory" effect on K secretion. However, this term has additional implications which are inappropriate in the present context. The term " $K(0)$  sensitivity" has been chosen to indicate that net K transport along the tubule may be influenced to varying degrees by the initial K concentration



entering the tubule. Shown in Figure II.3a are examples of different  $K(0)$  sensitivities. "A" shows a linear relationship between net K transport and  $K(0)$ . The degree of  $K(0)$  sensitivity can be quantified by the slope of "A",  $\Delta \text{net K transport} / \Delta K(0)$ . Note that K transport ranges from net secretion to net reabsorption. "B" shows a non-linear net K transport vs.  $K(0)$  profile.  $K(0)$  sensitivity is greater than "A" at lower ranges of  $K(0)$  concentrations. For higher values of  $K(0)$ , net reabsorption is relatively constant and insensitive to  $K(0)$ . As will be demonstrated later, flow rate will have a marked effect on  $K(0)$  sensitivity.

### 3. Secretory potency

Because many factors will be seen to affect the magnitude of K secretion demonstrated by a given model, a discussion of secretory potency is best deferred until specific models are considered. For the moment, it is relevant to point out that a flow-limited secretory model does not necessarily define a potent K secretory epithelium, and, conversely, a transport-limited system does not necessarily imply low rates of K secretion. This is illustrated in Figure II.3b where the four possible combinations of high and low secretory potency and flow- and transport-limited flow dependency are depicted.

In the presentation to follow, the K transport kinetics of each model will be characterized mathematically, graphically, and conceptually in a number of ways. For the purpose of discriminating among the models, the above three discussed aspects of K secretory behavior - flow dependency,  $K(0)$  sensitivity, and secretory potency - will be found to be particularly useful.



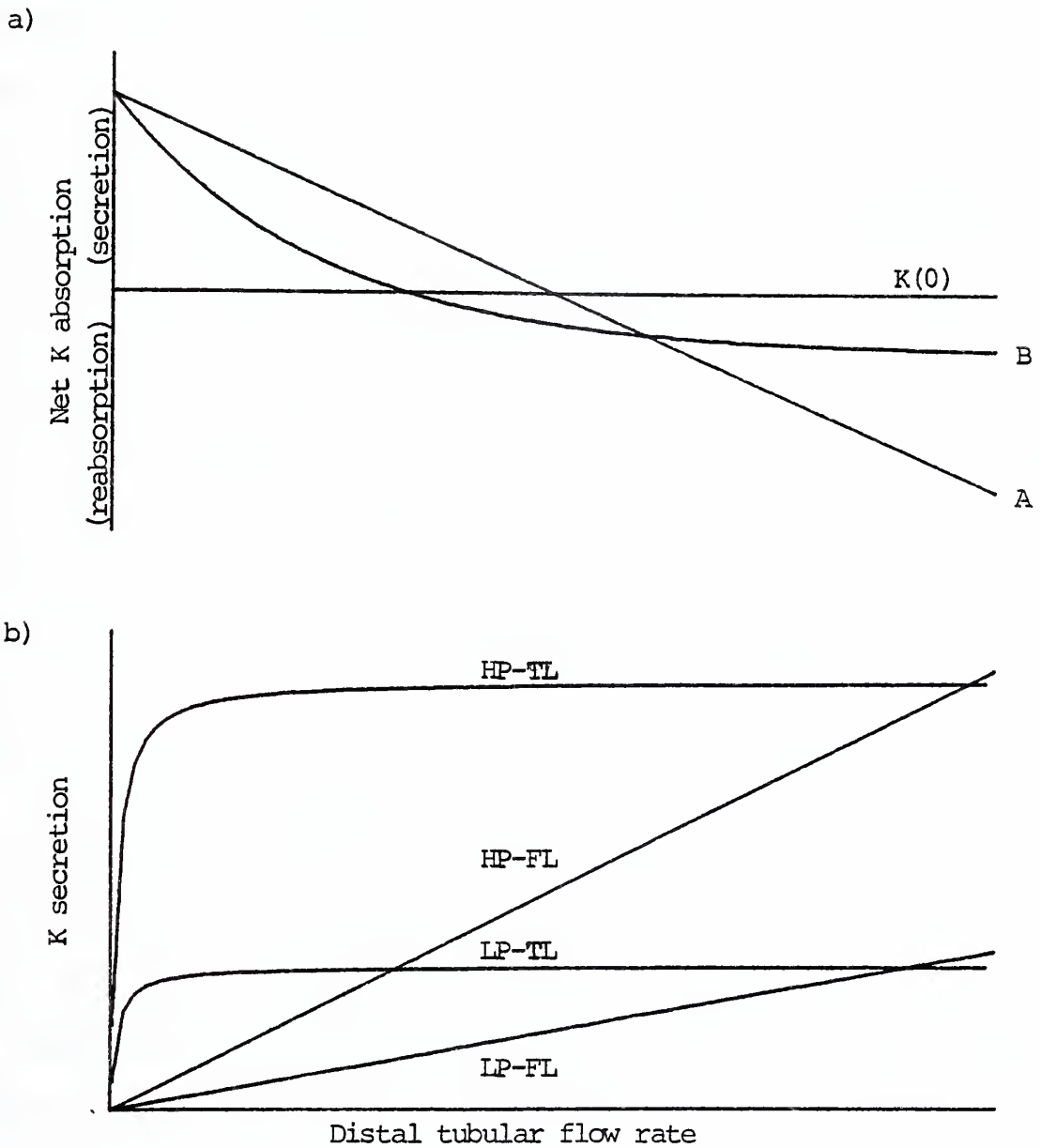


Figure II.3 a) Hypothetical linear "A" and nonlinear "B" relationship between net K absorption and  $K(0)$ .  
b) Four subsets of flow dependency - secretion potency: high potency, transport-limited (HP-TL); high potency, flow-limited (HP-FL); low potency, transport-limited (LP-TL); and low potency, flow-limited (LP-FL). See text for definition of terms.



### C. BASIC PARAMETERS

As shown in Figure II.4, the late distal tubule K secretory epithelium is represented as a tubular structure comprising a lumen enveloped by a layer of distal tubule cells. The tubule is bathed by interstitial fluid which will be assumed to have an electrolyte composition identical to that of blood perfusing the vicinity of the tubule. Flux parameters relating to the lumen, cell layer, and interstitial fluid (or blood) will be identified by the subscripts 1, 2, and 3 respectively. The axial dimension of the tubule ranges from  $x = 0$  to  $x = L$  millimeters. The cross-sectional area of the tubular lumen,  $a_1$ , and the cell layer,  $a_2$  ( $\text{cm}^2 \times 10^{-5}$ ), are constant as a function of  $x$  and independent of flow rate. The interstitial fluid is assumed to have quasi-infinite dimensions and therefore an unvarying electrolyte composition.

Fluid perfusing the tubule enters at  $x = 0$  and subsequently emerges at  $x = L$  with a potassium concentration of  $K(0)$  and  $K(L)$  respectively. The initial and final luminal flow rates are similarly identified as  $V(0)$  and  $V(L)$ . The luminal K concentration and the flow rate at any point along the tubule,  $K(x)$  and  $V(x)$ , may vary as a function of  $x$  depending on transepithelial potassium transport and volume reabsorption processes. The cell K concentration will be designated as  $C_K(x)$  which may also vary as a function of  $x$ . All concentrations will be given in  $\text{mmol/l}$  (equivalent to  $\text{pmol/nl}$ ), volume flow rates in  $\text{nl/min}$ , and fluxes in  $\text{pmol/min}$ .

$\Phi(x)$ , the axial flux of potassium, may be considered to represent the product of luminal flow rate and potassium concentration at  $x$ :





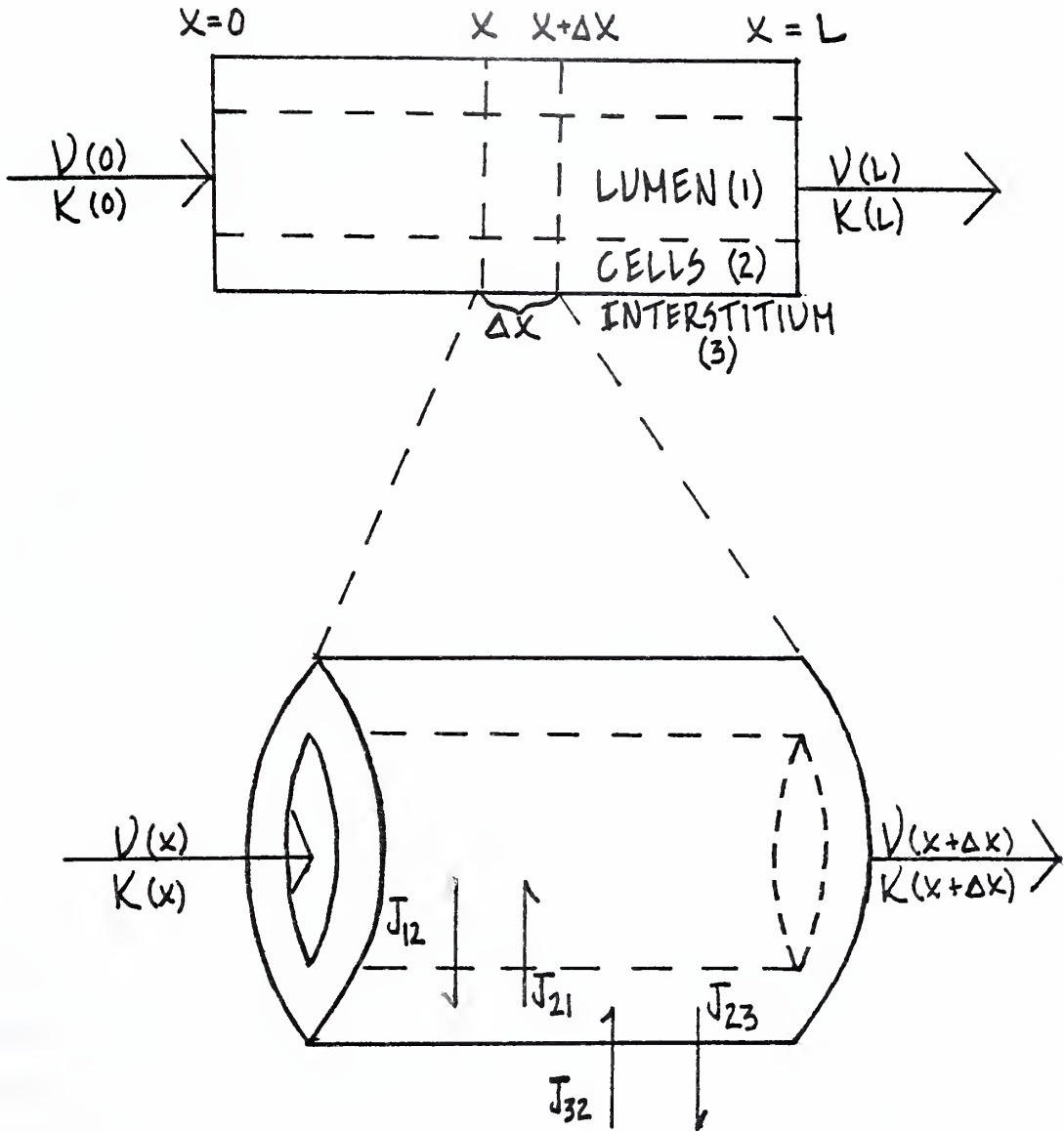


Figure II.4 Distal tubule potassium secretion model and basic parameters. See text for description.



$$\Phi(x) = V(x) \cdot K(x)$$

For the entire segment, net potassium absorption,  $\Phi(\text{net})$ , is defined as:

$$\Phi(\text{net}) = V(L) \cdot K(L) - V(0) \cdot K(0) \quad (1)$$

which, if positive, represents net potassium secretion and, if negative, net potassium reabsorption.

If we now consider a small section of the tubule of length  $\Delta x$  as depicted in Figure II.4, the fluid entering at point  $x$  and emerging at  $x + \Delta x$  may be modified by transepithelial potassium and volume fluxes. The transmembrane potassium fluxes,  $J_{12}$ ,  $J_{21}$ , and  $J_{23}$ , indicating the unidirectional potassium flux per unit length of tubule from lumen to cell, cell to lumen, and cell to blood respectively, can be given by

$$\begin{aligned} J_{12}(x) &= K(x) \cdot k'_{12} \cdot \left(\frac{v_1}{\Delta x}\right) \\ J_{21}(x) &= C_K(x) \cdot k'_{21} \cdot \left(\frac{v_2}{\Delta x}\right) \\ J_{23}(x) &= C_K(x) \cdot k'_{23} \cdot \left(\frac{v_2}{\Delta x}\right) \end{aligned}$$

where  $v_1$  and  $v_2$  are the volumes of the lumen and cell layer in the segment of length  $\Delta x$ , and  $k'_{ij}$  is the flux coefficient ( $\text{min}^{-1}$ ) mediating the flow of potassium from  $i$  to  $j$ . In accordance with the Giebisch cellular model,  $J_{21}$  and  $J_{23}$  are assumed to represent passive, non-carrier-mediated fluxes. Therefore, the electrical potential difference (PD) and the K permeability of the luminal and basolateral membranes will determine the values of  $k'_{21}$  and  $k'_{23}$ . The magnitude of the rate coefficient,  $k'_{12}$ , may be additionally influenced by the kinetics of the K reabsorptive luminal pump.



Since  $v_1/\Delta x$  and  $v_2/\Delta x$  define the cross-sectional area of the lumen and cell layer respectively, we have

$$J_{12}(x) = K(x) \cdot k'_{12} \cdot a_1$$

$$J_{21}(x) = C_K(x) \cdot k'_{21} \cdot a_2$$

$$J_{23}(x) = C_K(x) \cdot k'_{23} \cdot a_2$$

In order to maintain a degree of clarity in the mathematical treatment which follows, it will be convenient to define a flux coefficient,  $k_{ij}$ , as follows:

$$k_{ij} \equiv k'_{ij} \cdot a_i \quad (\text{cm}^2 \times 10^{-5}/\text{min} \equiv \text{nl}/\text{min}/\text{mm})$$

$$\text{for } k_{ij}: k_{12}, k_{21}, k_{23}$$

thereby eliminating geometrical terms in the mathematical development of the transport models. Thus the three transmembrane fluxes are defined simply as

$$J_{12}(x) = K(x) \cdot k_{12}$$

$$J_{21}(x) = C_K(x) \cdot k_{21}$$

$$J_{23}(x) = C_K(x) \cdot k_{23}$$

At this point, no specific characterization will be given to the blood to cell potassium flux,  $J_{32}$ , a significant component of which is mediated by the Na-K-ATPase pump. The mathematical models will be defined partly in terms of alternative postulates regarding the behavior of  $J_{32}$ .



D. FUNDAMENTAL EQUATIONS

It is presumed that for any imposed initial condition,  $V(0)$  and  $K(0)$ , a steady state will eventually prevail in which there will be no net change over time in the amount of potassium or volume within the lumen or cell layer. Specifically, over any given segment,  $\Delta x$ , consideration of mass balance dictates that during the steady state, the amount of  $K$  entering the tubular lumen and the cell layer must equal the amount of  $K$  leaving. That is,

for cell:

$$(\Delta x \cdot a_1) \cdot \frac{dK(\bar{x})}{dt} = 0 = [J_{32}(\bar{x}) + K(\bar{x}) \cdot k_{12} - C_K(\bar{x}) \cdot (k_{21} + k_{23})] \cdot \Delta x \quad (2)$$

for lumen:

$$\begin{aligned} (\Delta x \cdot a_1) \cdot \frac{dK(\bar{x})}{dt} = 0 = & K(x) \cdot V(x) + C_K(\bar{x}) \cdot k_{21} \cdot \Delta x \\ & - K(x + \Delta x) \cdot V(x + \Delta x) - K(\bar{x}) \cdot k_{12} \cdot \Delta x \end{aligned}$$

or,

$$\frac{K(x + \Delta x) \cdot V(x + \Delta x) - K(x) \cdot V(x)}{\Delta x} = C_K(\bar{x}) \cdot k_{21} - K(\bar{x}) \cdot k_{12} \quad (3)$$

where  $K(\bar{x})$  and  $C_K(\bar{x})$  represent the mean luminal and cellular  $K$  concentrations in the  $\Delta x$  segment, and  $J_{32}(\bar{x})$ , the mean rate of blood to cell  $K$  flux per unit length.

Since the macroscopic kinetics of the system can be very adequately approximated by assuming cell boundaries to have infinitesimally small dimensions, we may consider the limits for equations (2) and (3) as  $\Delta x \rightarrow 0$ .

For equation (2), evaluating the limit and then solving for  $C_K(x)$  gives

$$C_K(x) = \frac{J_{32}(x) + K(x) \cdot k_{12}}{k_{21} + k_{23}}$$





and for equation (3),

$$\frac{d[V(x) \cdot K(x)]}{dx} = J_s(x) = C_K(x) \cdot k_{21} - K(x) \cdot k_{12}$$

where  $J_s(x)$  is the rate of net transepithelial potassium secretion per unit length by the tubule at  $x$ .

The differential equation and the accompanying equation for cell K concentration,

$$J_s(x) = \frac{d[V(x) \cdot K(x)]}{dx} = C_K(x) \cdot k_{21} - K(x) \cdot k_{12} \quad (4)$$

where:

$$C_K(x) = \frac{J_{32}(x) + K(x) \cdot k_{12}}{k_{21} + k_{23}} \quad (5)$$

represent the fundamental kinetic description of late distal tubular K transport under the assumptions set forth up to this point. In order to integrate equation (4), the various parameters must be further defined.

Several assumptions basic to all models to be described will facilitate the integration of equation (4).

Assumption 1: The K secreting segment of the late distal tubule can be well approximated by considering it to be composed of identical K transporting cellular units.

From this assumption, it follows that the kinetics defined for any one cell (or infinitesimally small tubule segment) in the epithelium apply equally to the entire epithelium. As a consequence of this assumption, when there is no luminal flow in the hypothetical tubule, there will be no variation along  $x$  in the value of any of the kinetic parameters. However, as flow is directed into the tubule, certain axial gradients may



develop in any or all of the parameter values of equations (4) and (5) depending on the characteristic kinetic behavior of a given model.

Assumption 2: The effects of all determinants of K transport other than the parameters identified in equations (4) and (5) are assumed to be constant.

This assumption places the secretory model in an unvarying physiological setting in which such factors as plasma potassium concentration, diet, acid-base balance, hormonal influences, and the like are deemed to be constant. An important corollary of this assumption is that the kinetics of potassium transport can be defined independent of any consideration of luminal sodium concentration variation which might be anticipated to occur with flow rate changes. This assumption is consistent with the observations of Good and Wright discussed in Part I which indicate that K secretion is not significantly influenced by the load of sodium delivered to the distal tubule when other physiological determinants of K transport (aside from flow rate) are held constant (26,27).

Assumption 3: Passive, non-carrier-mediated potassium fluxes are adequately approximated by the Goldman "constant field" equations for ion transport through charged biological membranes.

The Goldman equation for the net passive flux of a positive ion across a charged membrane is given by

$$J_0 - J_i = (P\pi d) \cdot \frac{\Delta EF}{RT} \cdot \frac{[C_i \cdot \exp(-\Delta EF/RT) - C_0]}{[1 - \exp(-\Delta EF/RT)]} \quad (6a)$$

where: P ≡ permeability

$\Delta E = E_0 - E_i$

d ≡ lumen diameter

C ≡ concentration of ion

$i,0$  ≡ inside, outside of cell

J ≡ flux per tubule unit length



For the unidirectional passive fluxes,  $J_{21}$  and  $J_{23}$ , we obtain

$$J_{21} = P_{\ell} \pi d \cdot \frac{\Delta E_{\ell} F}{RT} \cdot \frac{C_K \cdot \exp(-\Delta E_{\ell} F/RT)}{1 - \exp(-\Delta E_{\ell} F/RT)} \quad (6b)$$

$$J_{23} = P_b \pi d \cdot \frac{\Delta E_b F}{RT} \cdot \frac{C_K \cdot \exp(-\Delta E_b F/RT)}{1 - \exp(-\Delta E_b F/RT)} \quad (6c)$$

where:  $C_K \equiv$  cell K concentration

$\ell, b \equiv$  luminal, basolateral membranes

If the membrane potential difference,  $\Delta E$ , is constant under all luminal and cellular conditions, as will be assumed in several models, then equations (6b) and (6c) are related to the previously defined flux relationships as follows:

$$J_{21} = C_K \cdot k_{21} \quad J_{23} = C_K \cdot k_{23}$$

therefore:

$$k_{21} = \frac{\Delta E_{\ell} F}{RT} \cdot \frac{P_{\ell} \pi d \cdot \exp(-\Delta E_{\ell} F/RT)}{1 - \exp(-\Delta E_{\ell} F/RT)}$$

$$k_{23} = \frac{\Delta E_b F}{RT} \cdot \frac{P_b \pi d}{1 - \exp(-\Delta E_b F/RT)}$$

Thus for a passive unidirectional flux across a membrane of constant  $\Delta E$  and  $P$ ,  $k_{ij}$  is constant, and  $J_{ij}$  is linearly dependent on  $C_K$  (in the case of  $J_{21}$  and  $J_{23}$ ). In one of the models to be discussed, the membrane PD is permitted to vary, and therefore  $k_{ij}$  will not be a constant term but dependent in part on the magnitude of  $\Delta E$ .



## E. WORKING POSTULATES

With the preceding basic assumptions in hand, it remains to define more specifically the parameters of equations (4) and (5):  $k_{ij}$ ,  $C_K$ , and  $J_{32}$ . The following postulates regarding these parameters will establish the basis for the various mathematical model solutions of the fundamental differential equation (4).

### 1. The luminal membrane rate coefficients: $k_{21}, k_{12}$

As previously noted, the rate coefficient,  $k_{ij}$ , incorporates into one term the effects of membrane permeability, electrical potential difference, and carrier-mediated transport mechanisms (active or facilitated) on the flux  $J_{ij}$ . Membrane K permeability is assumed to be independent of  $x$  and electrical PD and constant over physiological ranges of cell, blood or luminal K concentrations.

Postulate 1: The luminal membrane PD is constant and independent of  $x$  and cell or luminal ion concentrations.

Several experimental observations indicate that variations in the transepithelial PD of the late distal tubule are relatively small over a wide range of flow rates and changes in luminal Na and K concentrations (26,29,60). Whether this relative stability of the transepithelial PD reflects parallel PD changes in the luminal and basolateral membranes or whether it indicates a constancy of both membrane PD's during changes in luminal conditions is uncertain. There is no experimental data to clarify this issue. However, in order to gain insight into the significance of the luminal membrane PD on K secretory behavior, a





model in which the luminal membrane PD arises entirely as a consequence of a K diffusion potential will be examined and contrasted with models based on Postulate 1.

From Postulate 1 it follows that  $k_{21}$ , the rate coefficient mediating the passive flux,  $J_{21}$ , is a constant parameter, independent of  $x$ ,  $K(x)$ , and  $C_K(x)$ .

Postulate 2: The carrier-mediated flux component of  $J_{12}$  is nonsaturable over physiological ranges of luminal K concentrations and obeys linear kinetics; that is, the carrier-mediated flux from lumen to cell is directly proportional to the luminal K concentration.

Combining Postulates 1 and 2, we have, therefore, that  $k_{12}$  is a constant parameter, independent of  $x$ ,  $K(x)$  and  $C_K(x)$ . There is no experimental data which bears directly on Postulate 2. Therefore, the K secretory behavior resulting from the linear kinetics of  $J_{12}$  will be contrasted with a model which incorporates a hypothetical saturable K reabsorptive pump in the luminal membrane.

## 2. Cell Potassium

Again, there is no experimental data which permits a definition of the behavior of cell K concentration in the face of varied luminal conditions. The mathematical modeling will therefore contrast two plausible but quite opposed assumptions regarding cell K.

Postulate 3a: Cell K concentration is constant and independent of  $x$  and  $J_S(x)$



Postulate 3b:  $J_{32}$  and  $k_{23}$  are constant and independent of  $x$  and  $J_S(x)$ , and

$$C_K(x) = \frac{J_{32} + K(x) \cdot k_{12}}{k_{21} + k_{23}} \quad (\text{equation (5)})$$

In effect, Postulate 3a assigns to the basolateral membrane the function of regulating cell potassium at a constant level.  $J_{32}$  and  $J_{23}$ , therefore, do not need to be characterized specifically. Challenges to the stability of cell K concentration arising from changes in luminal conditions are assumed to be met by appropriate adjustments in the fluxes  $J_{32}$  and  $J_{23}$ .

A somewhat speculative argument may be advanced to defend Postulate 3a. It can be argued, for instance, that as luminal flow rate increases and luminal K concentration falls, the net flux of potassium from the cell to the lumen would be augmented, thus resulting in a lowering of cell K concentration. An increase in cell Na concentration would probably occur concurrently. The changed cell ionic milieu would then be favorable to an accelerated extrusion of Na and uptake of K at the basolateral membrane, a kinetic behavior that is consistent with some kinetic descriptions of the Na-K-ATPase dependent transport system (32,33,53). It is postulated that the sum effect of such events would be the restoration of cell K to its original concentration.

The alternative Postulate 3b - a constant  $J_{32}$  flux - is posed as a means of sharply contrasting two very different views of the role of the carrier-mediated transport at the basolateral membrane. Several important questions will be answered from the analysis of a model formulated on the basis of Postulate 3b. For example: If  $J_{32}$  is constant, to



what extent will cell K concentration decrease as luminal flow rate is increased, and to what degree will net K transport be affected?

Finally, it will be noted here and proved later that Postulates 3a and 3b actually represent special cases of a more general hypothesis: that cell K concentration decreases in direct proportion to increases in the net transepithelial potassium flux,  $J_s$ , that is,

$$\frac{dC_K(x)}{dJ_s(x)} = - \alpha \quad (7)$$

where  $\alpha$  is an arbitrary constant. Under Postulate 3a,  $\alpha$  equals zero. The value of  $\alpha$  for the model formulated on the basis of Postulate 3b will be derived later.

The main body of the presentation will concentrate on exploring two mathematical models, each of which incorporates Postulates 1 and 2, but which are distinguished by the alternative forms of Postulate 3. They will be described as MODEL A - constant cell K model and MODEL B - constant  $J_{32}$  model. After these models are examined in detail, other models will be developed and analyzed to explore alternatives to the luminal membrane behavior defined by Postulates 1 and 2. Formally stated, Models A and B are:

MODEL A - constant cell K

- (1) Cell K concentration is constant and independent of  $x$  and  $J_s(x)$
- (2)  $k_{12}$  and  $k_{21}$  are constant parameters independent of  $x$ ,  $K(x)$ ,  $C_K(x)$  and  $V(x)$



MODEL B - constant  $J_{32}$

- (1)  $J_{32}$  is constant and independent of  $x$  and  $J_s(x)$
- (2)  $k_{12}$ ,  $k_{21}$ , and  $k_{23}$  are constant parameters independent of  $x$ ,  $K(x)$ ,  $C_K(x)$  and  $V(x)$





F. MODELS A AND B MATHEMATICAL SOLUTIONS WITH NO VOLUME REABSORPTION

For the initial evaluation of the fundamental differential equation (4), the special case of no volume reabsorption will be considered.  $V$ , the luminal flow rate is therefore considered to be independent of  $x$ .  $V(0)$ , the initial flow rate, equals  $V(L)$ , the end segment flow rate. The differential equation (4) as applied to Model A simplifies to

$$\text{Model A} \quad \frac{dK(x)}{dx} = \frac{1}{V} [C_K \cdot k_{21} - K(x) \cdot k_{12}]$$

constant parameters:  $C_K, k_{12}, k_{21}$

Combining equations (4) and (5) and simplifying gives for Model B

$$\text{Model B} \quad \frac{dK(x)}{dx} = \frac{1}{V} [J_{32} \cdot k_s - K(x) \cdot k_r]$$

constant parameters:  $J_{32}$

$$k_s = k_{21} / (k_{21} + k_{23})$$

$$k_r = (k_{12} \cdot k_{23}) / (k_{21} + k_{23})$$

The complex rate coefficients  $k_s$  and  $k_r$  are defined as a matter of convenience.

The two equations represent linear, 1st order differential equations where  $\frac{dK(x)}{dx}$  is a function of  $K(x)$  and constant parameters independent of  $x$  and  $K(x)$ . Solutions to the equations may be found by formal separation of the variables and integration over the boundary conditions.

$$\int_{x=0}^x \quad \text{and} \quad \int_{K(0)}^{K(x)}$$

The results are:

Model A (constant cell  $K$ )

$$K(x) = K(0) \cdot \exp(-k_{12} \cdot x/V) + \frac{C_K \cdot k_{21}}{k_{12}} [1 - \exp(-k_{12} \cdot x/V)] \quad (8)$$



Model B (constant  $J_{32}$ )

$$K(x) = K(0) \cdot \exp(-k_r \cdot x/V) + \frac{J_{32} \cdot k_s}{k_r} [1 - \exp(-k_r \cdot x/V)] \quad (9)$$

Equations (8) and (9) mathematically define the axial profile of potassium concentration as a function of the initial conditions,  $V$  and  $K(0)$ , the rate coefficients, and the cell  $K$  concentration for Model A and the magnitude of  $J_{32}$  for Model B.

Net  $K$  absorption has been defined as

$$\phi(\text{net}) = V(L) \cdot K(L) - V(0) \cdot K(0) \quad (1)$$

Substituting for  $K(L)$  from equations (8) and (9) gives, after rearrangement of the terms,

Model A

$$\phi(\text{net}) = V \cdot \left[ \frac{C_K \cdot k_{21}}{k_{12}} - K(0) \right] [1 - \exp(-k_{12} \cdot L/V)] \quad (10)$$

Model B

$$\phi(\text{net}) = V \cdot \left[ \frac{J_{32} \cdot k_s}{k_r} - K(0) \right] [1 - \exp(-k_r \cdot L/V)] \quad (11)$$

These equations are further simplified by considering the following definitions.

$K(\text{max})$ : the limiting concentration of  $K$  uniformly attained within the tubular lumen as flow rate approaches zero.

$$K(\text{max}) = \lim_{V \rightarrow 0} K(x)$$



$\frac{\phi_s^{\max}}{S}$ : the maximum rate of K secretion which is approached when  $K(0) = 0$  and  $V \rightarrow \infty$

$$\phi_s^{\max} = \lim_{\substack{V \rightarrow \infty \\ K(0) = 0}} \phi(\text{net})$$

$K(\max)$  and  $\phi_s^{\max}$  are operationally defined as limits in order to facilitate the handling of equations (8), (9), (10) and (11) in which  $V$  arises as a denominator in the exponential term.  $K(\max)$  represents the equilibrium value of luminal  $K$  concentration under zero flow rate conditions. Though perhaps not immediately apparent from the above definition,  $\phi_s^{\max}$  will be seen to represent the maximum  $K$  secretion capability of the epithelium as defined by Models A and B.

The evaluation of the above limits for equations (8), (9), (10) and (11) is facilitated by noting the existence of the following limits, proofs of which are provided in the Appendix.

$$\lim_{V \rightarrow 0} \exp(-b/V) = 0$$

$$\lim_{V \rightarrow 0} A \cdot [1 - \exp(-b/V)] = A$$

$$\lim_{V \rightarrow \infty} \frac{V}{b} [1 - \exp(-b/V)] = 1$$

where:  $A$  and  $b$  are arbitrary constants

Therefore, for Model A

$$K(\max) = \frac{J_{32} \cdot k_s}{k_r}$$

$$\phi_s^{\max} = J_{32} \cdot k_s \cdot L$$



and similarly for Model B

$$K(\max) = \frac{C_K \cdot k_{21}}{k_{12}}$$

$$\phi_s^{\max} = C_K \cdot k_{21} \cdot L$$

Substituting the results from above into the original solutions, we obtain the general equations

$$K(x) = K(0) \cdot \exp(-k_a \cdot x/V) + K(\max) \cdot [1 - \exp(-k_a \cdot x/V)] \quad (12)$$

$$\phi(\text{net}) = V \cdot [K(\max) - K(0)] [1 - \exp(-k_a \cdot L/V)] \quad (13)$$

$$\phi_s^{\max} = K(\max) \cdot k_a \cdot L \quad (14)$$

where:

Model A

$$k_a = k_{12}$$

$$K(\max) = \frac{C_K \cdot k_{21}}{k_{12}}$$

$$\phi_s^{\max} = C_K \cdot k_{21} \cdot L$$

Model B

$$k_a = (k_{12} \cdot k_{23}) / (k_{21} + k_{23}) \equiv k_r$$

$$K(\max) = \frac{J_{32} \cdot k_{21}}{k_{12} \cdot k_{23}} \equiv \frac{J_{32} \cdot k_s}{k_r}$$

$$\phi_s^{\max} = \frac{J_{32} \cdot k_{21}}{k_{21} + k_{23}} \cdot L \equiv J_{32} \cdot k_s \cdot L$$

Models A and B thus yield mathematical solutions which differ only in the definition of the two constant parameters:  $k_a$ , the "absorption" rate coefficient, and  $K(\max)$ .





$J_s(x)$ , the rate of transepithelial potassium secretion per unit length of tubule may be derived readily by recalling from equation (4) that  $J_s(x)$  also indicates the rate of change of the axial flux of potassium per unit length; that is,

$$J_s(x) = V \cdot \frac{dK(x)}{dx}$$

Differentiating equation (12), we have

$$\begin{aligned} \frac{dK(x)}{dx} &= \frac{K(\max) \cdot k_a}{V} \exp(-k_a \cdot x/V) - \frac{K(0) \cdot k_a}{V} \exp(-k_a \cdot x/V) \\ &= \frac{1}{V} [K(\max) - K(0)] \cdot k_a \cdot \exp(-k_a \cdot x/V) \end{aligned}$$

and multiplying both sides by  $V$  gives

$$J_s(x) = [K(\max) - K(0)] \cdot k_a \cdot \exp(-k_a \cdot x/V) \quad (15)$$

and for the special case of  $K(0) = 0$

$$J_s(x) = K(\max) \cdot k_a \cdot \exp(-k_a \cdot x/V) \quad (16)$$

An alternative expression for  $J_s(x)$  can be found by noting that a rearrangement of equation (12) gives

$$[K(\max) - K(0)] \cdot \exp(-k_a \cdot x/V) = K(\max) - K(x) \quad (17)$$

Combining equations (15) and (17), we obtain

$$J_s(x) = K(\max) \cdot k_a - K(x) \cdot k_a \quad (18)$$

and since we can define  $J_s(\max)$  as

$$J_s^{\max} = \Phi_s^{\max}/L = K(\max) \cdot k_a \quad (19)$$

equation (18) further simplifies to

$$J_s(x) = J_s^{\max} - K(x) \cdot k_a \quad (20)$$



In terms of Models A and B:

$$J_s^A(x) = C_K \cdot k_{21} - K(x) \cdot k_{12} \quad (21)$$

$$J_s^B(x) = \frac{J_{32} \cdot k_{21}}{k_{21} + k_{23}} - K(x) \cdot \frac{k_{12} \cdot k_{23}}{k_{21} + k_{23}} \quad (22)$$

The equation for Model A is immediately identifiable as the net flux of K across the luminal membrane.

$$J_s^A(x) = J_{21} - J_{12}(x)$$

For Model B, we can draw from the formulation by Ussing (58) who derived the following relationships (modified to the present context):

$$J_{31} = J_{32} \cdot \frac{k_{21}}{k_{21} + k_{23}}$$

$$J_{13} = J_{12} \cdot \frac{k_{23}}{k_{21} + k_{23}}$$

where  $J_{31}$  is that proportion of the unidirectional K flux from blood to cell which reaches the lumen, and  $J_{13}$  is that proportion of  $J_{12}$  which reaches the blood. Therefore,

$$J_s^B(x) = J_{31} - J_{13}(x)$$

Note that  $J_{21}$  of Model A and  $J_{31}$  of Model B are constant fluxes equivalent to  $J_s^{\max}$  as defined for each model. Therefore, the secretory potency of Model A is limited by the luminal membrane flux,  $J_{21}$ , the magnitude of which is determined by  $C_K$  and  $k_{21}$ . For Model B, the upper limit of secretion capability is determined by  $J_{31}$ , the proportion of cell K uptake from the blood which is transported to the lumen. The magnitude of  $J_{32}$  and the fraction  $k_{21}/(k_{21} + k_{23})$  will determine the secretory potency of Model B.



For Model B, it will be important to identify the variability of cell K concentration resulting from changes in luminal flow rate and K concentration. We will restrict ourselves to deriving a mathematical statement for the mean cell K concentration along the tubule.

Equation (5) defines  $C_K(x)$  as a function of  $K(x)$ .

$$C_K(x) = \frac{J_{32}}{k_{21} + k_{23}} + \frac{k_{12}}{k_{21} + k_{23}} \cdot K(x) \quad (5)$$

Rearranging equation (18) gives

$$K(x) = K(\max) - J_s(x)/k_a$$

$$\text{where: } k_a = (k_{12} \cdot k_{23}) / (k_{21} + k_{23})$$

(Model B)

and substituting for  $K(x)$  in equation (5), we have, after simplification,

$$C_K(x) = \frac{J_{32}}{k_{21} + k_{23}} + K(\max) \cdot \frac{k_{12}}{k_{21} + k_{23}} + \frac{J_s(x)}{k_{23}} \quad (23)$$

The mean cell K concentration along the tubule may be defined by

$$\bar{C}_k = \frac{1}{L} \int_0^L C_K(x) dx \quad (24)$$

and since

$$\frac{1}{L} \int_0^L J_s(x) dx = \phi(\text{net})/L$$

integration of equation (23) in the manner defined by (24) gives

$$\bar{C}_K = \frac{J_{32}}{k_{21} + k_{23}} + \frac{K(\max) \cdot k_{12}}{k_{21} + k_{23}} - \frac{\phi(\text{net})}{k_{23} \cdot L}$$

Since for Model B,

$$K(\max) = J_{32} \cdot \frac{k_{21}}{k_{12} \cdot k_{23}}$$



after substituting and combining terms,

$$\bar{C}_K = J_{32} \left[ \frac{1}{k_{21} + k_{23}} + \frac{k_{12} \cdot k_{21}}{(k_{12} \cdot k_{23})(k_{21} + k_{23})} \right] - \frac{\phi(\text{net})}{k_{23} \cdot L}$$

which simplifies to

$$\bar{C}_K = \frac{J_{32}}{k_{23}} - \frac{\phi(\text{net})}{k_{23} \cdot L}$$

If we define  $C_K^{\text{max}}$  as that cellular K concentration attained under conditions of no net K transport, that is,  $\phi(\text{net}) = 0$ , then<sup>2</sup>

$$\bar{C}_K = C_K^{\text{max}} - \frac{\phi(\text{net})}{k_{23} \cdot L} \quad (25)$$

$$\text{where: } C_K^{\text{max}} = \frac{J_{32}}{k_{23}} \quad (26)$$

It can be shown that the minimum cell K concentration will be attained when K secretion is at its maximal rate,  $\phi_s^{\text{max}}$ , and that

$$C_K^{\text{min}} = C_K^{\text{max}} \cdot \frac{k_{23}}{k_{21} + k_{23}} \quad (27)$$

Equation (27) indicates that cell K concentration under the assumptions of Model B will always be greater than zero but less than  $C_K^{\text{max}}$  by the fraction  $k_{21}/(k_{21} + k_{23})$ .

This completes the derivation of the Model A and B solutions, a summary statement of which is given in Table II.1.

Although our attention has been confined exclusively to Models A and B up to this point, it was briefly noted earlier that the two models are formulated as special cases of a broader definition of the postulated behavior of cell K in relation to K transport: that cell potassium





Table II.1 Model A and B equations

A. General equations

$$\begin{aligned}
 & \frac{K(0) \neq 0}{K(0) = 0} \\
 K(x) &= K(0) \cdot \exp(-k_a \cdot x/V) + K(\max) [1 - \exp(-k_a \cdot x/V)] & K(\max) [1 - \exp(-k_a \cdot x/V)] \\
 \Phi(\text{net}) &= V[K(\max) - K(0)] [1 - \exp(-k_a \cdot L/V)] & V \cdot K(\max) [1 - \exp(-k_a \cdot L/V)] \\
 J_s(x) &= [K(\max) - K(0)] \cdot k_a \cdot \exp(-k_a \cdot x/V) & K(\max) \cdot k_a \cdot \exp(-k_a \cdot x/V)
 \end{aligned}$$

Model A

$$k_a = k_{12}$$

$$K(\max) = \frac{C_K \cdot k_{21}}{k_{12}} = \frac{\Phi_S^{\max}}{k_{12} \cdot L}$$

$$\Phi_{1S}^{\max} = K(\max) \cdot k_a \cdot L = C_K \cdot k_{21} \cdot L$$

Model B

$$\frac{k_{12} \cdot k_{23}}{k_{21} + k_{23}}$$

$$\frac{J_{32} \cdot k_{21}}{k_{12} \cdot k_{23}} = \frac{\Phi_S^{\max} \cdot (k_{21} + k_{23})}{k_{12} \cdot k_{23} \cdot L}$$

$$\frac{J_{32} \cdot k_{21}}{k_{21} + k_{23}} \cdot L$$

B. Cell K concentration, Model B

$$\bar{C}_K = C_K^{\max} - \frac{\Phi(\text{net})}{k_{23} \cdot L}$$

$$C_K^{\max} = \frac{J_{23}}{k_{23}}$$

$$C_K^{\min} = C_K^{\max} \cdot \frac{k_{23}}{k_{21} + k_{23}}$$



concentration is linearly related to the net transepithelial secretory flux,  $J_s(x)$ , such that

$$\frac{dC_K(x)}{dJ_s(x)} = -\alpha \quad (28)$$

where  $\alpha$  is a constant with the dimensions  $\text{min/cm}^2 \times 10^{-5}$ .

The assumption defined by equation (28) permits a more generalized treatment of the basic differential equation (4). If we again define operationally the maximum cell K concentration,  $C_K^{\text{max}}$ , as that concentration attained under conditions of zero net K transport, then we may integrate equation (28) over the boundary conditions

$$\left[ \begin{array}{l} C_K(x) \\ C_K^{\text{max}} \end{array} \right] \quad \text{and} \quad \left[ \begin{array}{l} J_s(x) \\ J_s = 0 \end{array} \right]$$

which gives the simple expression

$$\begin{aligned} C_K(x) &= C_K^{\text{max}} - \alpha \cdot J_s(x) \\ &= C_K^{\text{max}} - \alpha \cdot V \cdot \frac{dK(x)}{dx} \end{aligned} \quad (29)$$

Substituting equation (29) into the basic differential equation (4),

$$V \cdot \frac{dK(x)}{dx} = C_K^{\text{max}} \cdot k_{21} - \alpha \cdot k_{21} \cdot V \cdot \frac{dK(x)}{dx} - K(x) \cdot k_{12}$$

and then rearranging,

$$\frac{dK(x)}{dx} + \frac{k_{12}}{V(1+\alpha \cdot k_{21})} \cdot K(x) = C_K^{\text{max}} \cdot \frac{k_{21}}{V(1+\alpha \cdot k_{21})}$$

Integration of this equation is straightforward. The solution is

$$K(x) = K(0) \cdot \exp(-k_a \cdot x/V) + K(\text{max}) \cdot [1 - \exp(-k_a \cdot x/V)] \quad (30a)$$

$$\text{where: } k_a = k_{12}/(1 + \alpha \cdot k_{21}) \quad (30b)$$



$$K(\max) = C_K^{\max} \cdot k_{21}/k_{12} \quad (30c)$$

$$\Phi_s^{\max} = C_K^{\max} \cdot k_{21} \cdot L/(1 + \alpha \cdot k_{21}) \quad (30d)$$

which is the same solution format obtained for Models A and B, equations (12-14,26). It is a matter of algebraic manipulation to show that

$$\text{for Model A:} \quad \alpha = 0$$

$$\text{for Model B:} \quad \alpha = 1/k_{23}$$

Thus it can be appreciated that Models A and B represent special cases of the more general solution defined by equations (30a-d). It will be useful to keep in mind in the sections which follow that the analysis and conclusions formulated on the basis of the kinetic behavior of Models A and B can be frequently generalized to include any epithelium characterized by a constancy of the rate coefficients for the luminal membrane,  $k_{12}$  and  $k_{21}$ , and a cell K concentration that decreases in direct proportion to increases in net transepithelial K transport.



G. QUALITATIVE EXAMINATION OF THE K SECRETORY BEHAVIOR OF MODELS A AND B

In this section, graphs of three functional relationships among the parameters of the basic model equations will be examined:

$$K(L) = f[V]: K(L) = K(\max) \cdot [1 - \exp(-k_a \cdot L/V)] \quad (31)$$

$$\phi(\text{net}) = f[V]: \phi(\text{net}) = V \cdot K(\max) \cdot [1 - \exp(-k_a \cdot L/V)] \quad (32)$$

$$\phi(\text{net}) = f[K(0)]: \text{equations defined below}$$

For the limited purposes here of illustrating the qualitative character of these functions in terms of graphical plots, the dependent variable of the first two functions will be made dimensionless by dividing both sides of equations (31) and (32) by  $K(\max)$  and  $\phi_s^{\max}$  (which equals  $K(\max) \cdot k_a \cdot L$ ) respectively.

$$\%K(\max) = [1 - \exp(-k_a \cdot L/V)] \cdot 100\% \quad (33)$$

$$\%\phi_s^{\max} = \frac{V}{k_a \cdot L} [1 - \exp(-k_a \cdot L/V)] \cdot 100\% \quad (34)$$

The independent variable of the first two equations,  $V$ , will be varied from 0 to 40 nl/min which extends somewhat beyond the range of distal tubular flow rates observed under in vivo conditions. The functions will be studied with the rate coefficient,  $k_a$ , set at three values, 3, 10, and 30 nl/min/mm, which are representative of kinetic data derived from in vivo experiments (to be presented in subsequent sections) under a variety of physiological conditions. The length of the tubular segment,  $L$ , will be taken at 1 mm corresponding approximately to the length of the late distal tubule. Note that  $k_a \cdot L$  has the dimensions of flow rate, nl/min.





1. K(L) and  $\phi(\text{net})$  as a function of flow rate

Plots of equations (33) and (34) are illustrated in Figure II.5 for the three indicated values of  $k_a$ . The graph of  $K(L) = f(V)$  is sigmoidal in character with an inflection point at  $V = k_a \cdot L$ . As flow through the system is increased beyond zero,  $K(L)$  is initially maintained near its maximal value but falls towards zero at higher flow rates. The fall in  $K(L)$  with increasing flow rate is less precipitous when  $k_a$  takes on higher values. The corresponding plot of  $\phi(\text{net})$  vs.  $V$  is shown in Figure II.5b. Here,  $K$  secretion is seen to rise in a quasi-exponential fashion, approaching a maximal rate at high flow rates. On each graph, the point where  $k_a \cdot L = V$  is indicated, corresponding to the inflection point of the  $K(L)$  vs.  $V$  plot. Locating this point conveniently divides each graph into two characteristic phases of flow dependency. For flow rates less than  $k_a \cdot L$ , the dependency of  $K$  secretion on flow rate approximates a flow-limited secretion model. For flow rates exceeding  $k_a \cdot L$ , secretion is established relatively close to its maximal rate, and secretory behavior can be said to be predominantly transport-limited in character. Accordingly, it can be generalized that  $k_a \cdot L$  approximately characterizes the upper limit of flow rate for which flow-dependent  $K$  secretory behavior will be flow-limited in character for Models A and B.

The functional plot of  $\phi(\text{net}) = f(V)$  has been described as "quasi-exponential" since its mathematical features are quite distinct from the more familiar exponential function  $Y(x) = A(1 - e^{-bx})$ . The independent variable,  $x$ , arises as an exponent to Euler's number,  $e$ . In most of the functions to be described for Models A and B, the exponent to  $e$  will



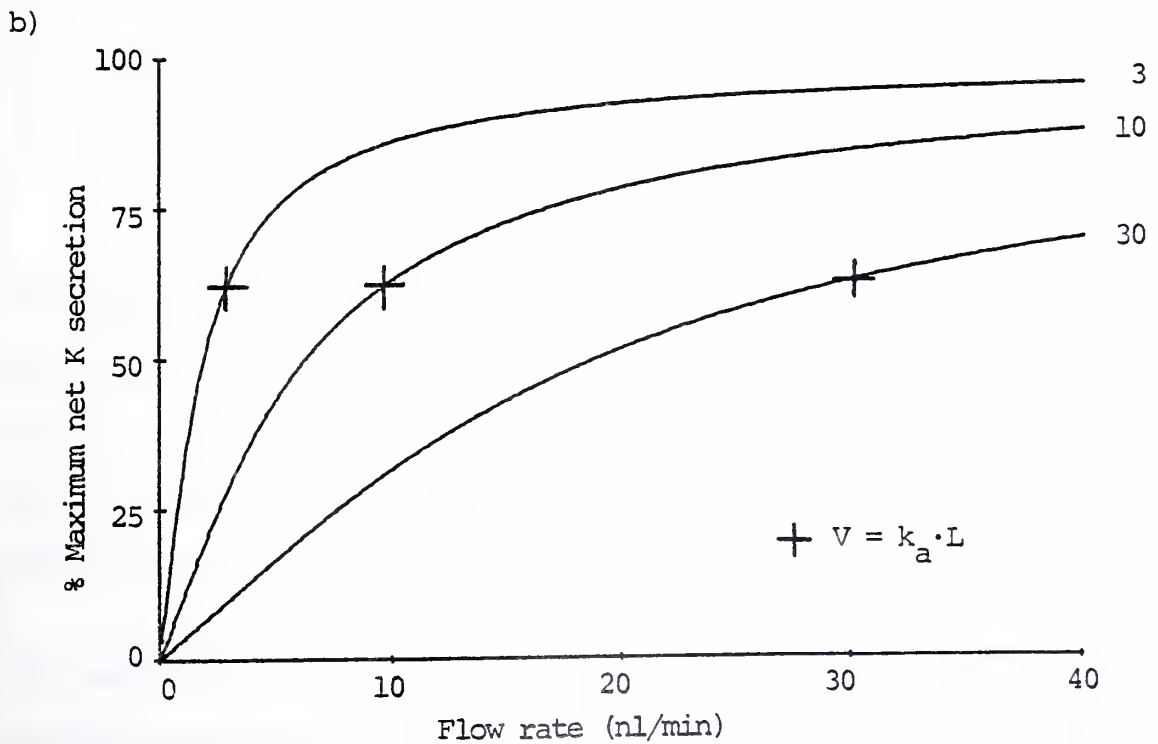
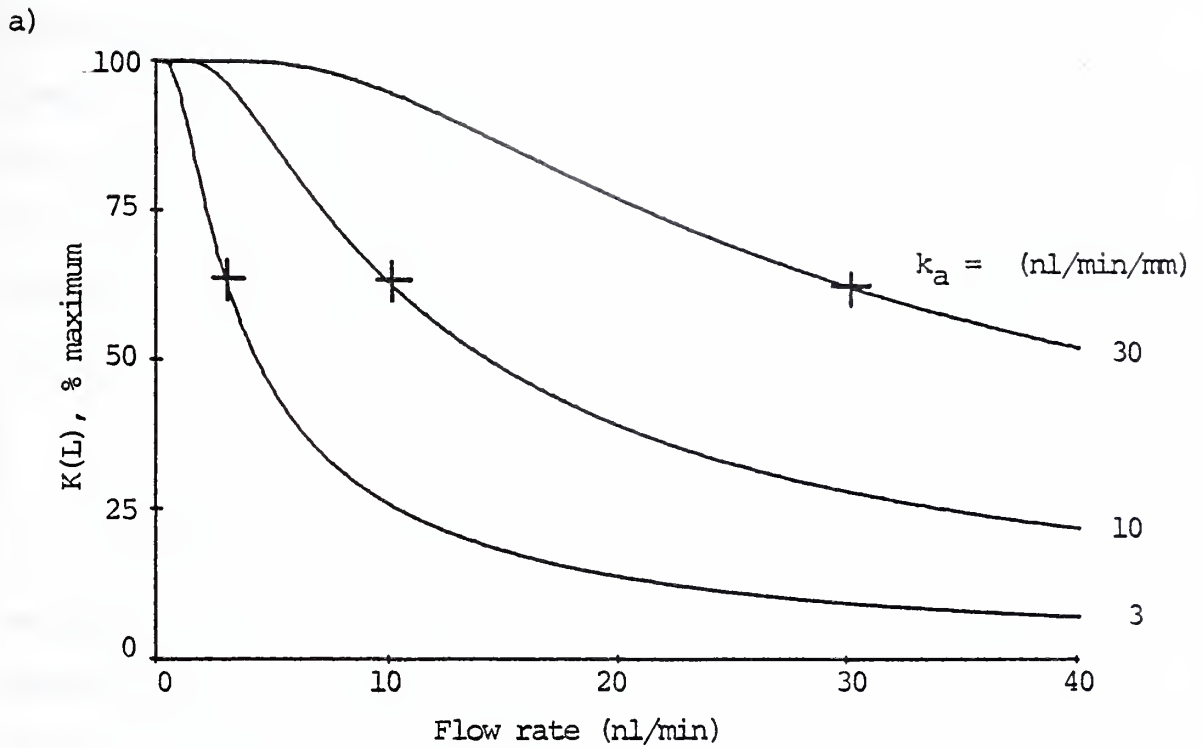


Figure II.5 Plots of % K(max) attained at  $x=L$  in relation to flow rate (a) and % maximum rate of K secretion in relation to flow rate (b). Model rate coefficient,  $k_a$ , as shown.  $K(0) = 0$  for all plots.



occur in the form  $(k_a \cdot L)/V$ , with the dependent variable  $V$  occurring in the denominator of the exponent. Accordingly, the mathematical behavior frequently will be difficult to appreciate without careful scrutiny. As a useful guide for future reference, the functions (in general form) to be encountered in subsequent sections are identified and graphed in Table II.2 with comparisons made to the more familiar exponential functions.

## 2. Net K secretion as a function of $K(0)$

An appreciation of the effect that  $K(0)$  has on net K transport is demonstrated in Figure II.6a where  $\% \phi_s^{\max}$  is plotted as a function of  $V$  for several different values of  $K(0)$ . (The value of  $k_a \cdot L$  is set at 10 nL/min for all plots.) The graphs arise from plotting equation (13) after dividing both sides of the equation by  $\phi_s^{\max}$  ( $= K(\max) \cdot k_a \cdot L$ ).

$$\% \phi_s^{\max} = \frac{V}{k_a \cdot L} [1 - K(0)/K(\max)] [1 - \exp(-k_a \cdot L/V)] \cdot 100\%$$

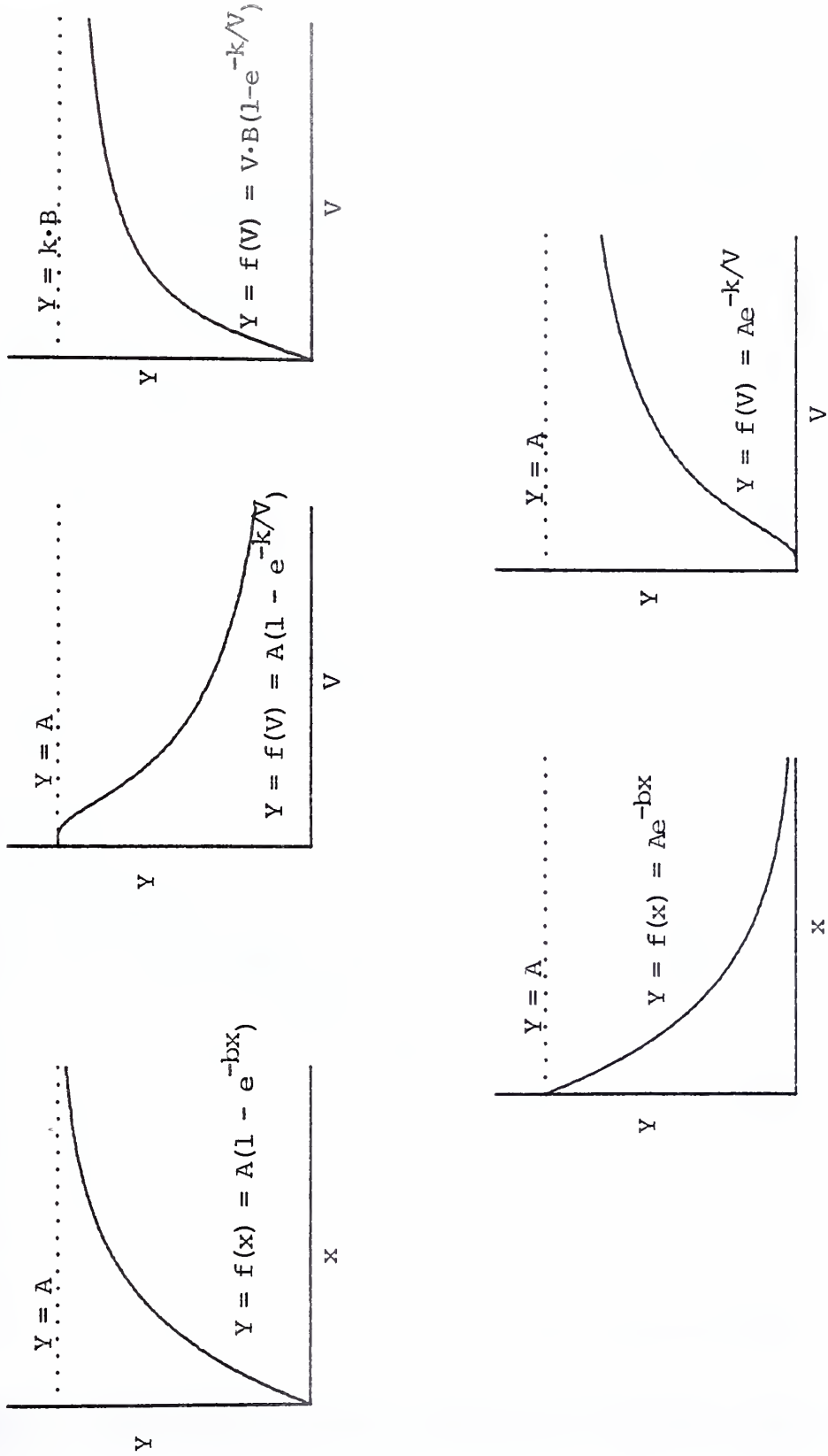
From Figure II.6a it is clear that the epithelium's capability to secrete potassium is diminished as  $K(0)$  is elevated. When  $K(0)$  equals  $K(\max)$ , net K secretion is, of course, zero. Higher  $K(0)$  values result in reabsorption of a portion of the potassium load entering the modeled tubule.

The sensitivity of net K absorption to the initial K load is more usefully examined by defining the mathematical expression for  $\phi(\text{net})$  as a function of  $K(0)$ . Rearranging equation (13) to a more suitable form gives

$$\phi(\text{net}) = -V \cdot [1 - \exp(-k_a \cdot L/V)] \cdot K(0) + V \cdot K(\max) \cdot [1 - \exp(-k_a \cdot L/V)]$$



Table II.2 Comparison of exponential functions in model equations with more familiar exponential functions



Model functions shown as  $Y = f(V)$ ; others as  $Y = f(x)$





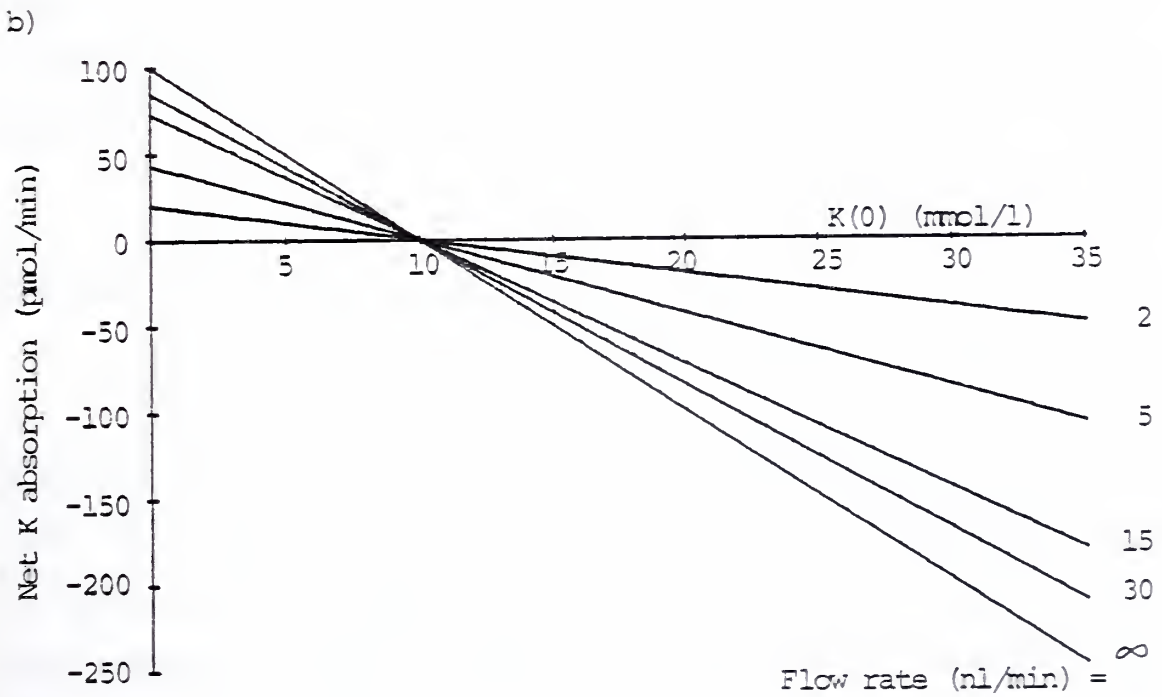
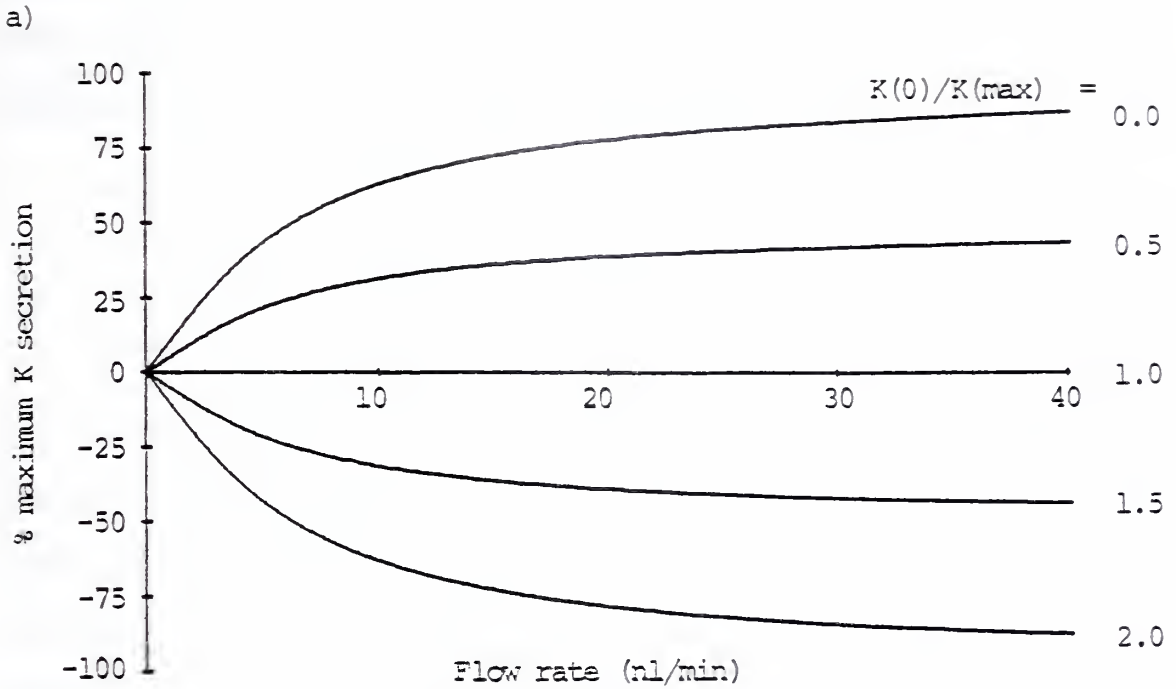


Figure II.6 a) The effect that the initial K concentration,  $K(0)/K(\max)$ , has on flow-dependent K transport ( $k_a=10$  nl/min/mm).  
 b) The relationship between  $K(0)$  and net K absorption at different flow rate ( $k_a=10$  nl/min/mm,  $K(\max)=10$  mmol/l).



From the above expression, it is evident that if flow rate and  $k_a$  are held constant and  $K(0)$  allowed to vary, the resulting plot will be a straight line with the following characteristic parameters:

Slope:  $-V \cdot [1 - \exp(-k_a \cdot L/V)]$

"Y" intercept:  $V \cdot K(\max) \cdot [1 - \exp(-k_a \cdot L/V)]$

"X" intercept:  $K(\max)$

The slope quantifies the  $K(0)$  sensitivity of the secretory model - the change in net  $K$  absorption that will arise from changes in  $K(0)$ , all other things being held constant. The more negative the slope, the higher the degree of sensitivity. Though not obvious from the mathematical expression for the slope, it will be seen that  $K(0)$  sensitivity increases as flow rate and/or  $k_a$  increase. Finally, it is of note to point out that as  $V \rightarrow \infty$ , the value of the slope approaches  $k_a \cdot L$ , that is,

$$\lim_{V \rightarrow \infty} -V \cdot [1 - \exp(-k_a \cdot L/V)] = -k_a \cdot L \quad (\text{see Appendix})$$

and the "Y" intercept approaches  $\phi_s^{\max}$  since

$$\lim_{V \rightarrow \infty} V \cdot K(\max) \cdot [1 - \exp(-k_a \cdot L/V)] = K(\max) \cdot k_a \cdot L = \phi_s^{\max}$$

Figure II.6b illustrates a plot of net  $K$  absorption as a function of  $K(0)$  for a number of different flow rates. The rate coefficient,  $k_a$ , is the same for all lines, 10 nl/min/mm. A value of 10 mmol/l has been assigned to  $K(\max)$ . ( $\phi_s^{\max}$  therefore equals 100 pmol/min.) Note that when  $K(0) = K(\max)$ , all plots intersect at the  $x$  axis since net  $K$  absorption will be zero regardless of flow rate. As indicated above, net  $K$  absorption is more markedly influenced by  $K(0)$  at higher flow rates.



Of the models considered here in Part II, the linear  $K(0)$  sensitivity shown in Figure II.6b is unique to Models A and B, and as will be seen, this feature will be quite helpful in distinguishing the  $K$  secretory behavior of these two models from others.

From what has been demonstrated up to this point, several observations will be made regarding Models A and B.

### Secretory potency

The maximal rate of  $K$  secretion is defined in relation to the parameters  $k_a$  and  $K(\max)$ :

$$\Phi_S^{\max} = K(\max) \cdot k_a \cdot L$$

and for Models A and B

$$A : \quad \Phi_S^{\max} = C_K \cdot k_{21} \cdot L \quad (35)$$

$$B : \quad \Phi_S^{\max} = J_{32} \cdot \frac{k_{21}}{k_{21} + k_{23}} \cdot L \quad (36a)$$

Since for Model B,  $C_K^{\max} = J_{32}/k_{23}$

$$B : \quad \Phi_S^{\max} = C_K^{\max} \cdot k_{21} \cdot \frac{k_{23}}{k_{21} + k_{23}} \cdot L \quad (36b)$$

It is apparent that in comparing equations (35) and (36b), for equivalent rate parameters and maximum cell  $K$  concentrations, the secretory potency of Model A will be stronger than Model B since the term  $k_{23}/(k_{21} + k_{23})$  is necessarily less than unity. On the other hand, it should be noted that either model will achieve any arbitrarily assigned  $\Phi_S^{\max}$  if the flux parameters are appropriately valued.



It is worth pointing out that both models accord well with the notion that the magnitude of K secretion is dependent in part on the activity of the Na-K-ATPase mediated flux,  $J_{32}$  and the consequent effect on cell K concentration (19,23,60). For example, elevation of the blood K concentration could stimulate an augmentation of  $J_{32}$ , an increase in cell K concentration (all other things being equal), and an enhanced rate of K secretion by both models. Also noteworthy is that an increase in the value of the rate coefficient,  $k_{21}$ , resulting from a decreased luminal membrane PD and/or increased K permeability would enhance K secretion for both models. Aldosterone has been claimed to be a hormonal mediator of such changes, though this view remains controversial (31,59,60).

#### Flow dependency

As concluded earlier, K secretion flow dependency can best be related to the parameter  $k_a$ . That is,

-predominantly flow-limited flow dependency when  $V < k_a \cdot L$

-predominantly transport-limited flow dependency when  $V > k_a \cdot L$

For a given set of rate coefficients, Model A will exhibit a wider flow rate range of flow-limited secretion since

$$k_a^A = k_{12}$$

$$k_a^B = k_{12} \cdot \frac{k_{23}}{k_{21} + k_{23}}$$

and,

$$\frac{k_{23}}{k_{21} + k_{23}} < 1$$





K(0) sensitivity

Since the luminal K concentration entering the late distal tubule is usually 2.0 mmol/l or less, K(0) sensitivity is relevant in the physiological setting only in those few instances where K(0) has been recognized to exceed this value (20,23). However, the linear K(0) sensitivity of Models A and B is distinct from all other models to be considered, and, therefore, experimental data bearing on the relationship of  $\Phi(\text{net})$  to K(0) over a broader than physiological range of initial K concentrations would be valuable in relating in vivo kinetic behavior to the theoretical predictions of Models A and B. Limited work in this area has been undertaken already by Good and Wright (27), and the relevance of their results to Models A and B will be discussed towards the end of Part II.



#### H. INCORPORATION OF IN VIVO KINETIC DATA INTO PARAMETERS OF MODELS A AND B

In order to develop a quantitative assessment of Models A and B appropriate to in vivo K secretory kinetics, it will be necessary to assign realistic values to the various kinetic parameters of the model equations. The only available experimental data suitable for this purpose comes from the classic distal tubule potassium kinetic study of DeMello-Aires et al (19). Briefly outlined, the experimental method involved the perfusion of capillary networks surrounding small segments of the late distal tubule with a  $^{42}\text{K}$  tracer solution while simultaneously perfusing the tubular lumen with a tracer-free solution; measurement of the steady-state flux of tracer from cell to lumen; and then, after discontinuance of the peritubular perfusion, measurement of the washout of tracer from cell to lumen. Based on a mathematical treatment of three compartment tracer kinetics applied to the experimental data, rate coefficients and fluxes for the luminal and peritubular membranes and cellular K transport pools were calculated. The perfusates used were characterized as "steady state" solutions - that is, their ionic compositions were tailored to nullify any net electrolyte or fluid transepithelial fluxes during the course of the experiment. Thus, the kinetic parameters were derived in the setting of this steady state condition.

Five experimental groups of rats were studied: normal diet, low K diet, high K diet, low Na diet, and acute bicarbonate infusion. A description of the five experimental classes, the peritubular and luminal steady state perfusate ionic compositions, and the derived rate parameters are outlined in Tables II.3 and II.4.



Table II.3 Experimental groups of DeMello-Aires et al (19)

	Luminal and Peritubular (L/P) Perfusate Compositions (mmol/l)					
	$\frac{K}{L/P}$	$\frac{Na}{L/P}$	$\frac{Cl}{L/P}$	$\frac{HCO_3}{L/P}$	$\frac{Ca}{L/P}$	
1) Normal diet 3% mannitol in saline @ 0.2 ml/min	10 / 5	30 / 145	40 / 127.5	0 / 25	0 / 2.5	
2) Low K diet 3% mannitol in saline @ 0.2 ml/min	3 / 2.5	30 / 145	33 / 125	0 / 25	0 / 2.5	
3) High K diet 3% mannitol in 0.15M KCl @ 0.1 ml/min	20 / 10	50 / 140	70 / 127.5	0 / 25	0 / 2.5	
4) Bicarbonate load 5% NaHCO <sub>3</sub> @ 0.1 ml/min	20 / 4	70 / 145	20 / 101.5	70 / 50	0 / 2.5	
5) Low Na diet 5% mannitol @ 0.1 ml/min	5 / 4.5	30 / 125	35 / 107.5	0 / 25	0 / 2.5	



Table II.4 DeMello-Aires et al kinetic data (19)

	$\frac{J_{12} - J_{21}}{(\text{pmol min}^{-1} \text{mm}^{-1})}$	$\frac{J_{32} - J_{23}}{(\text{min}^{-1} \text{mm}^{-1})}$	$\frac{k^*_{12}}{(\text{min}^{-1})}$	$\frac{k^*_{21}}{(\text{min}^{-1})}$	$\frac{k^*_{23}}{(\text{pmol mm}^{-1})}$	$\frac{S^*_2}{(\text{pmol mm}^{-1})}$	$\frac{C^*_K(1)}{(\text{mmol l}^{-1})}$
Normal diet	91.5	67.6	29.1	0.66	0.59	126	91
Low K	41.6	24.1	32.3	0.64	0.42	65.5	.47
High K	183	167	25.2	0.63	0.82	221	159
NaHCO <sub>3</sub>	186	134	29.7	0.75	0.57	245	176
Low Na	166	127	85.5	0.85	0.63	216	155

$S^*_2$  = cellular K transport pool

(1)  $C^*_K$ , cell K concentration, calculated by DeMello-Aires et al from  $S^*_2$  and estimates of tubular geometry. In the report, it is noted that "the calculated cellular potassium concentrations are highly sensitive to small differences in tubular geometry."





Since the rate coefficients of Models A and B are assumed to be constant, independent of  $x$ , flow rate, and luminal or cell  $K$  concentration, the parameters measured during the steady state condition of the DeMello-Aires experiment are assumed to represent values applicable to the model equations. Although the dimensions of the rate coefficients  $k_{ij}^*$  ( $\text{min}^{-1}$ ) differ from those of the model equations ( $\text{cm}^2 \text{min}^{-1}$ ), it is possible to derive values for  $k_{ij}$  as follows. First, the  $K$  concentration of the luminal steady state perfusate is equivalent to  $K(\text{max})$  in the model equations. (Recall that when the model system is perfused with  $K(0) = K(\text{max})$ , no net transport results, the situation which is stated to exist in the DeMello-Aires experiment.) Knowing the luminal and cell  $K$  concentrations permits one to calculate  $k_{12}$ ,  $k_{21}$ , and  $k_{23}$  as follows (\* designates DeMello-Aires parameters;  $K_p^*$ , the luminal  $K$  perfusate concentration):

$$k_{12} = J_{12}^* / K_p^*$$

$$k_{21} = J_{21}^* / C_K^*$$

$$k_{23} = J_{23}^* / C_K^*$$

Table II.5a gives the results of the computations for the various rate coefficients.

The DeMello-Aires kinetic data does not offer a basis for testing the assumptions of Models A or B since the derived parameters apply to only one in vivo condition - the "steady state" - when no net transport of  $K$  occurs. With this as an initial point of reference for comparing Models A and B, it will be seen that their secretory kinetics will differ significantly.



Table II.5 DeMello-Aires kinetic data adjusted for use in Models A and B equations

A) Adjusted DeMello-Aires rate coefficients ( $\text{nl min}^{-1} \text{mm}^{-1}$ )

	$\underline{k_{12}}$	$\underline{k_{21}}$	$\underline{k_{23}}$
Normal diet	9.15	1.00	0.74
Low K	13.87	0.89	0.51
High K	9.15	1.15	1.05
$\text{NaHCO}_3$	9.30	1.09	0.82
Low Na	33.20	1.07	0.82

B) Models A and B parameters calculated from DeMello-Aires kinetic data

	$\underline{k_a}$		$\underline{K(\text{max})}$	$\underline{\frac{\gamma_{\text{max}}}{I_s}/L}$		$\underline{C_K^{\text{max}}}$	$\underline{C_K^{\text{min}}}$
	$(\text{nl min}^{-1} \text{mm}^{-1})$		$(\text{mmol/l})$	$(\text{pmol min}^{-1} \text{mm}^{-1})$		$(\text{mmol l}^{-1})$	
	A	B	A & B	A	B	A & B	B
Normal diet	9.15	3.89	10	91.5	38.9	91	39
Low K	13.87	5.05	3	41.6	15.2	47	17
High K	9.15	4.37	20	183	87.4	159	76
$\text{NaHCO}_3$	9.30	3.88	20	186	77.6	176	73
Low Na	33.20	14.40	5	166	72.0	155	67



Applying the adjusted rate coefficients for normal diet animals to the model equations,

	$\frac{k_a}{(\text{nl}/\text{min}/\text{mm})}$	$\frac{K(\text{max})}{(\text{mmol}/\text{l})}$	$\frac{\phi_s^{\text{max}}/\text{L}}{(\text{pmol}/\text{min}/\text{mm})}$
Model A	9.15	10.0	91.5
Model B	3.89	10.0	38.9

Table II.5b gives  $K(\text{max})$ ,  $k_a$ ,  $\phi_s^{\text{max}}/\text{L}$ ,  $C_K^{\text{max}}$ , and  $C_K^{\text{min}}$  for all the experimental groups. The presentation which follows will concentrate primarily on the data from the normal diet animals. Later, when a more general solution for Models A and B incorporating volume reabsorption is developed, a brief comparison of the model predictions for all five experimental classes will be made.

1. Axial K Concentration Profile as a function of V and K(0)

Figure II.7 represents a plot of  $K(x)$  as a function of  $x$  for Models A and B,

$$K(x) = K(\text{max}) \cdot [1 - \exp(-k_a \cdot x/V)], \quad 0 \leq x \leq 1.0 \text{ mm}$$

which is equation (12) with  $K(0) = 0$  and the tubule length set at 1 mm (a value to be used throughout the remainder of the presentation). The potassium concentration is seen to rise exponentially from  $x = 0$  to  $x = L$ , the rate and overall magnitude of the rise being less at higher flow rates. Since  $K(\text{max})$  is the same for both models, each plot is approaching asymptotically the value of  $K(\text{max})$ , 10 mmol/l. Model A, the more potent of the two secretory models, shows K concentrations that



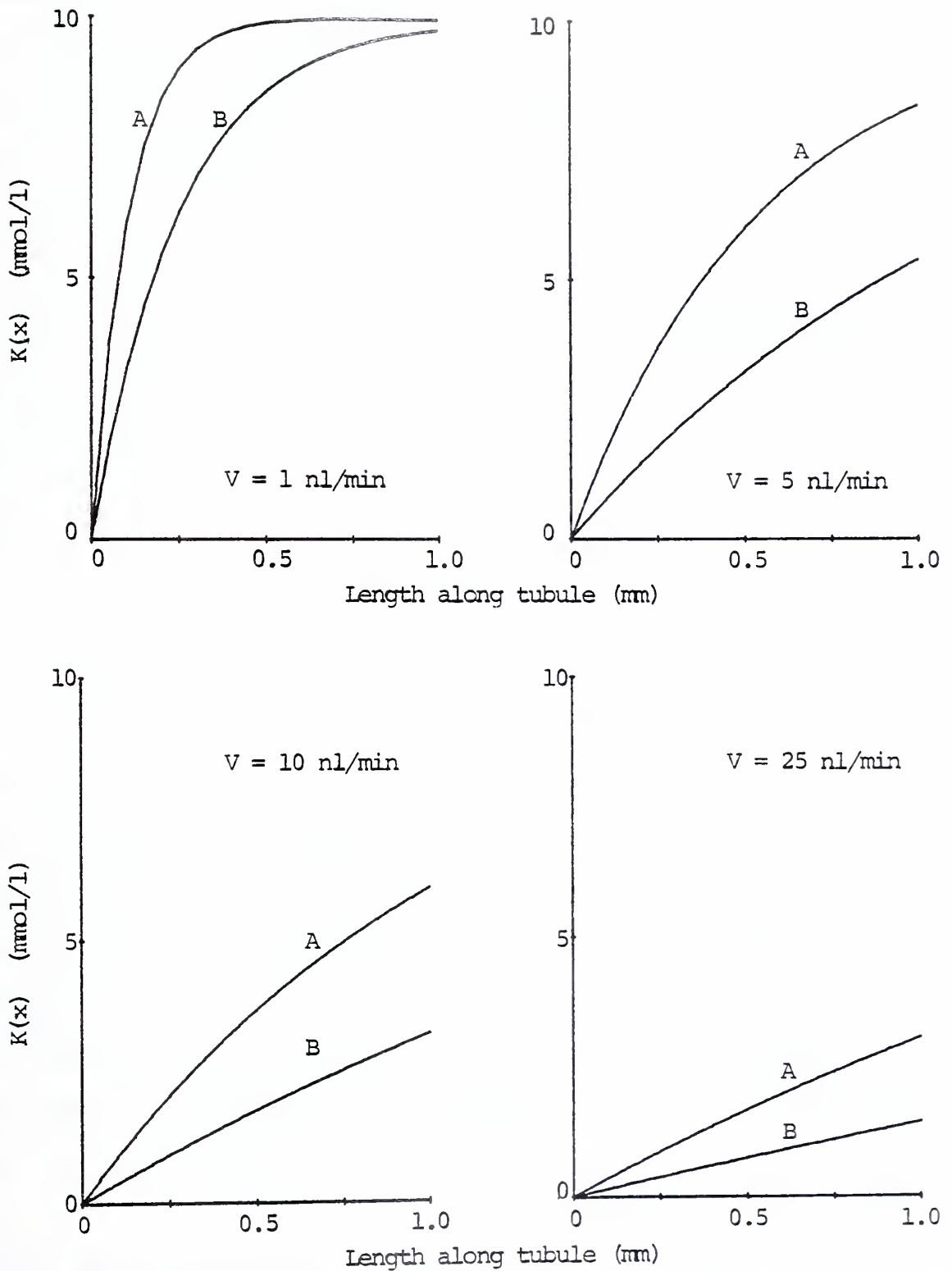


Figure II.7  $K(x)$  plotted as a function of  $x$ , the length along the modeled tubule. Plots are for Models A and B at different flow rate.  $K(0) = 0$  for all plots.





exceed those attainable by Model B in all comparable instances. Figure II.8 demonstrates the effect of raising the initial K concentration while holding V constant at 5 nl/min. When K(0) is less than K(max), the modeled epithelia progressively elevate the luminal K concentration, but at a slower rate as K(0) approaches K(max). For K(0) values exceeding K(max), the epithelia reabsorb luminal K resulting in a lowering of K concentration as fluid progresses along the tubule. All lines converge asymptotically towards K(max) at x = L. A comparison of the luminal profiles for Models A and B indicates that the former is both a more potent K secretory and K reabsorptive model.

## 2. K(L) as a function of K(0) and V

$$K(L) = K(0) \cdot \exp(-k_a \cdot L/V) + K(\max) \cdot [1 - \exp(k_a \cdot L/V)]$$

The plots of K(L) vs. V for several initial K concentrations are shown in Figure II.9. At zero flow rate, both models achieve the same equilibrium state with K(L) = K(max). With increasing flow rate, K concentration falls (or rises when K(0) > K(max)) to a greater extent in Model B than in A. The diminution of K concentration with increasing flow rate is significantly influenced by the initial K concentration. Note that in all instances K(L) approaches K(max) at low flow rates and K(0) at high flow rates.

## 3. Net K absorption as a function of V and K(0)

$$\phi(\text{net}) = V \cdot K(L) - V \cdot K(0)$$



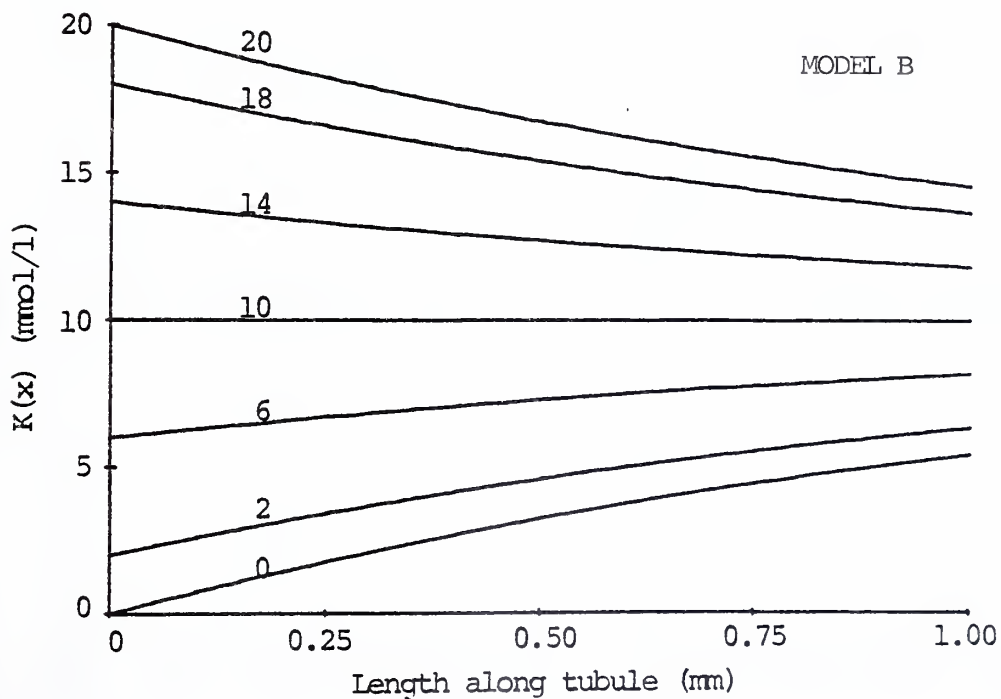
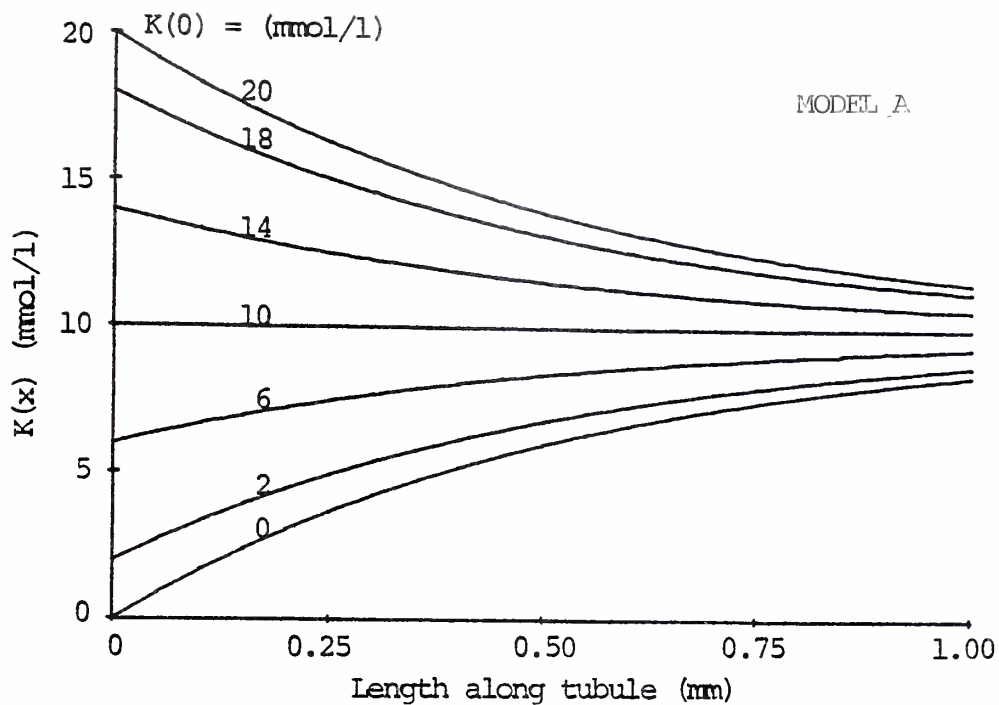


Figure II.8  $K(x)$  as a function of  $x$ , the length along the modeled tubule at different initial  $K$  concentrations,  $K(0)$ , for Models A and B.



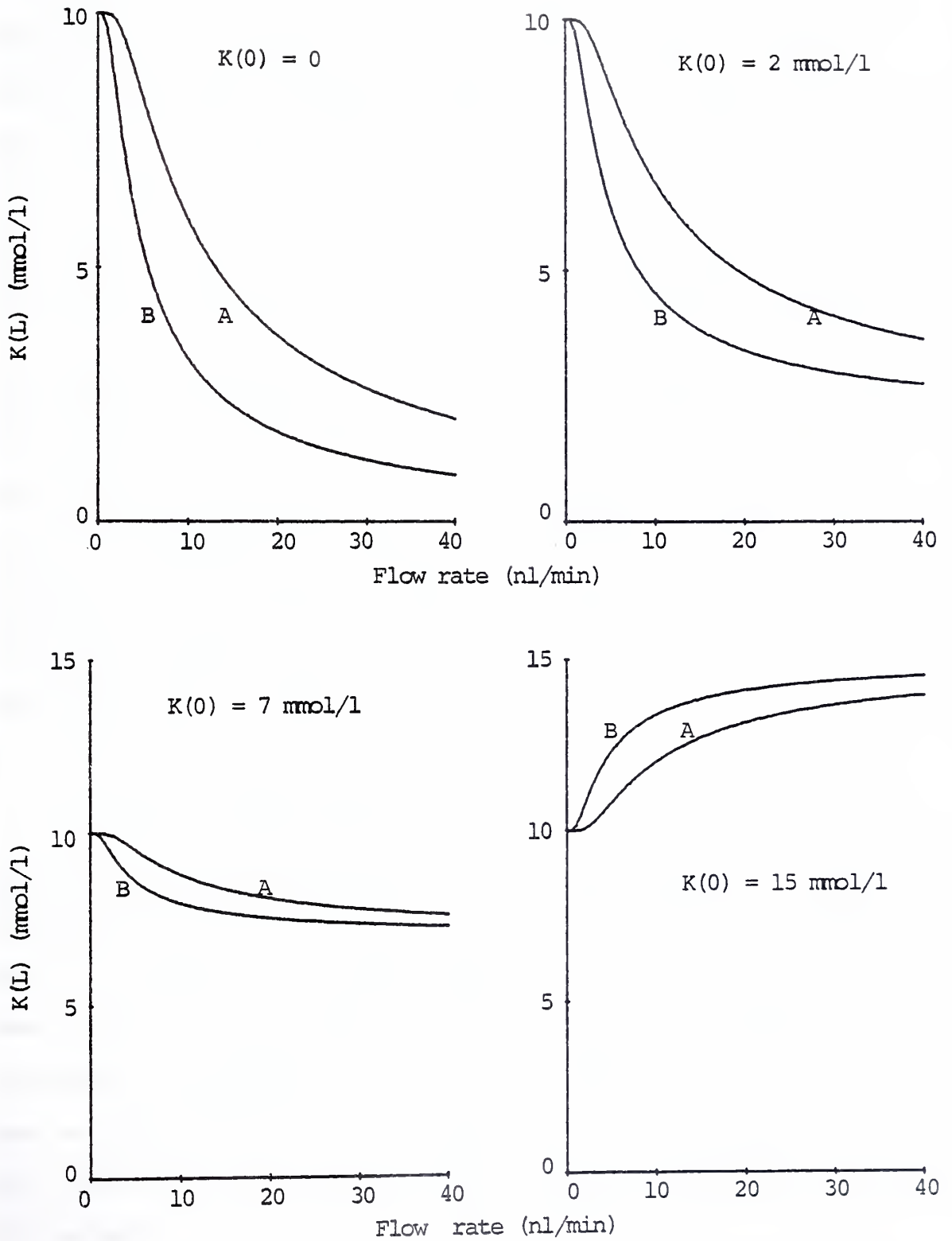


Figure II.9  $K(L)$  as a function of flow rate at several initial  $K$  concentrations,  $K(0)$ , for Models A and B.



The K transport-flow rate profiles for Models A and B are demonstrated in Figure II.10. The greater secretory potency of Model A over B is evident, the secretory maximum of Model A being 2.35 times greater than that for B. Importantly, for Model A the range of flow-limited secretory behavior, which as previously noted, occurs at flow rates less than  $k_a \cdot L$ , extends up to 9 nl/min as compared to approximately 4 nl/min for Model A. K secretion begins to plateau beyond these flow rates.

Also apparent from Figure II.10 is the significant sensitivity that both models exhibit to the changes in initial K concentration. Net K reabsorption is demonstrated when  $K(0) = 15$  mmol/l, a value which exceeds concentrations found in physiologic settings. However, it is noteworthy that a reabsorptive capability is predicted by the models since this phenomenon has been demonstrated in in vivo microperfusion experiments to be discussed later (27).

#### 4. Total K axial flux at $x = L$ , $\Phi(L)$

The K load entering the cortical collecting duct represents a contribution not only from K secreted by the late distal tubule but also from K delivered to the distal segment. Since, as we have seen,  $K(0)$ , when elevated, acts to decrease the magnitude of net K secretion, it is relevant to consider what effect varying concentrations of  $K(0)$  will have on the total axial K flux emerging from the modeled distal tubule. What proportion of this flux is accounted for by the distal tubule secretory segment?





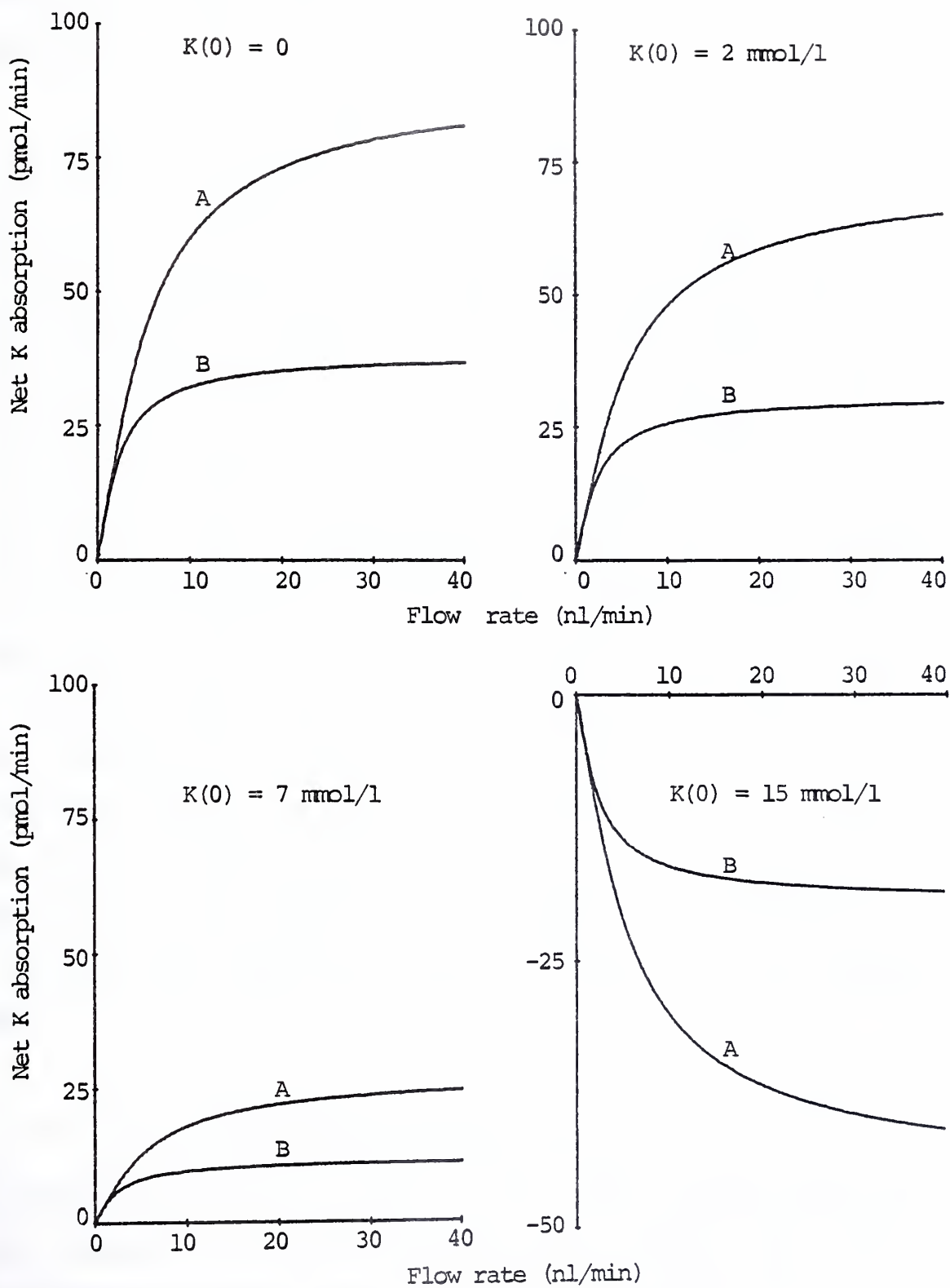


Figure II.10 Net K absorption plotted as a function of flow rate at several initial K concentrations,  $K(0)$ , for Models A and B.



The axial K flux at the end of the modeled secretory tubule is given simply by

$$\Phi(L) = V \cdot K(L)$$

In Figure II.11,  $\Phi(L)$  and  $\Phi(\text{net})$  are plotted as a function of V for Model A only. What is striking is that when  $K(0)$  equals 3 to 5 mmol/l, at moderate to high flow rates, the contribution of the secretory segment (net K secretion) to the total emerging flux is significantly less than fifty per cent. Thus, if Model A represents a good approximation of in vivo behavior, it can be concluded that under physiological circumstances in which the K load entering the late distal tubule ( $K(0) \cdot V(0)$ ) is significantly elevated, the K load delivered to the cortical collecting duct may in fact represent proportionally more of the K escaping proximal nephron reabsorption than K secreted by the distal tubule. It will be recalled that in the discussion in Part I regarding the prolonged K infusion series of experiments, the possibility that the delivered load of K to the distal tubule might significantly influence urinary K excretion was discussed and hypothesized to be one among several possible explanations for the augmented K secretion seen during the prolonged K infusion and volume expansion state.

##### 5. Net K absorption as a function of $K(0)$

The linear relationship of  $\Phi(\text{net})$  to  $K(0)$  when flow rate is held constant, previously demonstrated, is again shown in Figure II.12 utilizing the parameters of Models A and B. Note that for any given flow rate,



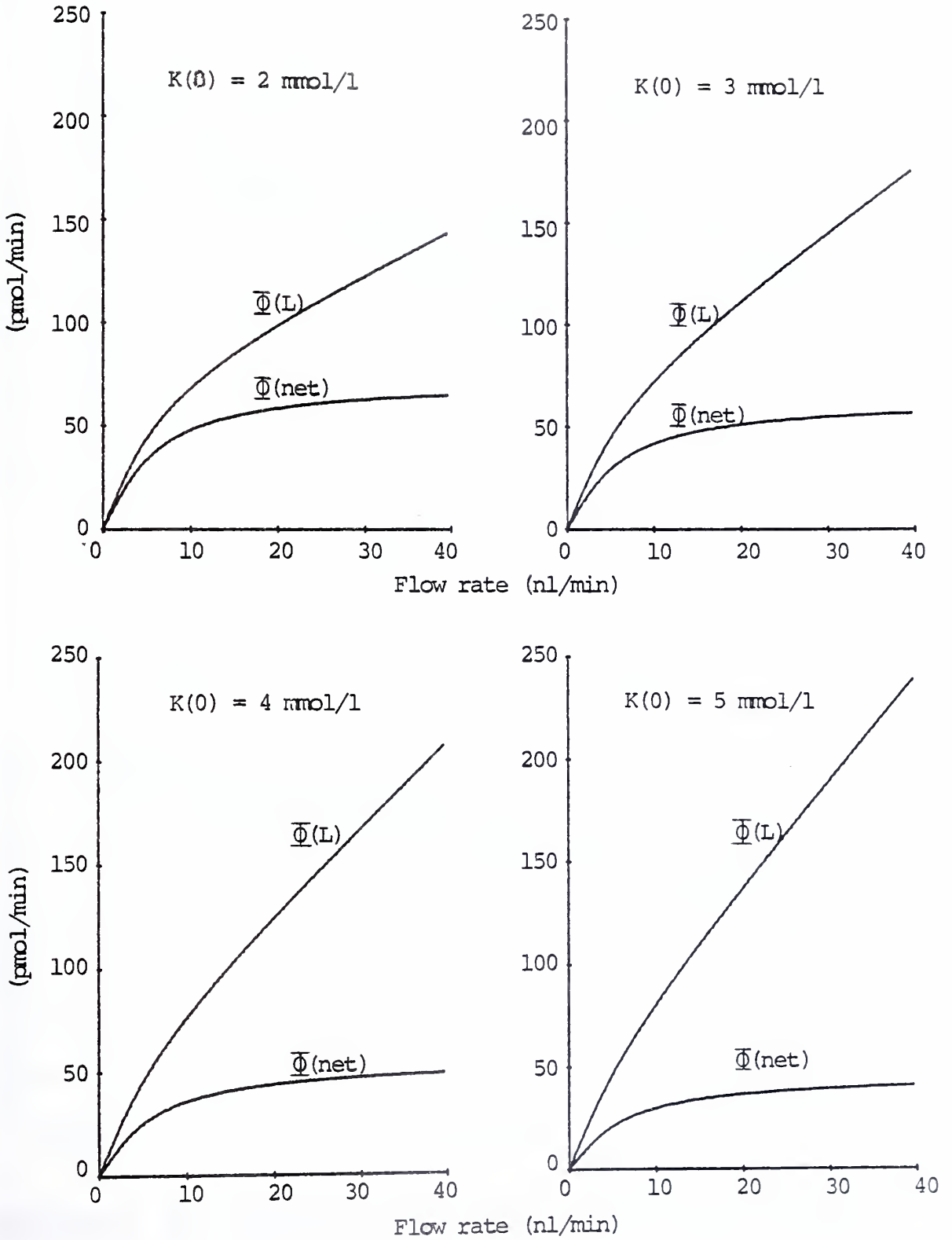


Figure II.11  $\bar{\Phi}(L)$  and  $\bar{\Phi}(\text{net})$  as a function of flow rate for several initial K concentrations,  $K(0)$ . Plots are for Model A.



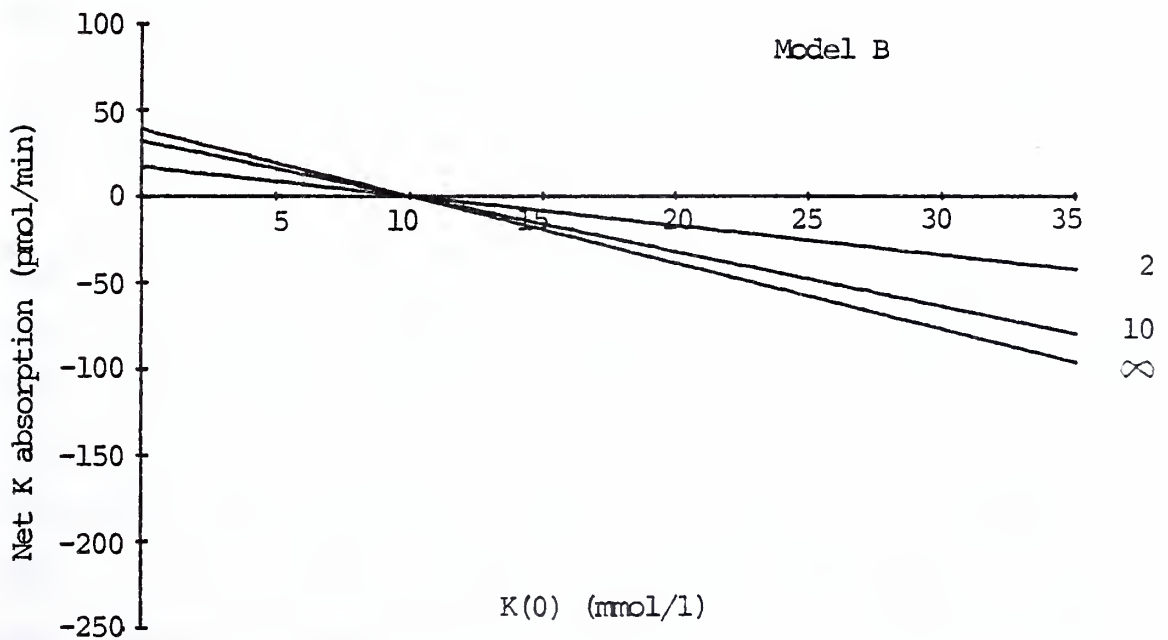
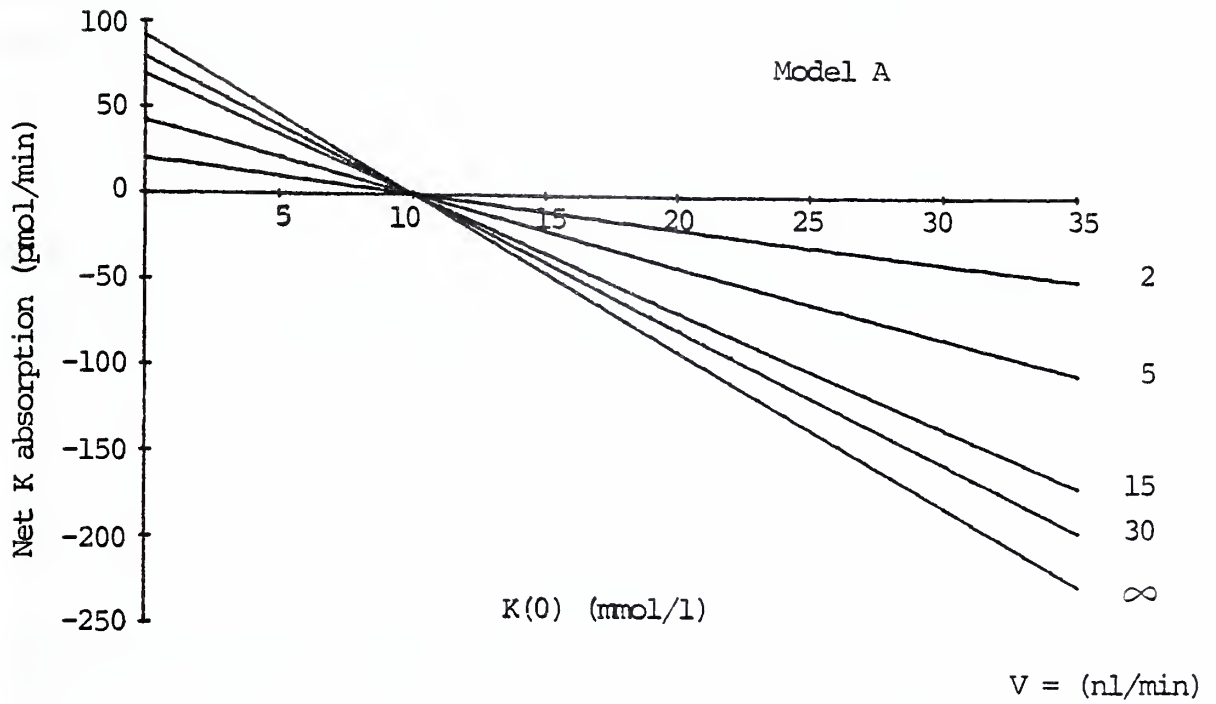


Figure II.12 Net K absorption plotted as a function of K(0) at several flow rates for Models A and B.





Model A has a greater  $K(0)$  sensitivity, that is, a more negative slope, than Model B, which translates to both a higher secretory and reabsorptive capability.

### 6. Cell potassium concentration variability in Model B

Equations (25-27) give the expressions necessary for assessing mean cell potassium concentrations under varying luminal conditions.

$$\bar{C}_K = C_K^{\max} - \Phi(\text{net}) / (k_{23} \cdot L) \quad (25)$$

$$C_K^{\max} = J_{32} / (k_{23}) \quad (26)$$

$$C_K^{\min} = C_K^{\max} \cdot k_{23} / (k_{21} + k_{23}) \quad (27)$$

The above equations indicate that mean cell  $K$  will vary in direct proportion to  $\Phi(\text{net})$  between the two limiting values  $C_K^{\max}$  and  $C_K^{\min}$ .

The proportionality factors equals  $1/k_{23} \cdot C_K^{\max}$  for Model B, 91 mmol/l, is equal to the constant cell  $K$  concentration maintained by Model A.

$C_K^{\min}$  may be calculated from equation (25) to equal 39 mmol/l.

Figure II.13a gives the plots of mean cell  $K$  vs.  $V$  for Model B

( $K(0) = 0$ ) with the constancy of Model A's cell  $K$  indicated for reference. Interestingly, mean cell  $K$  drops relatively quickly as flow rate increases from 0 to 10 nl/min in Model B and virtually stabilizes near its minimum value thereafter. Indeed, the apparent near constancy of cell  $K$  from 10 nl/min upwards, if experimentally measured, would seem to confirm the postulate of a constant cell  $K$  invoked for Model A.



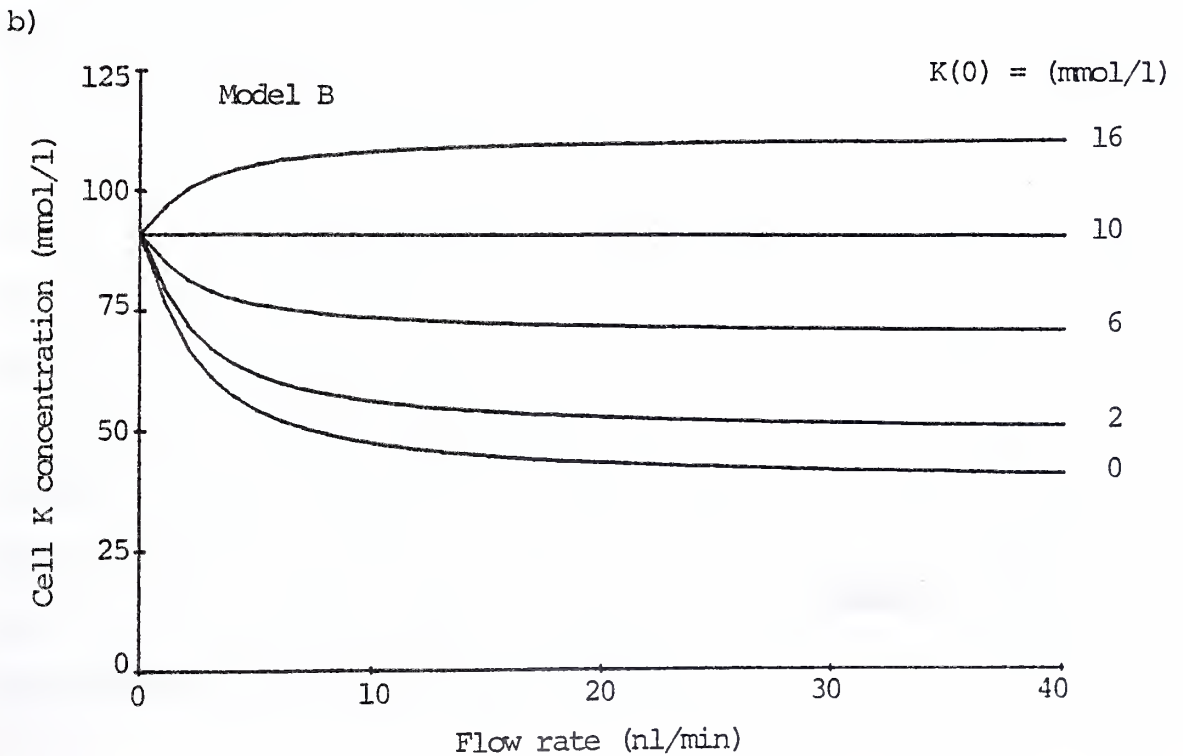
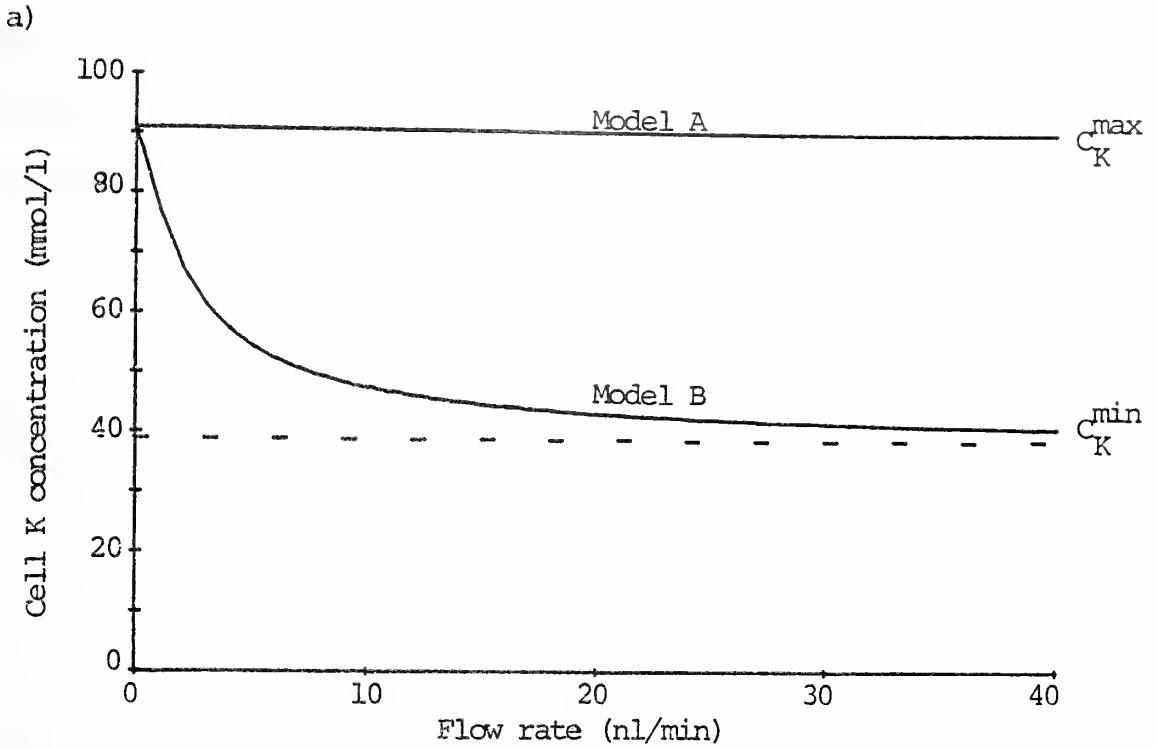


Figure II.13 Cell K concentration as a function of flow rate in Model B. In (a), the constant cell K concentration of Model A is contrasted with Model B. In (b), the effect of  $K(0)$  on cell K in Model B is demonstrated.



As cautioned in an earlier footnote to Table II.4, the absolute values of cell  $K$ , as depicted in Figure II.13, must be interpreted with caution because of the substantial margin for error noted by DeMello-Aires et al in their calculation of cell  $K$  concentrations. Nonetheless, it is interesting to point out that the seemingly low values of cell  $K$  predicted by Model B are not inconsistent with the experimental findings of Khuri et al who measured with a  $K$  sensitive intracellular liquid ion-exchange microelectrode a mean cell  $K$  concentration of 46.5 mmol/l in the late distal tubule of normally dieted rats under free flow conditions (35).

Figure II.13b shows the variation of mean cell  $K$  with flow rate for Model B at different  $K(0)$  concentrations. With increasing initial  $K$  concentrations, cell  $K$  is maintained closer to its maximum concentration as flow rate increases. When  $K(0) = K(\max)$ , cell  $K$  is stabilized at its maximum value for all flow rates. This, incidentally, is the condition under which the DeMello-Aires experiments were performed, and thus Figure 13b graphically illustrates why the cell  $K$  estimates determined in that experiment are identical with the value of  $C_K^{\max}$  as used in the model equations. The variability of the response of cell  $K$  to changes in luminal conditions is clearly emphasized by the fact that Model B predicts that the cells will gain potassium with increasing flow rate if  $K(0)$  exceeds  $K(\max)$ . In this circumstance, the epithelium is reabsorbing rather than secreting potassium.

In summary, the models predict a flow-dependent potassium secretion characterized by a rising rate of  $K$  secretion with increasing luminal flow



rates.  $K$  secretion plateaus within physiological flow rate ranges for both models. The constant cell  $K$  concentration maintained by the epithelium as postulated by Model A exhibits a more potent and flow-limited secretory behavior than Model B in which the blood to lumen flux,  $J_{32}$ , is unresponsive to luminal events. Model B more closely approximates a transport-limited  $K$  secretory system. The  $K$  secreting capability of both models is conditioned in part by the concentration of  $K$  entering the beginning of the tubule segment. That is, net  $K$  secretion is reduced as  $K(0)$  increases, reverting to net  $K$  reabsorption when  $K(0)$  exceeds  $K(\max)$ . The total flux of  $K$  leaving the tubule becomes proportionally more dependent on the entering  $K$  load when  $K(0)$  is raised beyond 2 mmol/l. Cell  $K$  concentrations in Model B vary over a range of 39 to 91 mmol/l with luminal flow rate when  $K(0)$  is less than  $K(\max)$ . This variability is largely confined to low flow rates.





## I. VOLUME REABSORPTION EFFECTS ON K SECRETION

In order to assess the effect volume reabsorption will have on the K secretory behavior of Models A and B, it is necessary to define volume flow rate as a function of  $x$  - a "flow function." The flow function to be utilized here will be derived somewhat speculatively since there is little experimental data or analysis which can be drawn on to accurately characterize the nature of volume reabsorption in the distal tubule. Before giving the derivation of this function, the discussion will first address the question: Is it possible to define the maximum and minimum effects that a given magnitude of volume reabsorption,  $\Delta V = V(0) - V(L)$ , can be expected to have on K secretion?

From the kinetics of Models A and B already analyzed, it can be stated from the outset that volume reabsorption will always act to reduce net K secretion from the level attained under conditions of no volume reabsorption. This statement derives its validity from the fact that the reabsorption of fluid at any point along the tubule will raise luminal K concentration. From equation (20),

$$J_s(x) = J_s^{\max} - K(x) \cdot k_a \quad (20)$$

we know that  $J_s(x)$  will necessarily be diminished by the elevated luminal K concentration. Since the raised luminal K concentration effected by volume reabsorption does not augment the axial flux of potassium, the depressant action of the increased  $K(x)$  on  $J_s(x)$  will be the only relevant effect.

The magnitude of the effect that volume reabsorption will have on K secretion will depend in part on whether the bulk of fluid is absorbed



early or late along the course of the tubule. If early, the raised luminal K concentration will depress  $J_s$  throughout the remainder of the tubule. If late, the tubule will be able to maximize its secretory K flux before volume reabsorption effects become manifest. Thus, it is appropriate to consider two hypothetical flow functions which might be anticipated to exert maximal and minimal volume reabsorption depressant effects on K secretion.

1) Minimum K secretion inhibition flow function

$$V(x) = \begin{cases} V(0), & 0 \leq x < L \\ V(0) - \Delta V, & x = L \end{cases} \quad \left. \begin{array}{l} V(x) \\ \left. \begin{array}{c} \text{---} \\ \text{---} \\ \text{---} \end{array} \right\} \Delta V \\ \text{---} \\ \text{---} \\ \text{---} \end{array} \right\} \Delta V$$

2) Maximum K secretion inhibition flow function

$$V(x) = \begin{cases} V(0), & x = 0 \\ V(0) - \Delta V, & 0 < x \leq L \end{cases} \quad \left. \begin{array}{l} V(x) \\ \left. \begin{array}{c} \text{---} \\ \text{---} \end{array} \right\} \Delta V \\ \text{---} \\ \text{---} \end{array} \right\} \Delta V$$

where:  $\Delta V = V(0) - V(L)$

In the first case, the entire volume is reabsorbed "instantly" at  $x = L$  thus enabling the tubule to carry out its secretory function with minimal inhibition. In the second case,  $\Delta V$  is transported across the epithelium at  $x = 0$  after which flow remains constant at a rate  $V(x) = V(L)$ . Thus the inhibiting effect of volume reabsorption on  $J_s$  is maximally exerted by allowing the rise in luminal K concentration to occur at the earliest possible point along the tubule. It will be theorized that flow



functions 1 and 2 in fact represent modes of volume reabsorption which exert minimum and maximum effects respectively on K secretion in Models A and B.

For the purpose of illustration, the basic differential equation incorporating the two flow functions will be solved for the case of Model A only. The appropriate equations are:

$$\text{Case 1)} \quad [V(0) - H_1(x) \cdot \Delta V] \frac{dK(x)}{dx} = C_K \cdot k_{21} - K(x) \cdot k_{12}$$

$$\text{Case 2)} \quad [V(L) + H_2(x) \cdot \Delta V] \frac{dK(x)}{dx} = C_K \cdot k_{21} - K(x) \cdot k_{12}$$

where  $H(x)$  is the Heaviside unit step function,

$$H_1(x) = \begin{cases} 0, & 0 \leq x < L \\ 1, & x = L \end{cases} \quad H_2(x) = \begin{cases} 1, & x = 0 \\ 0, & 0 < x \leq L \end{cases}$$

The integrated solutions are readily found.

Case 1: minimum K secretion inhibition flow function

$$\phi(\text{net}) = V(0) \cdot [K(\text{max}) - K(0)] [1 - \exp(-k_{12} \cdot L/V(0))] \quad (37)$$

Case 2: maximum K secretion inhibition flow function

$$\phi(\text{net}) = [V(L) \cdot K(\text{max}) - V(0) \cdot K(0)] [1 - \exp(-k_{12} \cdot L/V(L))] \quad (38)$$

$$\text{where: } V(L) = V(0) - \Delta V$$

$$K(\text{max}) = C_K \cdot k_{21} / k_{12} \quad .$$

It is immediately evident from equation (37) that for a given  $V(0)$  and  $\Delta V$ , net K secretion can never exceed the rate of K secretion attained when no fluid is reabsorbed. The difference between equations (38) and (37) would mathematically express the theorized magnitude of



effect that volume reabsorption may have on inhibiting K secretion. Subtracting equation (38) from (37), however, creates a mathematical statement, the complexity of which defies facile interpretation, in part because of the many variables which may influence the magnitude of volume reabsorption effects ( $k_a$ ,  $\Delta V$ ,  $V(0)$ , and  $K(0)$ ). However, in the next section, equations (37) and (38) will be plotted in conjunction with the flow function to be derived next in order that the effects on K secretion resulting from a more realistic approximation of in vivo flow rate behavior can be located within the potential range of volume reabsorption effects.

1. Approximating flow function

Fluid reabsorption in the late distal tubule is generally believed to represent a process of equilibration between the hypotonic fluid leaving the early distal tubule and the isotonic environment of the cortical interstitium. The late distal segment is sensitive to ADH, and thus its hydraulic permeability is susceptible to the osmoregulatory influences of ADH.

The driving force for net fluid transport from the lumen to the interstitium will be assumed to arise from the difference in osmotic pressure,  $\Delta\pi$ . Therefore,

$$-\frac{dV(x)}{dx} \propto \Delta\pi(x)$$

Since the osmotic pressure of the luminal fluid will tend to change in parallel with luminal flow rate, as a first approximation, it will be assumed that

$$\Delta\pi(x) \propto V(x)$$





and therefore that

$$-\frac{dV(x)}{dx} = b \cdot V(x) \quad (39)$$

where  $b$  is a constant with the dimensions  $\text{mm}^{-1}$ .

Equation (39) integrates over the boundaries  $\int_{x=0}^x$  and  $\int_{V(0)}^{V(x)}$  to give

$$V(x) = V(0)e^{-bx} \quad (40)$$

Since a higher initial flow rate,  $V(0)$ , may be assumed to reflect systemic conditions favoring reduced volume reabsorption, as a second approximation, it will be assumed that  $b$ , the rate coefficient of volume reabsorption, varies inversely with  $V(0)$ , that is,

$$b \propto 1/V(0)$$

We may then define a second volume flux parameter,  $\beta$ , by the relationship

$$b = \beta/V(0)$$

where  $\beta$  has the dimensions,  $\text{nl}/\text{min}/\text{mm}$ . Substituting into equation (40), we have

$$V(x) = V(0) \cdot \exp[-\beta \cdot x/V(0)] \quad (41a)$$

and

$$V(L) = V(0) \cdot \exp[-\beta \cdot L/V(0)] \quad (41b)$$

The flow function defined by equation (41a) will be employed to approximate in vivo luminal flow rate. Empirically, it is found that by setting the value of  $\beta \cdot L$  at 7.5  $\text{nl}/\text{min}$ , equation (41b) predicts quite well the relationship between  $V(0)$  and  $V(L)$  as measured during in vivo saline volume expansion experiments. Shown in Figure II.14a is data



from three experiments where early and late distal luminal flow rates were recorded (36,39,51). Early distal flow is taken to be equivalent to  $V(0)$  and late distal to  $V(L)$ . The plotted line represents a graph of equation (41b). As seen, the predictive value of the equation is remarkably good. Figure II.14b demonstrates the axial profile of luminal flow rates predicted by the derived flow function for several values of  $V(0)$ . How well the plots reflect in vivo flow rate behavior is not known.

Having developed an approximating function for  $V = f(x)$ , we can now seek a more general solution to the fundamental differential equation.

Combining equations (4) and (41a), we obtain

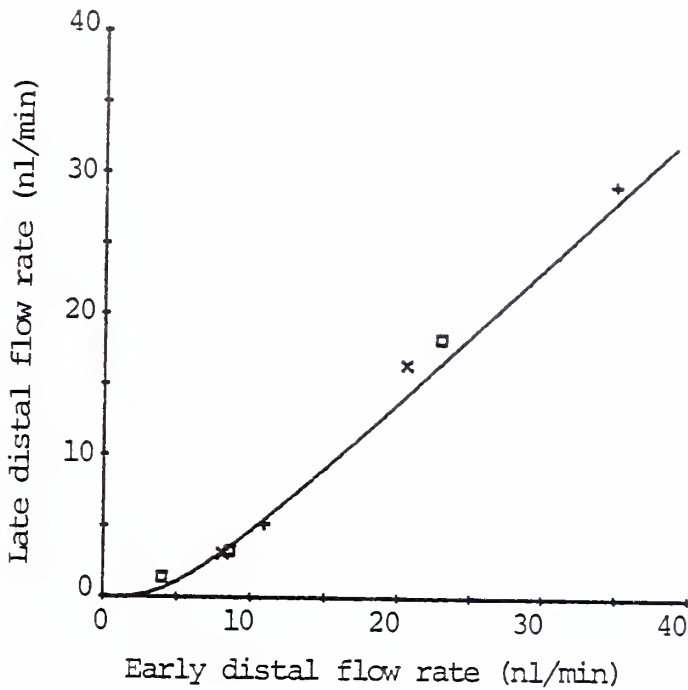
$$\begin{aligned} \frac{d[V(x) \cdot K(x)]}{dx} &= V(x) \frac{dK(x)}{dx} + K(x) \frac{dV(x)}{dx} \\ &= V(0) \cdot \exp[-\beta \cdot x/V(0)] \frac{dK(x)}{dx} - K(x) \cdot \beta \cdot \exp[-\beta \cdot x/V(0)] \\ &= C_K(x) \cdot k_{21} - K(x) \cdot k_{12} \end{aligned}$$

Under the assumptions of Models A and B, this expression cannot be integrated in closed form, and, therefore, methods of numerical analysis were employed to develop the graphs which follow. The method of Runge-Kutta, a fourth-order algorithm for approximating roots to differential equations was used. The solutions were generated by a Hewlett Packard computer (9815A) and plotter (9862A). The plots which follow are for the constant cell  $K$  concentration case only.

Plotted in Figure II.15 is  $\phi(\text{net})$  vs.  $V(0)$  for several initial  $K$  concentrations utilizing the parameters of DeMello-Aires as calculated for normal diet animals. As previously discussed, the potential range of fluid reabsorption effects is illustrated on each graph by plotting



a)



b)

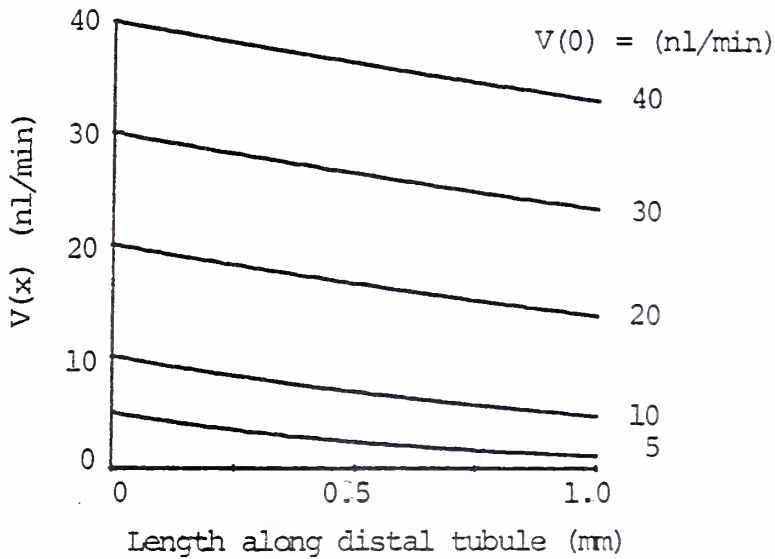


Figure II.14 a) Late distal flow rate as a function of early distal flow rate. Line represents a plot of approximating flow function (see text). Symbols correspond to data from in vivo experiments: squares, reference 36, '+'s, 39, and 'x's, 51.  
b) Axial flow rate profile of approximating flow function for several initial flow rates,  $V(0)$ .



equations (37) and (38).  $\Delta V$  is the same in all plots, being defined by equation (41a), that is,

$$\Delta V = V(0) - V(0) \cdot \exp[-\beta \cdot L/V(0)]$$

Although the derived flow function demonstrated luminal fluid flow rate profiles roughly intermediate between the two hypothetical flow functions (Figure II.14b), it is apparent from Figure II.15 that net K secretion in the fluid reabsorption model is maximally inhibited when  $K(0) = 0$  and only somewhat less so as  $K(0)$  is raised to 6 mmol/l. Also of interest is that when  $K(0)$  is greater than zero, net K reabsorption occurs at low flow rates. Net K secretion develops only when luminal flow rate is increased. The luminal K concentrating effect of fluid transport apparently is sufficiently great to result in net K reabsorption at low flow rates. (That is, luminal K is raised above  $K(\max)$  thus initiating K reabsorption). This effect of course becomes more pronounced at higher  $K(0)$  concentrations.

## 2. $\bar{\Phi}(\text{net})$ vs. $\bar{V}$ for DeMello-Aires five experimental groups

Having now developed a means for evaluating the fundamental differential equation with volume reabsorption taken into account, it is appropriate to return to the DeMello-Aires kinetic data and very briefly examine the K secretion-flow rate profiles of Models A and B for all five experimental groups. For the purposes here, it will be assumed that the flow function derived above is applicable to all experimental groups and that  $K(0)$  is fixed at 2.0 mmol/l under all conditions. The appropriate kinetic parameters to be applied to Models A and B are found in Table II.5.





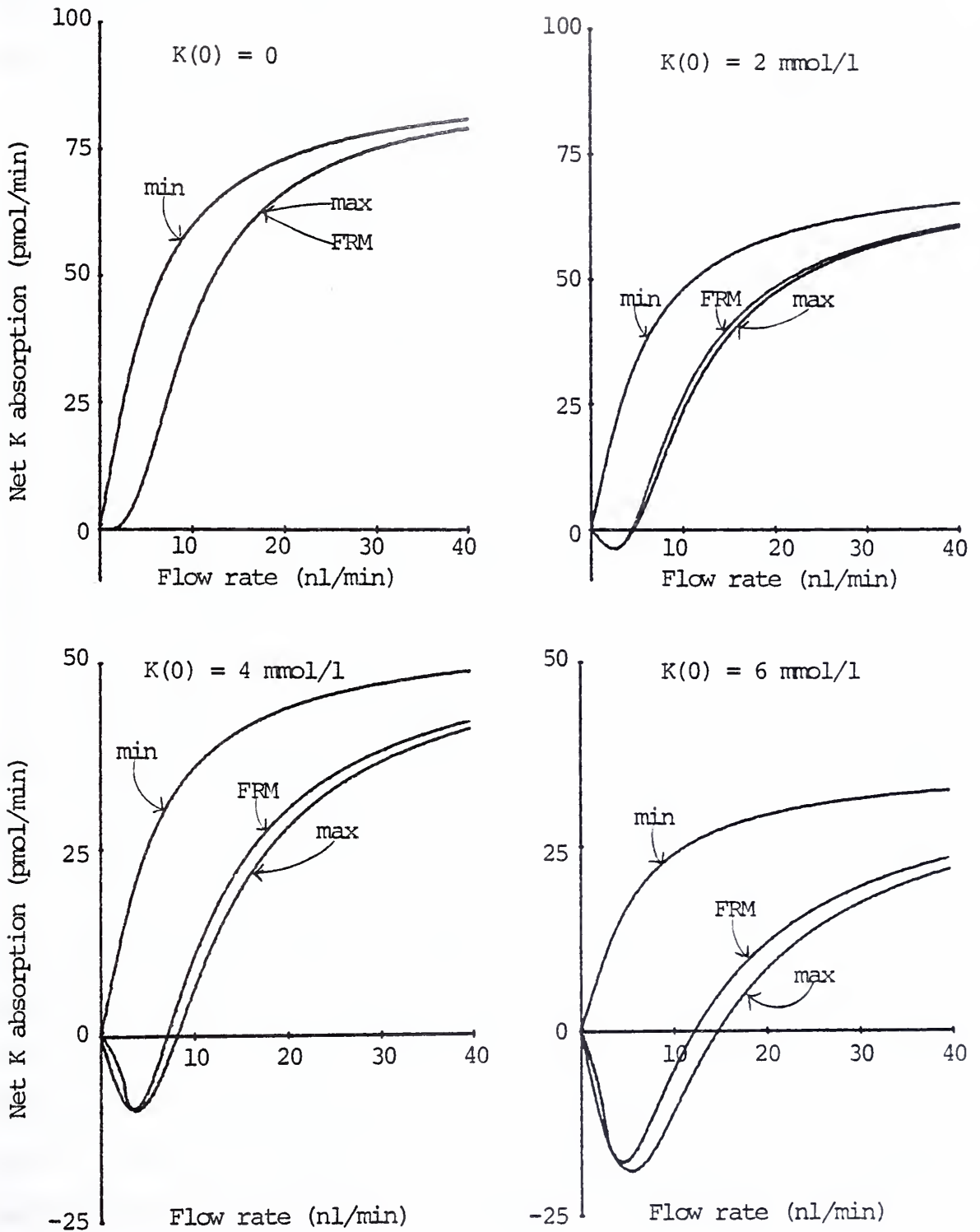


Figure II.15 Net K absorption as a function of flow rate. "Min" indicates minimum K secretion inhibition flow function; "max" - maximum K secretion inhibition flow function; and "FRM" - fluid reabsorption model. See text for explanation.



Shown in Figure II.16 for Models A and B are  $\Phi(\text{net})$  vs.  $\bar{V}$  plots, the mean flow rate being derived from equation (41b),

$$\begin{aligned}\bar{V} &= \frac{1}{L} \int_0^L V(0) \cdot \exp[-\beta \cdot x/V(0)] dx \\ &= \frac{V(0)^2}{\beta \cdot L} [1 - \exp[-\beta \cdot x/V(0)]]\end{aligned}$$

Since  $k_a$  is nearly the same in all but the low Na diet group, the plots are principally distinguished by their differences in secretory potency, with the bicarbonate infused and high K diet groups showing the highest rates of K secretion. As expected, the low K diet group is remarkable for its very low rate of net K transport. Additionally, it is seen that net K secretion in the low K group is not achieved until the mean luminal flow rate is greater than 12 nl/min and 15 nl/min in Models A and B respectively. The low Na diet group, with a  $k_a$  value approximately three times as great as the other experimental groups, demonstrates a secretory potency comparable to the normal diet group but a flow-dependent K secretion behavior that is more flow-limited in character over a substantially wider range of flow rates.

It is tempting to correlate the model predictions of Figure II.16 with in vivo K secretion data since the magnitude of K secretion, particularly in Model A for the normal and high K diet groups, approximately corresponds to in vivo measurements (see for example references 27,36, 39,51). However, the comparison would be quite speculative since in vivo results typically are given for K transport along the entire distal tubule segment accessible to micropuncture (including early and late



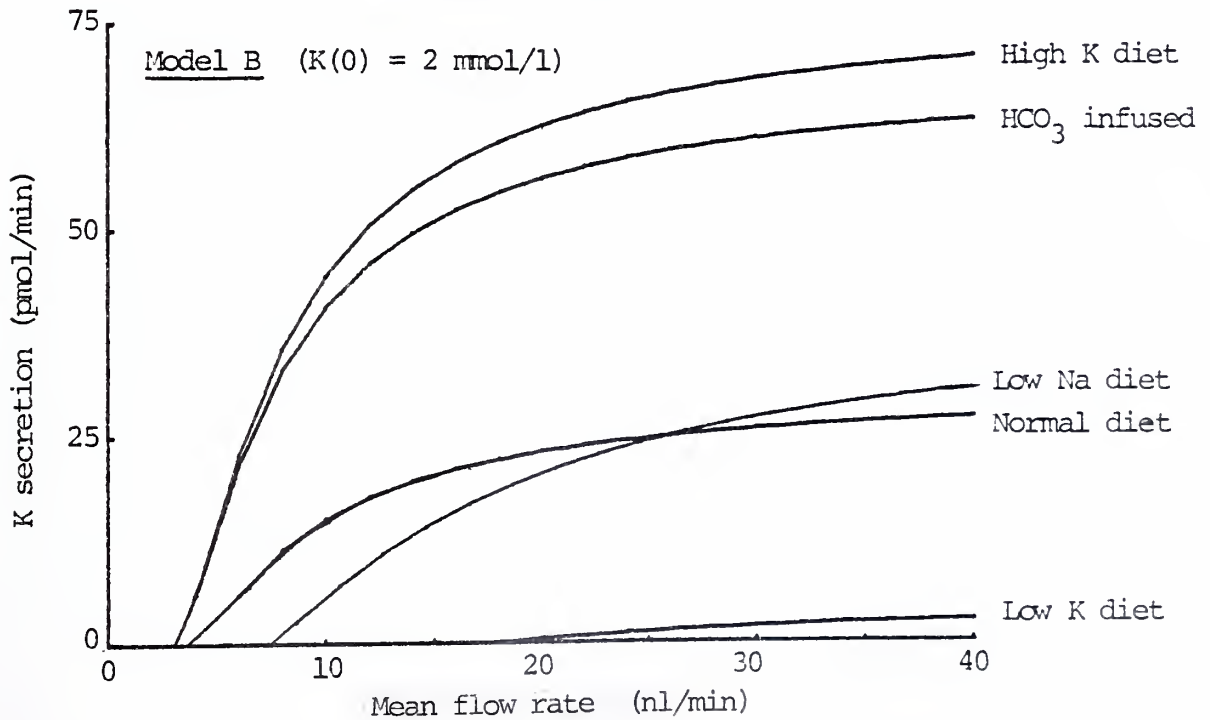
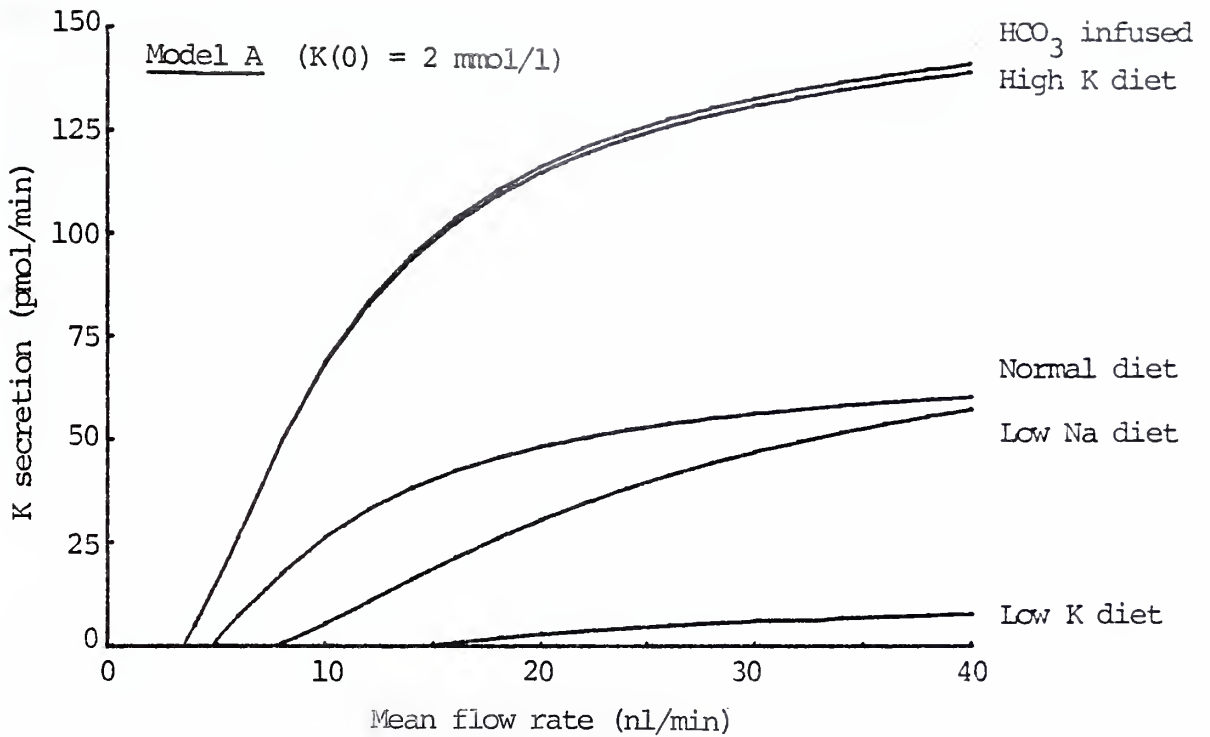


Figure II.16 Net K secretion as a function of flow rate for the five DeMello-Aires experimental groups. Models A and B are shown. Kinetic parameters for plots taken from Table II.5.



distal segments), and the length of the K secreting segment is uncertain. The temptation is therefore resisted, and the plots of Figure II.16 are presented primarily to summarize and illustrate the range of flow-dependent K secretory kinetics predicted by Models A and B under diverse physiological conditions.





J. NON-LINEAR LUMINAL REABSORPTIVE PUMP KINETICS

Greatly simplifying the modeling up to this point, both conceptually and mathematically, has been the assumption that the kinetics of the lumen to cell flux,  $J_{12}$ , are linear. This flux, according to the cellular model of Giebisch, contains both passive and carrier-mediated components, which hereafter, for convenience, will be identified, along with the corresponding rate coefficients, as:

$$J_{12}(x) = J_{12}^D(x) + J_{12}^M(x) \quad \text{total K flux } 1 \rightarrow 2$$

$$J_{12}^D(x) = K(x) \cdot k_{12}^D \quad \text{passive K flux } 1 \rightarrow 2$$

$$J_{12}^M(x) = K(x) \cdot k_{12}^M \quad \text{carrier-mediated flux } 1 \rightarrow 2$$

Because of the assumption of constancy of the luminal membrane PD and permeability,  $J_{12}^D$  is a linear flux; that is,  $k_{12}^D$  is a constant parameter. However, the kinetic behavior of  $J_{12}^M$ , the K reabsorptive pump flux, which until now has been assumed to follow linear kinetics, is unknown. The existence of a luminal K reabsorptive pump is postulated on the basis of several experimental observations discussed in detail by Giebisch and others (23,30,65). The presence of a carrier-mediated lumen to cell flux can be inferred though not proven by an evaluation of the relative magnitudes of the  $k_{12}$  and  $k_{21}$  rate coefficients from the DeMello-Aires kinetic data. Assuming that the passive fluxes are adequately described by the Goldman equation,

$$J_{12}^D(x) = P_{rd} \cdot \frac{\Delta EF}{RT} \cdot \frac{1}{1 - \exp(-\Delta EF/RT)} \cdot K(x)$$

$$J_{21}^D(x) = P_{rd} \cdot \frac{\Delta EF}{RT} \cdot \frac{\exp(-\Delta EF/RT)}{1 - \exp(-\Delta EF/RT)} \cdot C_K(x)$$

where: P = luminal membrane K permeability

$\Delta E$  = luminal membrane PD at x



then,

$$k_{12}^p = \frac{\Delta EF}{RT} \cdot \frac{P_{rd}}{1 - \exp(-\Delta EF/RT)} \quad k_{21} = \frac{\Delta EF}{RT} \cdot \frac{P_{rd} \cdot \exp(-\Delta EF/RT)}{1 - \exp(-\Delta EF/RT)} \quad (42a, b)$$

If we now divide  $k_{21}$  by  $k_{12}^p$ , we obtain

$$k_{21}/k_{12}^p = e^{-\frac{\Delta EF}{RT}}$$

Assuming a luminal membrane PD of 20, 30 or 40 mv, a range encompassing a variety of experimental measurements, the ratio of the two flux coefficients calculates to be:

	<u>20 mv</u>	<u>30 mv</u>	<u>40 mv</u>
$k_{21}/k_{12}^p$	0.72	0.61	0.51

Since  $k_{21}$  has been assumed to mediate an entirely passive flux, its value can be taken directly from Table II.5, 1.00 nl/min/mm for normal diet rats. The calculated  $k_{12}^p$  therefore equals:

	<u>20 mv</u>	<u>30 mv</u>	<u>40 mv</u>
$k_{12}^p$ calculated (nl/min/mm)	1.40	1.65	1.95

$$k_{12} \text{ (normal diet group)} = 9.15$$

The calculated values of  $k_{12}^p$  is substantially less than the experimentally derived value for  $k_{12}$ . This analysis thus supports the probable existence of a carrier-mediated transport mechanism, the rate coefficient of which,  $k_{12}^m$ , contributes to the overall magnitude of  $k_{12}$ .

### 1. No luminal K reabsorptive pump model

Before considering alternative kinetic formulations for  $J_{12}^m$ , it will



be useful to examine the K secretory behavior of Model A in the absence of the carrier-mediated flux. For illustration purposes, a 30 mv luminal membrane PD will be assumed and the appropriate values for  $k_{12}^D$  and  $k_{21}$  for normal diet animals drawn from the above calculations.

The net flux across the luminal membrane is given by

$$J_s(x) = V \cdot \frac{dK(x)}{dx} = C_K \cdot k_{21} - K(x) \cdot k_{12}^D$$

and the integrated solution is

$$K(x) = K(0) \cdot \exp(-k_{12}^D \cdot x/V) + K(\max) \cdot [1 - \exp(-k_{12}^D \cdot x/V)]$$

$$\Phi(\text{net}) = V \cdot [K(\max) - K(0)] [1 - \exp(-k_{12}^D \cdot L/V)]$$

$$K(\max) = C_K \cdot k_{21} / k_{12}^D = 55.5 \text{ mmol/l}$$

$$\Phi_s^{\max} = C_K \cdot k_{21} \cdot L = 91.5 \text{ pmol/min}$$

for 30 mv luminal membrane PD, normal diet group

These equations are identical in form to the previously derived solutions for Model A. The rate coefficient and  $K(\max)$  take on significantly different values than for Model A, whereas  $\Phi_s^{\max}$  remains unchanged.

Shown in Figure II.17 are graphs of  $K(L)$  vs.  $V$  and  $\Phi(\text{net})$  vs.  $V$  for the "no luminal pump" model and Model A. Since the maximum rate of K secretion is identical for both models, equal to the constant flux  $J_{21}$ , the secretory potency of the two models is the same. However, the K secretion-flow rate profiles are remarkably different, with the no luminal pump model very closely resembling the transport-limited model of Giebisch. From approximately a flow rate of 8 nl/min on up, secretion lies within 85% of its maximal value. At low flow rates, luminal K concentrations in the no luminal pump model are considerably higher than for Model A.



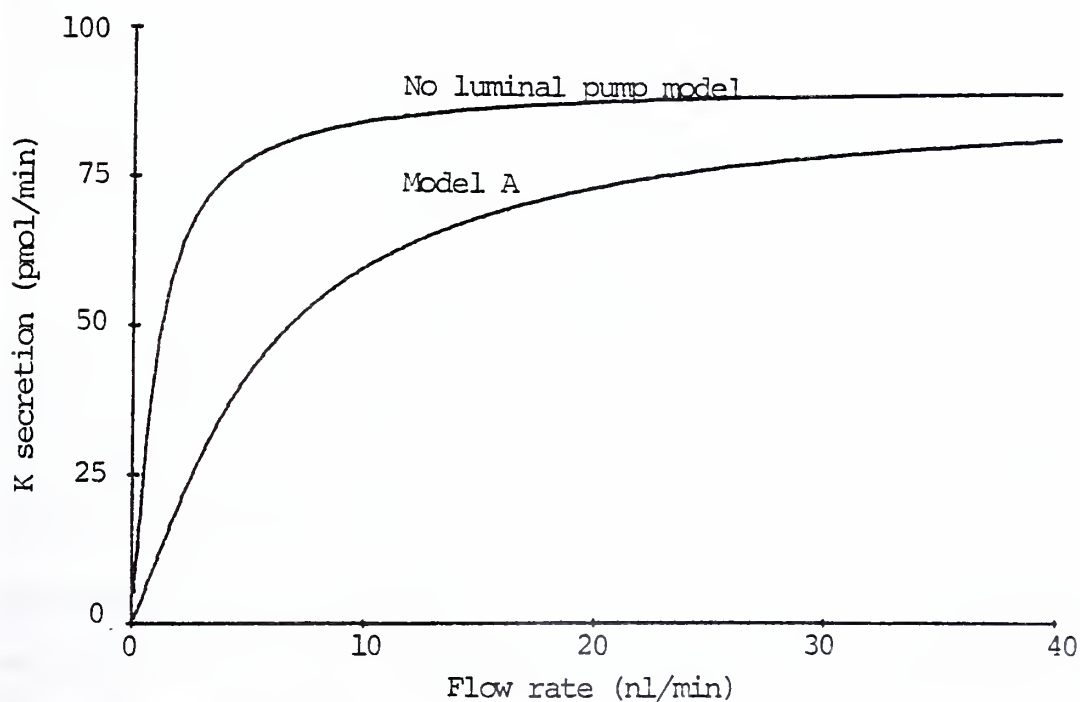
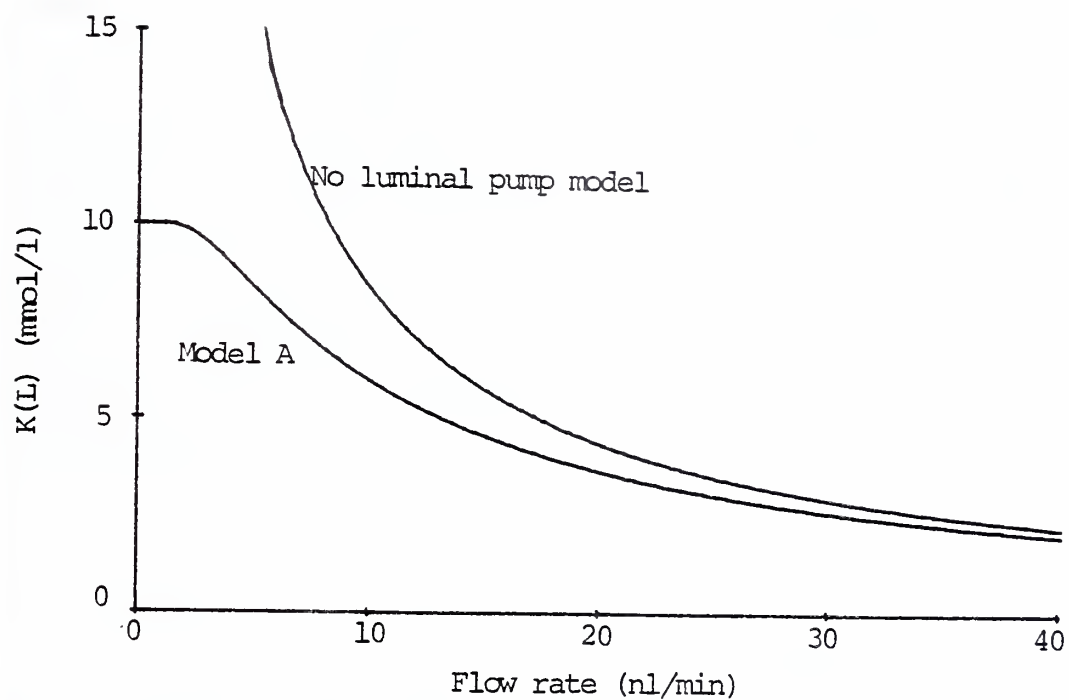


Figure II.17 Model A contrasted with no K reabsorption luminal pump model. (a)  $K(L)$  as a function of flow rate, (b) K secretion as a function of flow rate.  $K(0) = 0$  for all plots.





From the above, it can be appreciated that the reabsorptive pump figures strongly into the flow-dependent K secretory character of Model A. In effect, potentially high concentrations of luminal K at low flow rates are obviated by the action of the luminal K reabsorptive pump, thus giving rise to the flow-dependent K secretory behavior of Model A. Therefore, it is very appropriate to consider alternative kinetic formulations for  $J_{12}^m$  as we can expect that the flow-dependent K secretion behavior of Model A will depend significantly on the character of this carrier-mediated flux.

## 2. Non-linear, saturable luminal K reabsorptive pump model

In the absence of any specific guidelines from experimental work on which to base the kinetic representation of  $J_{12}^m$ , it is simplest and perhaps most illustrative to view the pump as a saturable, carrier-mediated transport mechanism following Michaelis-Menten kinetics. Thus we will assume that  $J_{12}^m$  can be defined by

$$J_{12}^m(x) = \frac{J_{12}^{\max} \cdot K(x)}{K(x) + K_{1/2}} \quad (43)$$

where  $J_{12}^{\max}$  is the maximum flux potentially generated by the pump, and  $K_{1/2}$  is the luminal K concentration at which  $J_{12}^m$  achieves one-half of its maximal rate.

Reformulating the fundamental differential equation to incorporate the activity of the luminal reabsorptive pump along with the passive lumen to cell flux, we have



$$\begin{aligned}
 J_s(x) &= V \frac{dK(x)}{dx} = J_{21}(x) - J_{12}^p(x) - J_{12}^m(x) \\
 &= C_K(x) \cdot k_{21} - K(x) \cdot k_{12}^p - \frac{J_{12}^{\max} \cdot K(x)}{K(x) + K_{1/2}}
 \end{aligned}
 \tag{44}$$

The above differential equation cannot be solved explicitly for  $K(x)$ , and therefore the numerical method of Runge-Kutta again will be employed.

We will consider the constant cell  $K$  case only, and therefore compare the above mathematically defined model with Model A. In order to make the appropriate comparisons, it will be necessary to define values for  $J_{12}^{\max}$  and  $K_{1/2}$  which are consistent with the DeMello-Aires data. Since during the steady state,  $J_s(x) = 0$  and  $K(x) = K(\max)$ , equation (44) transforms to

$$C_K \cdot k_{21} = J_{21} = K(\max) \cdot k_{12}^p + \frac{J_{12}^{\max} \cdot K(\max)}{K(\max) + K_{1/2}}$$

and,

$$J_{12}^{\max} = (K(\max) + K_{1/2}) \left( \frac{J_{21}}{K(\max)} - k_{12}^p \right)
 \tag{45}$$

Equation (45) defines  $J_{12}^{\max}$  in terms of  $K_{1/2}$  and three other parameters whose values may be derived from the DeMello-Aires data. We will arbitrarily choose to consider two values of  $K_{1/2}$ , 3 and 20 mmol/l, as representative of pump kinetics which saturate at low and high luminal  $K$  concentrations, and again take the value of  $k_{12}^p$  calculated for a 30 mv luminal membrane (normal diet animals). The corresponding values of  $J_{12}^{\max}$  are:

$K_{1/2}$ (mmol/l)	=	3	20
$J_{12}^{\max}$ (pmol/min/mm)	=	97.5	225



$$\left\{ \begin{array}{l} K(\text{max}) = 10 \text{ mmol/l} \\ k_{12}^p = 1.65 \text{ nl/min/mm} \\ \Delta E = 30 \text{ mv} \end{array} \right\}$$

The non-linear character of the  $J_{12}$  flux for the above kinetic parameters along with the linear flux of Model A are shown in Figure II.18 where  $J_{12}$  is plotted as a function of the luminal K concentration. The passive component of the flux is indicated by the dotted line and the difference between its value and the total  $J_{12}$  flux represents the magnitude of the carrier-mediated flux component.

We can now examine the behavior of the K secretory system defined by equation (44) in relation to Model A. Shown in Figure II.19 are the plots of  $\phi(\text{net})$  and  $K(L)$  vs.  $V$  for the three cases with  $K(0) = 0$ . Model A again exhibits the most potent K secreting capability within the range of flow rates shown (0 - 40 nl/min). However, since for all cases the maximal rate of K secretion is limited by the magnitude of the constant flux  $J_{21}$ , which is the same for each model, K secretion in all plots is rising asymptotically with flow rate towards the value of 91.5 pmol/min. The rate of rise is most rapid for Model A and less so as  $K_{1/2}$  is lowered from 20 to 3 mmol/l. Since the non-linear pump model generates a higher lumen to cell flux at lower flow rates (when luminal K concentrations are relatively elevated), K secretion is accordingly diminished relative to Model A.

Turning to Figure II.20 where net K absorption is plotted as a function of  $K(0)$ , the linear  $K(0)$  sensitivity of Model A contrasts sharply with the non-linear pump models. As  $K_{1/2}$  is lowered, the non-linear



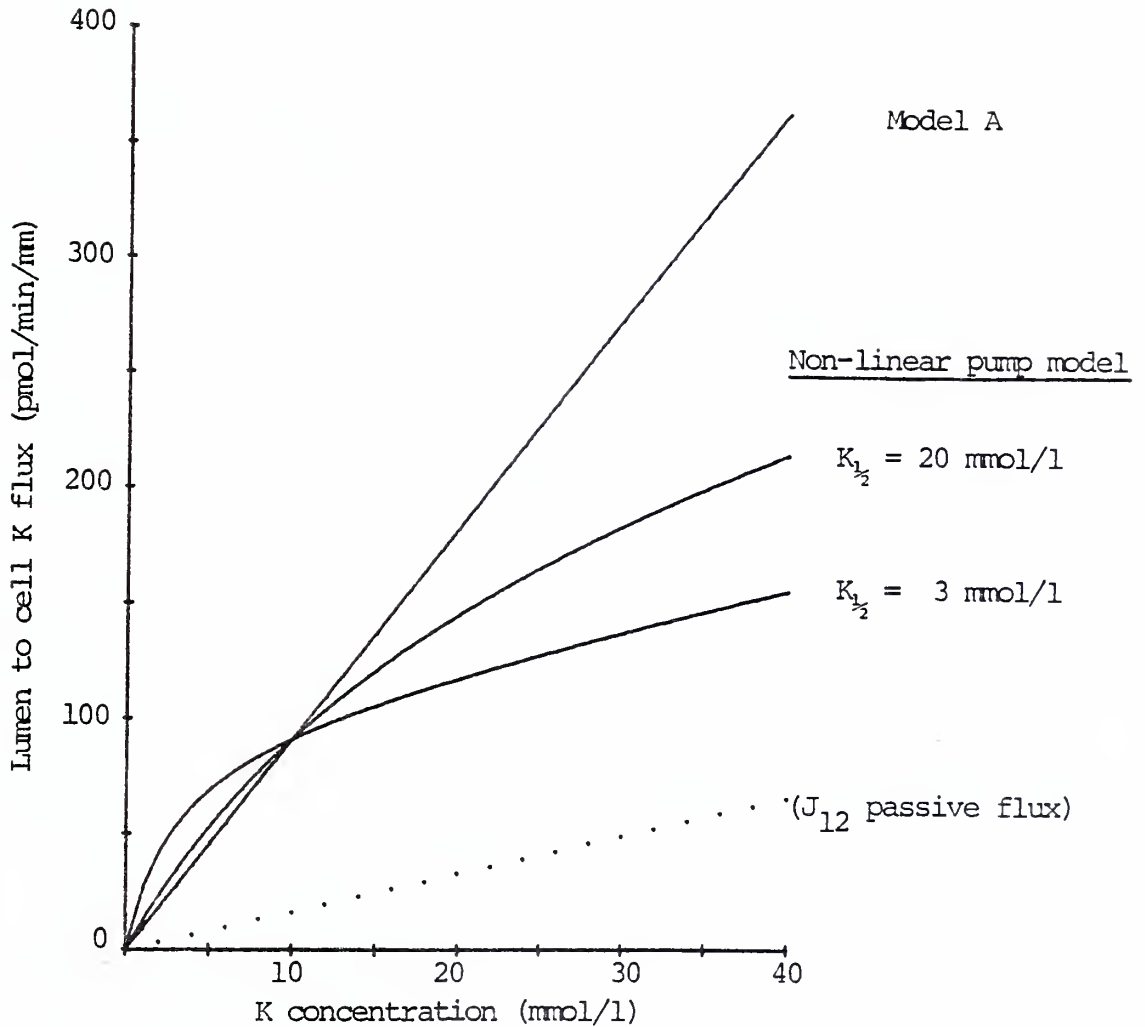


Figure II.18 Lumen to cell K flux,  $J_{12}$ , as a function of luminal K concentration for Model A and the non-linear luminal K reabsorptive pump model with  $K_{1/2}$  set at the values shown. Dotted line indicates the passive flux component of the total  $J_{12}$  flux represented by the other lines.





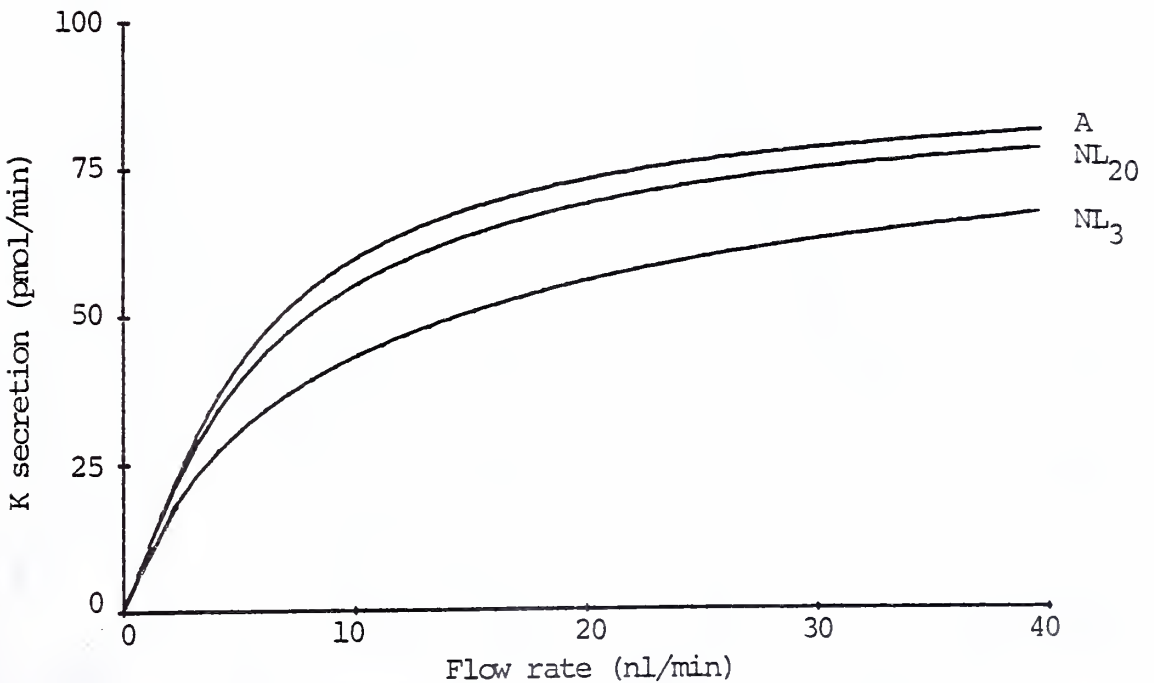
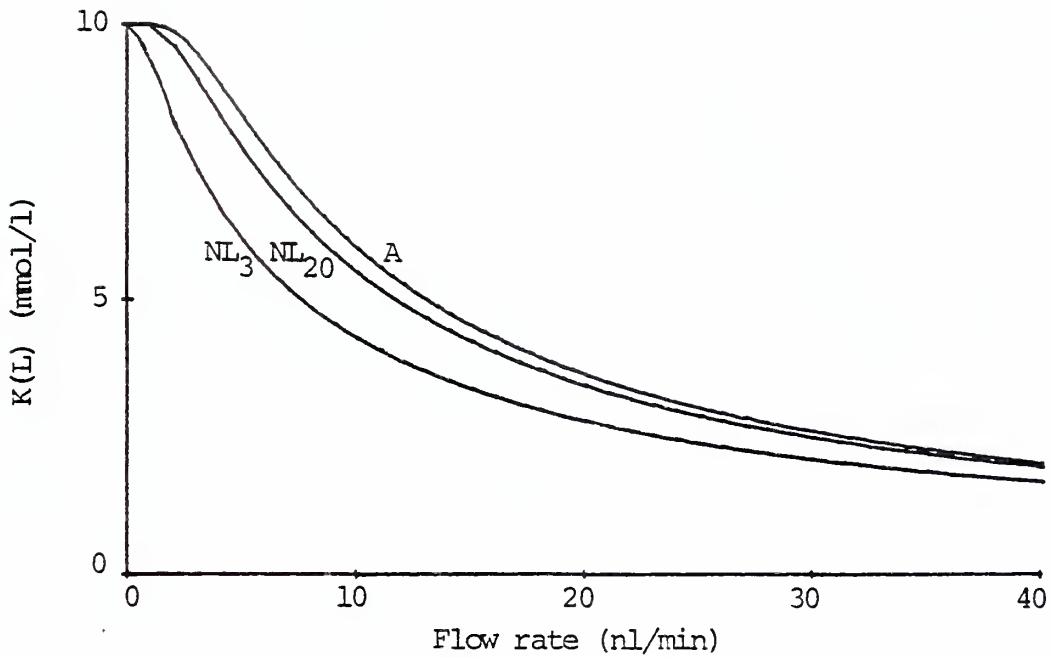


Figure II.19 K(L) and K secretion as a function of flow rate for Model A ("A"), and the non-linear K reabsorptive pump model: "NL<sub>3</sub>" -  $K_{1/2}=3\text{mmol/l}$ , "NL<sub>20</sub>" -  $K_{1/2}=20\text{mmol/l}$ .  $K(0) = 0$  for all plots.



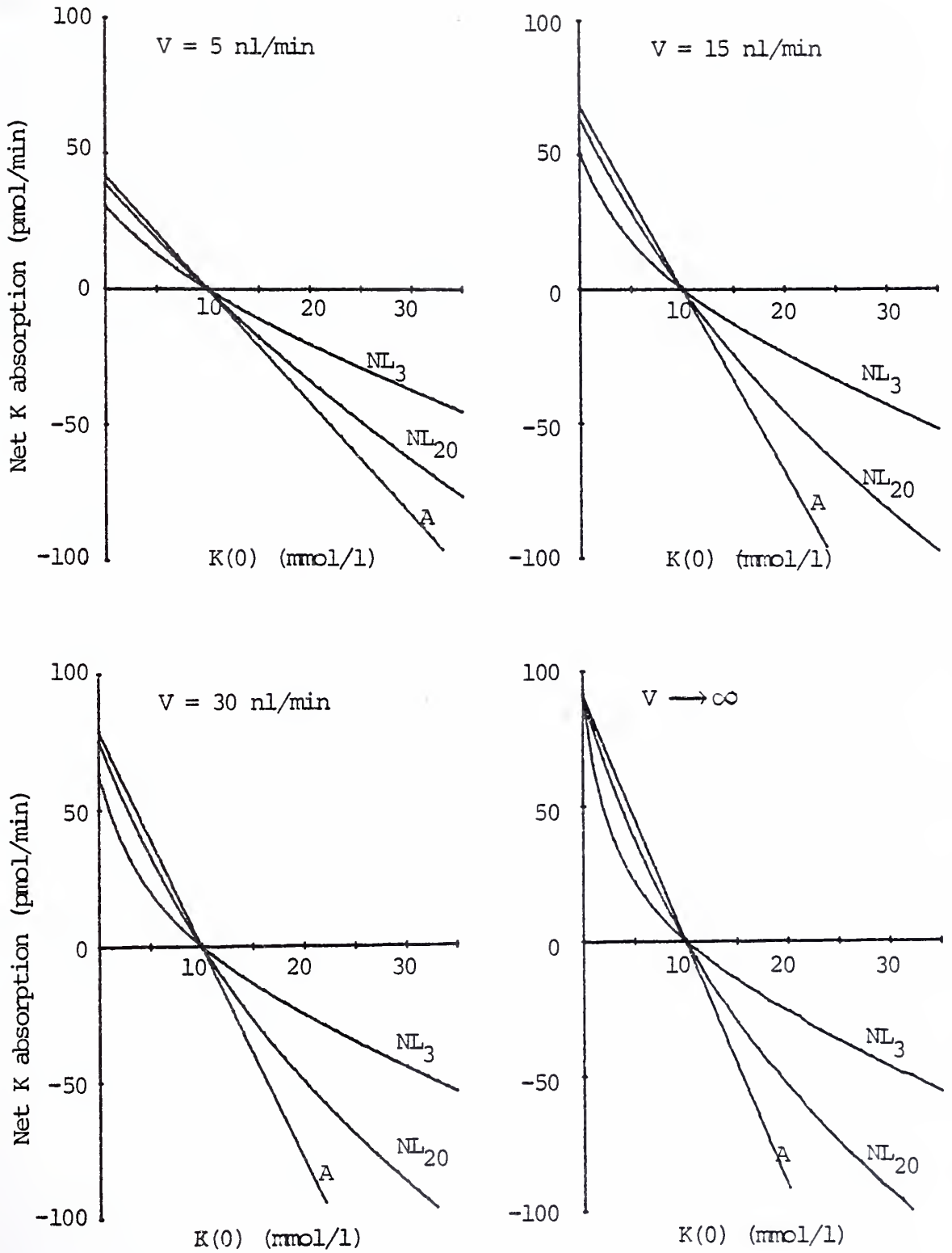


Figure II.20 Net K absorption as a function of  $K(0)$  at several flow rates. Model A is indicated by "A"; the non-linear K reabsorptive pump model by "NL<sub>3</sub>" ( $K_{1/2} = 3$  mmol/l) and "NL<sub>20</sub>" ( $K_{1/2} = 20$  mmol/l)



pump model plots become more curvilinear, particularly at high flow rates. Additionally, the potency of net K reabsorption is reduced in the non-linear pump model, most significantly when  $K_{1/2}$  equals 3 mmol/l, which corresponds to a  $J_{12}^{\max}$  of 97.5 pmol/min. The saturability of the reabsorptive pump limits the rate of net K reabsorption. The plots for  $V \rightarrow \infty$  maximally expose the non-linear character of the luminal pump and confirm that  $\phi_s^{\max}$  is identical for all cases.



## K. NON-CONSTANT LUMINAL MEMBRANE PD

In this section, a brief analysis will be undertaken of a purely hypothetical model to illustrate the importance of the assumption of a constant luminal membrane PD in Models A and B to flow-dependent K secretion. As noted in the Introduction to Part II, if the luminal membrane PD were to become more polarized as a consequence of a lowered luminal K concentration, the net K secretory flux would tend to diminish if electrical potential driving force were the sole factor to be considered. On the other hand, if cell K concentration were maintained at a constant level in spite of the fall in luminal K concentration, the chemical potential for net K secretion would be favorably enhanced. These considerations of the effect of luminal K concentration on electrical and chemical potentials across the luminal membrane briefly introduce the model to be considered below.

We will assume a hypothetical, homogeneous epithelium with the following characteristics:

- Cell K is maintained at a constant concentration, independent of  $x$  and  $J_s(x)$ .
- The luminal membrane net K flux is defined by the Goldman "constant field" equation for passive transport of a cation across a charged membrane.
- The luminal membrane PD arises solely as a Nernst K diffusion potential.

Clearly, this model is based on assumptions that are at odds with known membrane kinetic properties of the late distal tubule. However, its analysis will facilitate an appreciation of the effects of luminal membrane PD variability on K transport.





The appropriate Goldman equation (6a) was given previously:

$$J_s(x) = V \frac{dK(x)}{dx} = P_{nd} \cdot \frac{\Delta E F}{RT} \cdot \frac{[C_K \cdot \exp(-\Delta E F/RT) - K(x)]}{[1 - \exp(-\Delta E F/RT)]} \quad (46)$$

and  $\Delta E$  may be defined by the Nernst equation,

$$E = - \frac{RT}{F} \ln[C_K/K(x)] \quad (47)$$

A solution to equation (46) with the appropriate substitution from equation (47) can be found again by the numerical method of Runge-Kutta. The value of the term,  $P_{nd}$ , will be calculated from the DeMello-Aires kinetic data assuming a 30 mv luminal membrane PD and  $k_{21} = 1.0$  nl/min/mm (normal diet group). From equation (42b)

$$k_{21} = \frac{\Delta E F}{RT} \cdot \frac{P_{nd} \cdot \exp(-\Delta E F/RT)}{1 - \exp(-\Delta E F/RT)} \quad (42)$$

or

$$P_{nd} = \frac{RT}{\Delta E F} \cdot \frac{1 - \exp(-\Delta E F/RT)}{\exp(-\Delta E F/RT)} \cdot k_{21}$$

and for  $\Delta E = 30$  mv,  $k_{21} = 1.00$  nl/min/mm:

$$P_{nd} = 1.30 \text{ nl/min/mm}$$

Setting cell K concentration at 91 mmol/l, we have now defined all the parameters of equations (46) and (47).

Figure II.21a presents the net K secretion - flow rate profile for this model with  $K(0)$  values of 0, 2, and 5 mmol/l. At a zero initial K concentration, K secretion actually declines with increasing flow rate. The luminal membrane polarizing effect of a falling luminal K concentration with higher flow rate dominates K secretion behavior. However, when  $K(0)$  is raised to 2 or 5 mmol/l, the opposing effects



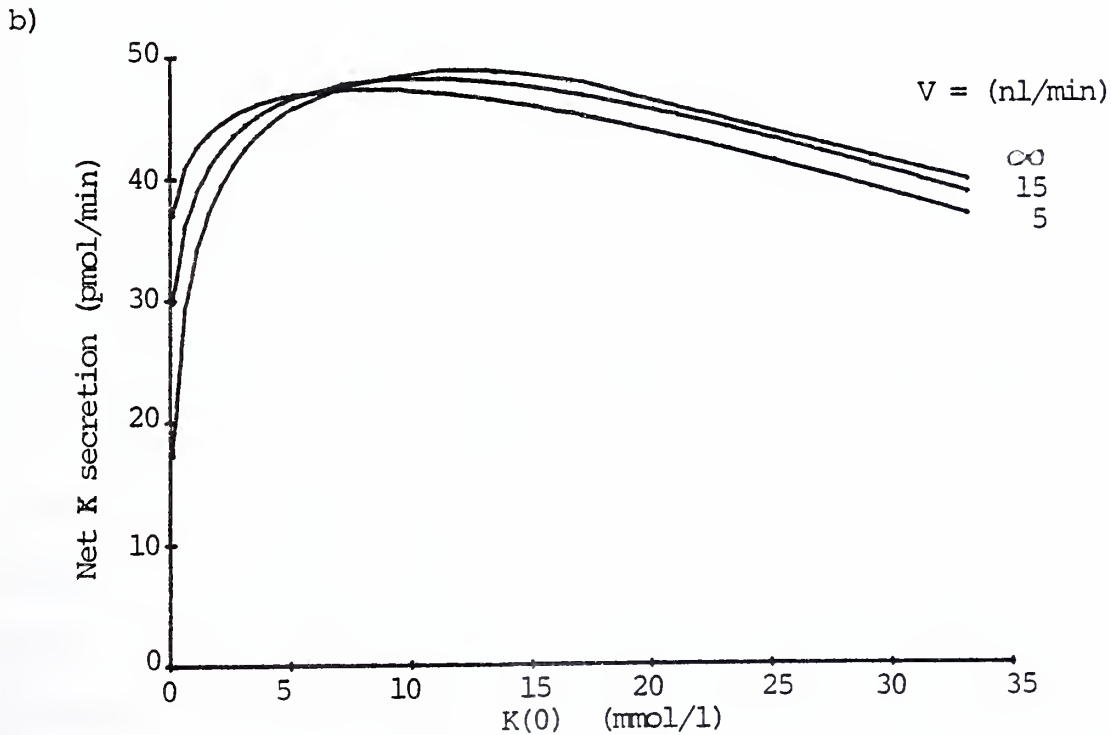
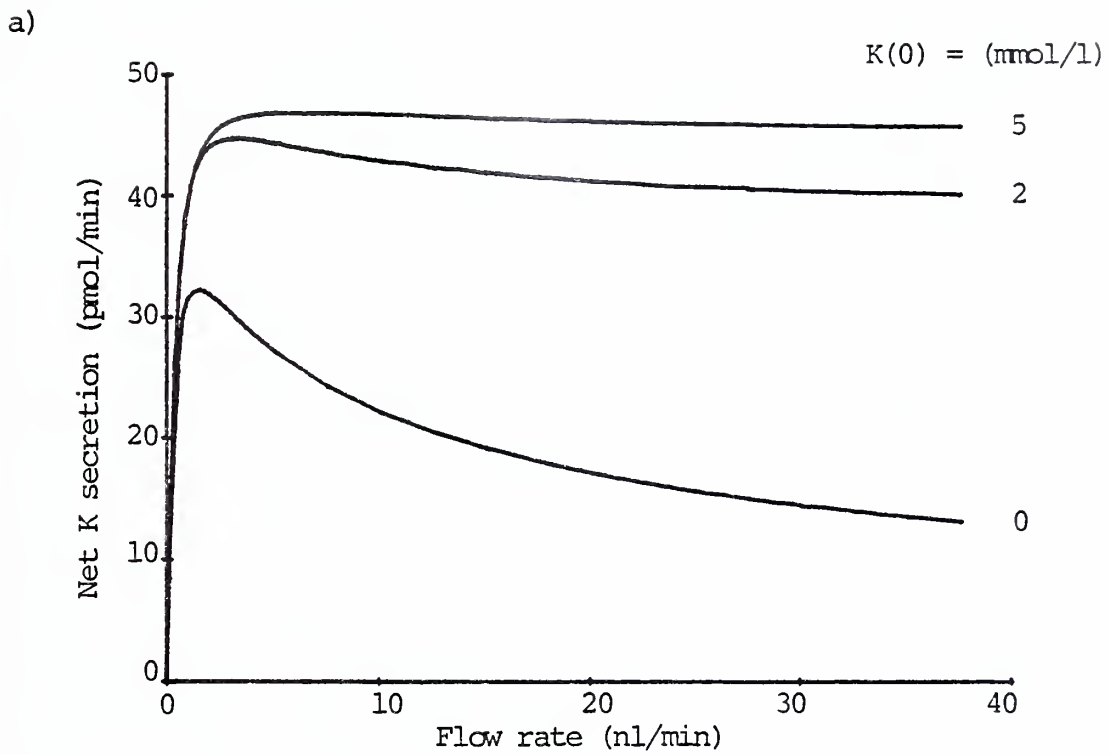


Figure II.21 K secretion as a function of flow rate (a) and net K secretion as a function of  $K(0)$  (b) for variable luminal membrane PD model. Several initial K concentrations (a) and flow rates (b) are shown.



of the electrical and chemical potential across the luminal membrane on K transport have apparently aligned in a manner that produces a near constancy of net K secretion under variable luminal conditions. Interestingly, when  $K(0) = 5 \text{ mmol/l}$ , flow dependent K secretion more closely approximates a strictly transport-limited system than any model previously considered.

Figure II.21b demonstrates a  $K(0)$  sensitivity plot radically different from any previously considered model. No net K reabsorption is demonstrated over the range of  $K(0)$  values plotted, 0 to 35 mmol/l. Indeed, net K secretion would not fall to zero until  $K(0)$  equaled 100 mmol/l. In this circumstance, luminal and cell K concentrations would be equal and the electrochemical potential of K transport would be zero. Also, in contrast to previous models, maximal rates of K secretion are attained when  $K(0)$  is greater than zero. From Figure II.21b, maximum net K secretion can be estimated to be approximately 50 pmol/min/mm, somewhat higher than  $\phi_S^{\text{max}}$  of Model B, 38.9 pmol/min/mm, and substantially less than  $\phi_S^{\text{max}}$  for Model A, 91.5 pmol/min/mm.

From the foregoing we may conclude generally that a luminal membrane PD partially or entirely dependent on a K diffusion potential will tend to favor transport-limited flow dependency of K transport. If a luminal K reabsorptive pump with linear kinetics were added to this model, it can be predicted that K secretion flow dependency would tend towards a more flow-limited character, but the peculiar curvilinear nature of  $\phi(\text{net})$  vs.  $K(0)$  plot in Figure II.21b would not be changed.

Having now considered a number of alternative luminal membrane properties that contrast with the postulates of Models A and B, we can now



proceed with an assessment of in vivo data which will permit a limited evaluation of the applicability of the various models to in vivo K secretion kinetics.





## L. IN VIVO $\phi(\text{net})$ VS. $K(0)$ RESULTS COMPARED TO MODEL PREDICTIONS

In this section, experimental data from work in progress in the laboratory of D. Good and F. S. Wright will be drawn from in order to evaluate the kinetic predictions of the various theoretical models presented in Part II. The data to be considered here was developed in the course of a microperfusion study of flow dependency of distal tubule K transport, the principal findings of which already have been reported (26,27).

The experimental approach illustrated in Figure II.22 involved the perfusion of single distal tubule segments of hydropenic rats at several flow rates with solutions of differing ionic compositions. Because only a few perfusion rates were employed, the results from this aspect of the work are not particularly helpful in evaluating the theoretical models. Most of the models considered in Part II predict an enhancement of K secretion with flow rate. This phenomenon was well demonstrated by the Good and Wright experiments (27). In addition to studying flow dependency, Good and Wright also investigated the effect of varying the perfusate K concentration on net K absorption rates. At a perfusion rate of 26 nl/min, net K absorption was measured during perfusion with solutions containing four different K concentrations: 0, 2, 14, and 35 mmol/l. These experiments are particularly relevant to the models, for they permit a plotting of in vivo data in the form of  $\phi(\text{net})$  vs.  $K(0)$ . This, of course, represents a  $K(0)$  sensitivity plot that has been shown to be the important discriminating feature among the theoretical models. As will be seen, the data from the Good and Wright experiments demonstrates a convincing linearity in the relationship between  $\phi(\text{net})$  and  $K(0)$ , a characteristic feature and prediction of Models A and B.



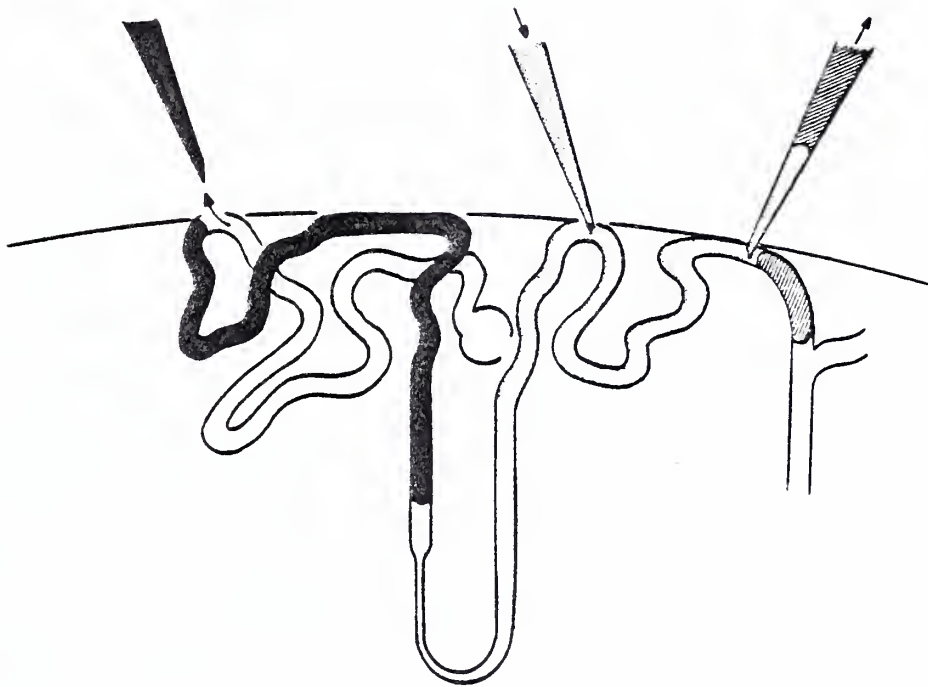


Figure II. 22 Distal tubular microperufsion experiment of Good and Wright (27). See text for explanation. (Reprinted with the permission of F. S. Wright.)



Before proceeding with an evaluation of this data, a cautionary note is warranted. Discussed in the preceding sections were several possible reasons for the existence of non-linearity in the  $\phi(\text{net})$  vs.  $K(0)$  functional relationship. Although not analyzed per se, it is also evident that the demonstration of a linear  $K(0)$  sensitivity plot based on in vivo experimental results by no means validates the assumptions of Models A and/or B. Appropriately aligned non-linearity in the kinetic behavior of the fluxes  $J_{12}$  and  $J_{21}$  as luminal conditions change could give rise to a linear  $\phi(\text{net})$  vs.  $K(0)$  relationship. For this and other reasons, the data from Good and Wright to be presented here may be judged as consistent with the predictions of Models A and B, but with the recognition that the varied complexities of in vivo K membrane transport may have combined to give an apparency of legitimacy to the simplifying postulates of these two models. At a minimum, it will be appreciated that the Model A and B solution equations offer a potentially useful mathematical description of in vivo distal tubular K transport kinetics.

The single nephron perfusion depicted in Figure II.22 was carried out over a distal tubule segment comprising both early and late portions. The model equations are thus not strictly applicable since the solutions assumed a homogeneous epithelium. Furthermore, volume reabsorption occurs over the experimentally perfused tubule segment, whereas the explicit model equations were found under zero fluid transport conditions. However, a mathematical solution to the fundamental differential equation (4) can be found that is consistent with the principal assumptions of Models A and B and which further takes into account volume reabsorption



and a non-homogeneous epithelium. The details of the solution are presented in the Appendix. The Model A and B assumptions remain the same except that  $k_a$  as defined for each model is permitted to vary as a function of  $x$ ; that is,  $k_a(x) = f(x)$ . The integrated solution to the differential equation (4) shown below yields a mean value for this parameter.

$$K(L) = K(0) \frac{V(0)}{V(L)} \exp(-\bar{k}_a \cdot L/V^*) + K^*(\max) \frac{V(0)}{V(L)} [1 - \exp(-\bar{k}_a \cdot L/V^*)] \quad (48)$$

$$\phi(\text{net}) = V(0) \cdot [K^*(\max) - K(0)] [1 - \exp(-\bar{k}_a \cdot L/V^*)] \quad (49)$$

where

$$V(L) \leq V^* \leq V(0)$$

$\bar{k}_a \equiv$  mean value of  $k_a(x)$  between  $x = 0$  and  $x = L$

$K^*(\max) \equiv K(0)$  when  $\phi(\text{net}) = 0$

( $K^*(\max)$  will vary with  $V(0)$ )

Model A:  $\bar{k}_a = \bar{k}_{12}(x)$

Model B:  $\bar{k}_a = \left[ \frac{k_{12}(x) \cdot k_{23}(x)}{k_{21}(x) + k_{23}(x)} \right]_{\text{mean}}$

Note that  $K^*(\max)$  is defined operationally as equal to that value of  $K(0)$  which results in zero net  $K$  absorption. Unlike the previously defined  $K(\max)$  parameter,  $K^*(\max)$  can be shown to vary with flow rate.

Accordingly,  $K^*(\max) \cdot \bar{k}_a$  does not equal  $\phi_s^{\max}$  except when  $V(0) \rightarrow \infty$ .

It can also be demonstrated that for an epithelium like the distal tubule where  $k_a(x)$  may be presumed to be greater in the late than early portion,  $K^*(\max)$  will increase as flow rate increases. Its maximum value is attained when  $V(0) \rightarrow \infty$ .  $V^*$  arises as defined because the flow function is





intentionally not characterized. (It will be recalled that the approximating flow function developed in an earlier section did not permit an explicit solution of the fundamental differential equation.)

It is important to note that equation (49) will plot as a straight line if  $V(0)$  and  $V(L)$  are held constant.  $\Phi(\text{net})$  will then vary directly as a function of  $K(0)$ , with the slope,  $S$ , equal to

$$S = - V(0)[1 - \exp(-\bar{k}_a \cdot L/V^*)] \quad (50)$$

$$V(L) \leq V^* \leq V(0)$$

from which a range for the value  $\bar{k}_a$  can be calculated if  $V(0)$  is known. The "X" intercept of a plot of equation (49) ( $\Phi(\text{net}) = 0$ ) will equal  $K^*(\text{max})$ .

Data from the Good and Wright experiments which may be evaluated in terms of equations (49) and (50) is shown in Table II.6. Note that  $V_{ED}$  and  $V_{LD}$  ( $\cong V(0)$  and  $V(L)$ ) are relatively constant for the various initial  $K$  concentrations, the magnitude of volume reabsorption is small, and  $\Phi(\text{net})$  ranges from net  $K$  secretion to net  $K$  absorption. The data, plotted in Figure II.23, yields the linear regression equation

$$y = - 6.91x + 115.7$$

$$r = 0.999$$

$$K^*(\text{max}) = 16.7 \text{ mmol/l}$$



Table II.6 Data from Good and Wright microperfusion experiments

A) Results from distal tubule perfusion with differing perfusate K concentrations

	$\frac{K_{ED}}{\text{(mmol/l)}}$	$\frac{K_{LD}}{\text{(mmol/l)}}$	$\frac{V_{ED}}{\text{(nl/min)}}$	$\frac{V_{LD}}{\text{(nl/min)}}$	$\frac{O(\text{net})}{\text{(pmol/min)}}$
0 K	0	4.8	25.3	23.0	113.5
2 K	2.2	7.0	25.9	23.3	105.4
15 K	14.5	16.7	26.5	23.9	11.3
34 K	34.3	33.2	25.6	22.8	-119.9

Mean length of perfused tubule segments = 1.3 mm

B) Perfusion solutions, ionic compositions (mmol/l)

	<u>0 K</u>	<u>2 K</u>	<u>15 K</u>	<u>34 K</u>
Na	43	43	43	43
K	0	2	15	34
Cl	33	35	50	68
urea	108	105	80	43

All perfusion solutions also contained phosphate (4.5 mmol/l) and sulfate (1.0 mmol/l).



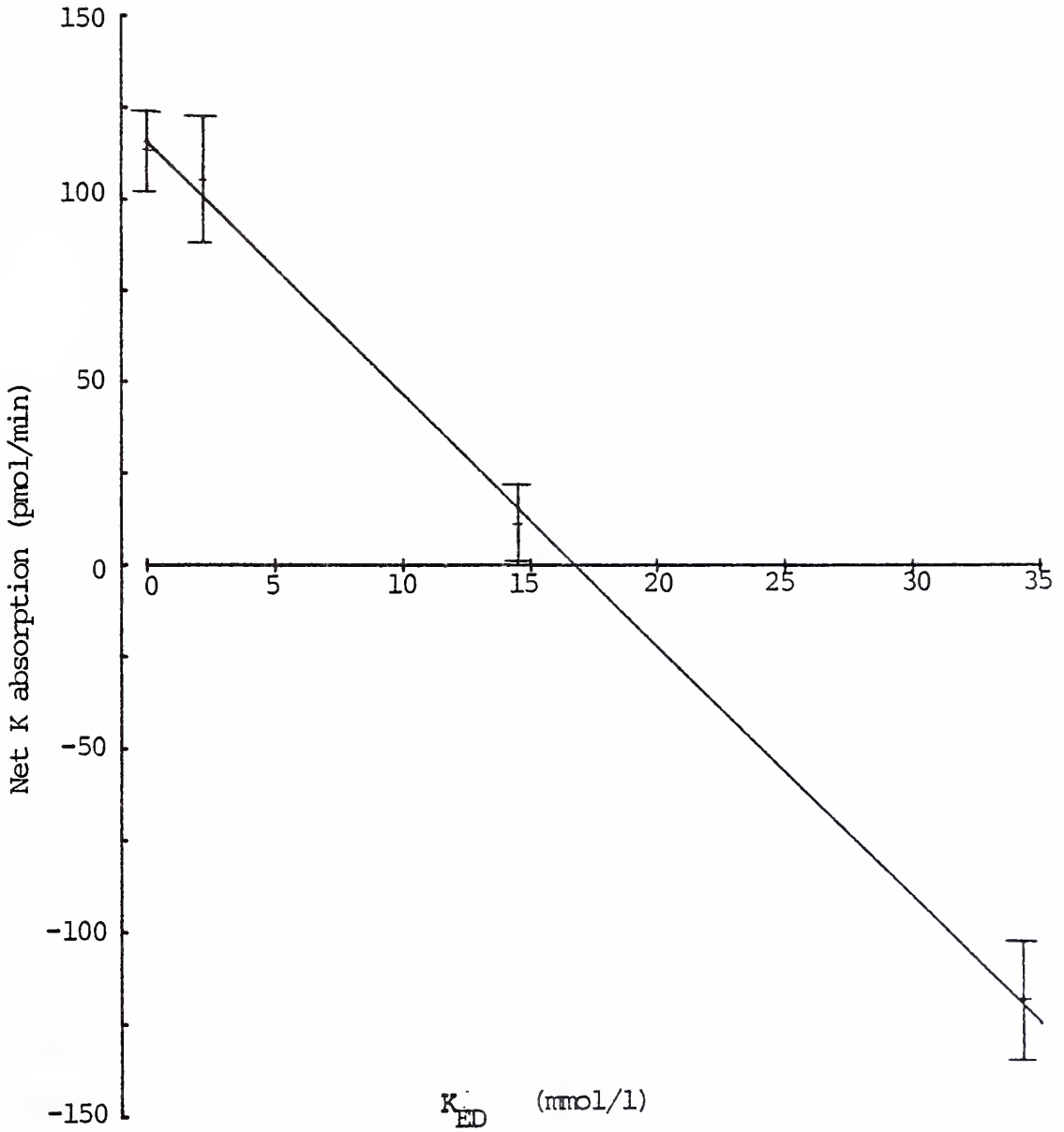


Figure II.23 Plot of net K absorption as a function of early distal K concentration ( $K_{ED}$ ) for data of Good and Wright shown in Table II.6. Mean net K absorption  $\pm$ SEM indicated. Line represents plot of best fit linear regression equation:  $y = -6.91x + 115.7$  ( $r = .999$ ).



The rate coefficient,  $\bar{k}_a$ , is calculated from equation (50) after solving for  $\bar{k}_a$ :

$$\frac{-V(L)}{L} \ln\left[\frac{S}{V(0)} + 1\right] \leq \bar{k}_a \leq -\frac{V(0)}{L} \ln\left[\frac{S}{V(0)} + 1\right]$$

$$S = 6.91 \text{ nl/min}$$

$$V(0) = 26 \quad "$$

$$V(L) = 23 \quad "$$

$$L = 1.3 \text{ mm}$$

$$5.47 \leq \bar{k}_a \leq 6.18 \text{ nl/min/mm}$$

The mean rate coefficient for the perfused segment has a value within the range of  $k_a$ 's calculated for the normal diet rats of the DeMello-Aires experiment (9.15 for Model A and 3.89 for Model B). As with the experimental results from DeMello-Aires, the data from Good and Wright does not permit a differentiation of Model A from B.

Clearly, the Good and Wright experiments are not ideally designed to test the assumptions of Models A and B. The inhomogeneity of the perfused segment (early and late distal segments) and the presence of volume reabsorption lead to experimental results which cannot be readily related to the parameters  $K(\max)$  and  $\Phi_s^{\max}$  of Models A and B. However, the data offer some support for a kinetic behavior of distal tubular K secretion along the lines predicted by Models A and B. Results from experiments carried out at different flow rates would be required to further evaluate the models. Moreover, a direct test of the particular assumptions of Models A and B regarding the luminal membrane PD, the luminal K reabsorptive pump, and cell K concentration would undoubtedly





necessitate experimental approaches of an entirely different type. The single isolated tubule perfusion method perhaps represents the most satisfactory approach presently available for directly evaluating the principal assumptions and predictions of the models considered here in Part II.



APPENDICES



APPENDIX A. Proof of limits employed in derivation of model equations

$$(1) \quad \lim_{V \rightarrow 0} y = f[V] = e^{-\frac{b}{V}} = 0$$

Proof: as  $V \rightarrow 0$ ,  $b/V \rightarrow \infty$

$$\text{and } e^{-\frac{b}{V}} \rightarrow \frac{1}{\infty} = 0$$

$$(2) \quad \lim_{V \rightarrow 0} y = f[V] = A[1 - e^{-\frac{b}{V}}] = A$$

Proof follows directly from (1).

$$(3) \quad \lim_{V \rightarrow \infty} y = f[V] = \frac{V}{b}[1 - e^{-\frac{b}{V}}] = 1$$

Proof:  $y(V)$  can be rewritten as an infinite series,

$$\begin{aligned} y(V) &= \frac{V}{b} \left[ \frac{b}{V} - \frac{1}{2!} \left(\frac{b}{V}\right)^2 + \frac{1}{3!} \left(\frac{b}{V}\right)^3 \dots \right] \\ &= 1 - \frac{1}{2!} \left(\frac{b}{V}\right) + \frac{1}{3!} \left(\frac{b}{V}\right)^2 \dots \end{aligned}$$

therefore,

$$\lim_{V \rightarrow \infty} y(V) = 1$$



APPENDIX B. General solution of fundamental differential equation

A general solution for the fundamental differential equation (4) is given below. The solution is derived for the case of a constant cell K concentration only.

The general solution to the differential equation

$$\frac{dV(x) \cdot K(x)}{dx} = C_K \cdot k_{21} - K(x) \cdot k_{12} \quad (4)$$

where  $K(x), V(x), k_{12}$ , and  $k_{21}$  may vary as a function of  $x$ , and  $C_K$  is a constant parameter

may be written as

$$K(x) = \frac{u(0)}{u(x)} \cdot K(0) + \frac{1}{u(x)} \int_0^x \left[ u(s) \cdot C_K \cdot k_{21} \right] dx \quad (B1)$$

where

$$u(x) = \exp \left[ \int \left[ \frac{1}{V(x)} \cdot \frac{dV(x)}{dx} + \frac{k_{12}}{V(x)} \right] dx \right] \quad (B2)$$

Evaluating the indefinite integral of (B2) gives

$$\begin{aligned} u(x) &= \exp \left[ \ln V(x) + \int \left[ \frac{k_{12}}{V(x)} \right] dx \right] \\ &= V(x) \cdot \exp \left[ \int \left[ \frac{k_{12}}{V(x)} \right] dx \right] \end{aligned}$$

or

$$u(x) = V(x) \exp[I(x)] \quad (B3)$$

$$\text{where: } I(x) = \left[ \int \left[ \frac{k_{12}}{V(x)} \right] dx \right]$$

We now note that

$$\frac{u(0)}{u(x)} = \frac{V(0)}{V(x)} \exp \left[ - \int_0^x \left[ \frac{k_{12}}{V(x)} \right] dx \right] \quad (B4)$$





and since by the First Integral Theorem of Mean Value,

$$\int_0^x \left[ k_{12} \sqrt{V(x)} \right] dx = \frac{1}{V^*} \int_0^x k_{12} dx$$

where:  $V(0) \leq V^* \leq V(x)$

and also

$$\int_0^x k_{12} dx = x \cdot \bar{k}_{12}$$

where:  $\bar{k}_{12}$  is the mean value of  $k_{12}$  over the interval  $0 \rightarrow x$

equation (B4) transforms to

$$\frac{u(0)}{u(x)} = \frac{V(0)}{V(x)} \exp(-\bar{k}_{12} \cdot x / V^*) \tag{B5}$$

Substituting (B3) and (B5) into (B1) gives

$$K(x) = \frac{V(0)}{V(x)} \exp[(-\bar{k}_{12} \cdot x / V^*)] \cdot K(0) + \frac{\exp[-I(x)]}{V(x)} \int_0^x \left[ u(s) \cdot C_K \cdot k_{21} \right] dx \tag{B6}$$

$\Phi(\text{net})$  has been defined as

$$\Phi(\text{net}) = V(L) \cdot K(L) - V(0) \cdot K(0) \tag{1}$$

Thus equation (B6) when substituted into (1) gives

$$\Phi(\text{net}) = V(0) \cdot K(0) [\exp(-\bar{k}_{12} \cdot L / V^*) - 1] + \exp[-I(L)] \cdot \int_0^{x=L} \left[ u(s) \cdot C_K \cdot k_{21} \right] dx \tag{B7}$$

It is useful to define  $K^*(\text{max})$  as that value of  $K(0)$  which results in zero net  $K$  absorption, that is,

$$K(0) = K^*(\text{max}) \text{ when } \Phi(\text{net}) = 0 \tag{B8}$$



Substituting (B8) into (B7), setting  $\Phi(\text{net}) = 0$ , and solving for  $\exp[-I(L)]$  gives

$$\exp[-I(L)] = \frac{V(0) \cdot K^*(\text{max}) \cdot [1 - \exp(-\bar{k}_{12} \cdot L/V^*)]}{\int_0^{x=L} [u(s) \cdot C_K \cdot k_{21}] dx} \quad (\text{B9})$$

and now substituting (B9) into (B6) and (B7) gives, after simplification,

$$K(L) = K(0) \frac{V(0)}{V(x)} \exp(-\bar{k}_{12} \cdot L/V^*) + K^*(\text{max}) \frac{V(0)}{V(L)} [1 - \exp(-\bar{k}_{12} \cdot L/V^*)]$$

$$\Phi(\text{net}) = [K^*(\text{max}) - K(0)] [1 - \exp(-\bar{k}_{12} \cdot L/V^*)]$$

which are equations (48) and (49) given in the text.



R E F E R E N C E S



1. Adam, W. R. and Dawborn, J. K. Potassium tolerance in rats. Australian J. Exp. Biol. Med. Sci. 50: 757-768, 1972.
2. Adler, S. An extrarenal action of aldosterone on mammalian skeletal muscle. Am. J. Physiol. 218: 616-621, 1970.
3. Alexander, E. A. and Levinsky, N. G. An extrarenal mechanism of potassium adaptation. J. Clin. Invest. 47: 740-748, 1968.
4. Ahterton, J. C., Hai, M. A., and Thomas, S. Effects of water diuresis and osmotic (mannitol) diuresis on urinary solute excretion, by the conscious rat. J. Physiol. (London) 197: 395-410, 1968.
5. Baylis, C., and O'Connor, W. J. The effect of plasma potassium in determining normal rates of excretion of potassium in dogs. QJ Exper. Physiol. 61: 145-157, 1976.
6. Beal, A. M., Budtz-Olsen, O. E., Clark, R. C., Cross, R. B., and French, T. J. Changes in renal haemodynamics and electrolyte excretion during acute hyperkalaemia in conscious adrenalectomized sheep. QJ Exper. Physiol. 60: 207-221, 1975.
7. Berliner, R. W. Renal mechanisms for potassium excretion. Harvey Lectures 55: 141-171, 1961.
8. Boulpaep, E. Electrical phenomenon in the nephron. Kidney Int. 9: 88-102, 1976.
9. Boyd, J. E., Palmore, W. P., and Mulrow, P. J. Role of potassium in the control of aldosterone secretion in the rat. Endocrinology 88: 556-565, 1971.
10. Boyd, J. E. and Mulrow, P. J. Further studies on the influence of potassium upon aldosterone production in the rat. Endocrinology 90: 299-301, 1972.
11. Brandis, M., Keyes, J., and Windhager, E. E. Potassium induced inhibition of proximal tubular fluid reabsorption in rats. Am. J. Physiol. 222: 421-427, 1972.
12. Brenner, B. M. and Berliner, R. W. Transport of potassium. In Handbook of Physiology (J. Orloff and R. W. Berliner, Eds.) Sect. 8., pp. 497-520. American Physiological Society, Washington, D.C., 1973.
13. Burg, M. B. and Orloff, J. Effect on temperature and medium K on Na and K fluxes in separated renal tubules. Am. J. Physiol. 211: 1005-1010, 1966.





14. Burg, M. B. and Abramow, M. Localization of tissue sodium and potassium compartments in rabbit renal cortex. *Am. J. Physiol.* 211: 1011-1017, 1966.
15. Cade, R. and Shalhoub, R. Effect of mineralocorticoids on renal handling of potassium. *J. Clin. Invest.* 40: 1028, 1961. Abstract.
16. Cortney, M. A., Nagel, W., and Thurau, K. A micropuncture study of the relationship between flow-rate through the loop of Henle and sodium concentration in the early distal tubule. *Pfluegers Archiv.* 287: 286-295, 1966.
17. Cox, M., Sterns, R. H., and Singer, I. The defense against hyperkalemia: The roles of insulin and aldosterone. *N. Engl. J. Med.* 229: 519-521, 1978.
18. Davis, J. O., Urquhart, J., and Higgins, J. T., Jr. The effects of alterations of plasma sodium and potassium concentration on aldosterone secretion. *J. Clin. Invest.* 42: 597-609, 1963.
19. DeMello-Aires, M., Giebisch, G., Malnic, G., and Curran, P. F. Kinetics of potassium transport across single distal tubules of rat kidney. *J. Physiol. (London)* 232: 47-70, 1973.
20. Duarte, C. G., Chamety, F., and Giebisch, G. Effect of amiloride, ouabain, and furosemide on distal tubular function in the rat. *Am. J. Physiol.* 221: 632-639, 1971.
21. Fimognari, G. M., Fanestil, D. D., and Edelman, I. S. Induction of RNA and protein synthesis in the action of aldosterone in the rat. *Am. J. Physiol.* 213: 954-962, 1967.
22. Giebisch, G. In The Kidney, Morphology, Biochemistry, Physiology (C. Rouiller and A. Muller, Eds.), Vol. 3, pp. 329-382. Academic Press, Inc., New York and London, 1971.
23. Giebisch, G. Some reflections on the mechanism of renal tubular potassium transport. *Yale J. Biol. Med.* 48: 315-336, 1975.
24. Giebisch, G. Effects of diuretics on renal transport of potassium. In Methods in Pharmacology (M. Martinez-Maldonado, Ed.), Vol 4A, pp. 121-164, Plenum Press, New York, 1976.
25. Gonick, H. C., Coburn, J. W., Rubini, M. E., Maxwell, M. H., and Kleeman, C. R. Effect of urea osmotic diuresis on potassium excretion. *Am. J. Physiol.* 206: 1118-1122, 1964.
26. Good, D. W. and Wright, F. S. Effects of sodium reabsorption, trans-epithelial voltage and fluid flow rate on potassium secretion in renal distal tubule. *Kidney Int.* 12: 558, 1977.



27. Good, D. W. and Wright, F. S. Luminal influences on potassium secretion: sodium concentration and fluid flow rate. *Am. J. Physiol.* 236: (Feb.), 1979. (In press).
28. Grantham, J. J. Action of antidiuretic hormone in the mammalian kidney. In MTP International Review of Science (K. Thurau, Ed.), Series I, Vol. 6, pp. 247-272. Butterworth & Co., London and Washington, D.C., 1974.
29. Hayslett, J. P., Boulpaep, E. L., and Giebisch, G. Factors influencing transepithelial potential difference in mammalian distal tubule. *Am. J. Physiol.* 234: F182-F191, 1978.
30. Hierholzer, K. and Widerholdt, M. Some aspects of distal tubular solute and water transport. *Kidney Int.* 9: 198-213, 1976.
31. Hierholzer, K. and Lang, S. The effects of adrenal steroids on renal function. In Kidney and Urinary Tract Physiology (K. Thurau, Ed.), MTP Int. Rev. of Science, 6: 273-333, 1974.
32. Hoffman, J. F. The active transport of sodium by ghosts of human red blood cells. *J. Gen. Physiol.* 45: 837-859, 1962.
33. Hoffman, P. G. and Tosteson, D. C. Active sodium and potassium transport in high potassium and low potassium sheep red cells. *J. Gen. Physiol.* 58: 438-466, 1971.
34. Hohenneger, M. Potassium escape phenomenon in rats during continuous application of amiloride. *Pharmacol.* 5: 301-306, 1971.
35. Khuri, R. N., Agulian, S. K., and Kalloghlian, A. Intracellular potassium in cells of the distal tubule. *Pfluegers Arch.* 335: 297-307, 1972.
36. Khuri, R. N., Wiederholt, M., Strieder, N., and Giebisch, G. The effects of flow rate and potassium intake on distal tubular potassium transfer. *Am. J. Physiol.* 228: 1249-1261, 1975.
37. Khuri, R. N., Wiederholt, M., Strieder, N., and Giebisch, G. The effects of graded solute diuresis on renal tubular sodium transport in the rat. *Am. J. Physiol.* 228: 1262-1268, 1975.
38. Knox, W. H. and Sen, A. K. Mechanism of action of aldosterone with particular reference to (Na + K)-ATPase. *Ann. N. Y. Acad. Sci.* 242: 471-488, 1974.
39. Kunau, R. T., Jr., Webb, H. L., and Borman, S. C. Characteristics of the relationship between the flow rate of tubular fluid and potassium transport in the distal tubule of the rat. *J. Clin. Invest.* 54: 1488-1495, 1974.



40. Kunau, R. T., Jr., Webb, H. L., and Borman, S. C. Characteristics of sodium reabsorption in the loop of Henle and distal tubule. *Am. J. Physiol.* 227: 1181-1191, 1974.
41. Landwehr, D. M., Klose, R. M., and Giebisch, G. Renal tubular sodium and water reabsorption in the isotonic sodium chloride loaded rat. *Am. J. Physiol.* 221: 1192-1208, 1971.
42. Malnic, G., Klose, R. M., and Giebisch, G. Micropuncture study of renal potassium excretion in rats. *Am. J. Physiol.* 206: 674-686, 1964.
43. Malnic, G., Klose, R. M., and Giebisch, G. Micropuncture study of distal tubular potassium and sodium transport in rat nephron. *Am. J. Physiol.* 211: 529-547, 1966.
44. Malnic, G. R., Klose, R. M., and Giebisch, G. Microperfusion study of distal tubular potassium and sodium transfer in rat kidney. *Am. J. Physiol.* 211: 548-599, 1966.
45. Morel, F., Chabardes, D., and Imbert, M. Functional segmentation of the rabbit distal tubule by microdetermination of hormone-dependent adenylate cyclase activity. *Kidney Int.* 9: 264-277, 1976.
46. Morgan, T. and Berliner, R. W. A study by continuous microperfusion of water and electrolyte movements in the loop of Henle and distal tubule of the rat. *Nephron* 6: 388-405, 1969.
47. Orloff, J. and Davidson, D. G. The mechanism of potassium excretion in the chicken. *J. Clin. Invest.* 38: 21-30, 1959.
48. Rabinowitz, L. and Gunther, R. A. Renal potassium excretion in sheep during sodium sulfate, phosphate, and chloride infusion. *Am. J. Physiol.* 234: F371-F375, 1978.
49. Rapaport, S. and West, C. D. Excretion of sodium and potassium during osmotic diuresis in the hydropenic dog. *Am. J. Physiol.* 163: 175-180, 1950.
50. Rector, F. C., Jr., Bloomer, H. A., and Seldin, D. W. Proximal tubular reabsorption of potassium during mannitol diuresis in rats. *J. Lab. Clin. Med.* 63: 100-105, 1964.
51. Reineck, H. J., Osgood, R. W., Ferris, T. F., and Stein, J. H. Potassium transport in the distal tubule and collecting duct of the rat. *Am. J. Physiol.* 229: 1403-1409.
52. Rose, B. D. Clinical Physiology of Acid-Base and Electrolyte Disorders, Chapter 8, pp. 109-135. McGraw-Hill, New York, 1977.
53. Sachs, J. R. and Welt, L. G. The concentration dependence of active potassium transport in the human red blood cell. *J. Clin. Invest.* 46: 65-76, 1967.





54. Silva, P., Ross, B. D., Charney, A. N., Besarab, A., and Epstein, F. H. Potassium transport by the isolated perfused kidney. *J. Clin. Invest.* 56: 862-869, 1975.
55. Silva, P., Brown, R. S., and Epstein, F. H. Adaptation to potassium. *Kidney Int.* 11: 466-475, 1977.
56. Stanton, B. and Giebisch, G. In vivo microperfusion study of potassium secretion by the distal convoluted tubule during acute K infusion. *Fed. Proc.* 37: 728, 1978. (Abstract).
57. Thatcher, J. S. and Radike, A. W. Tolerance to potassium intoxication in the albino rat. *Am. J. Physiol.* 151: 138-146, 1947.
58. Ussing, H. H. and Zerahn, K. Active transport of sodium as the source of electric current in short-circuited isolated frog skin. *Acta Physiol. Scand.* 23: 110-127, 1951.
59. Wiederholt, M., Schoormans, W., Fischer, F., and Behn, C. Mechanism of action of aldosterone on potassium transfer in the rat kidney. *Pfluegers Arch.* 345: 157-178, 1973.
60. Wiederholt, M., Agulian, S. and Khuri, R. N. Intracellular potassium in the distal tubule of the adrenalectomized and aldosterone treated rat. *Pfluegers Arch.* 347: 117-123, 1974.
61. Woodhall, P. B. and Tisher, C. C. Response of the distal tubule and cortical collecting duct to vasopressin in the rat. *J. Clin. Invest.* 52: 3095-3108, 1973.
62. Wright, F. S., Strieder, N., Fowler, N. B., and Giebisch, G. Potassium secretion by the distal tubule after potassium adaptation. *Am. J. Physiol.* 221: 437-448, 1971.
63. Wright, F. S. Potassium transport by the renal tubule. In MTP International Review of Science (K. Thurau, Ed.), Series I, Vol. 6, pp. 79-106. Butterworth & Co., London and Washington, D.C., 1974.
64. Wright, F. S. Potassium. In Pathophysiology of the Kidneys (N. Kurtzman and M. Martinez-Maldonado, Eds.), pp. 180-212, C. Thomas, Springfield, 1977.
65. Wright, F. S. Sites and mechanisms of potassium transport along the renal tubule. *Kidney Int.* 11: 415-432, 1977.
66. Wright, F. S. and Giebisch, G. Renal potassium transport: contributions of individual nephron segments and populations. *Am. J. Physiol.* (editorial) 235: F515-F527, 1978.













YALE MEDICAL LIBRARY

Manuscript Theses

Unpublished theses submitted for the Master's and Doctor's degrees and deposited in the Yale Medical Library are to be used only with due regard to the rights of the authors. Bibliographical references may be noted, but passages must not be copied without permission of the authors, and without proper credit being given in subsequent written or published work.

This thesis by \_\_\_\_\_ has been used by the following persons, whose signatures attest their acceptance of the above restrictions.

<u>Michael Canty</u>	<u>333 Cedar St.</u>	<u>12/30/81.</u>
NAME AND ADDRESS		DATE



